Université de Montréal

Validation of Synthetic Lethal Hits of Microtubule Targeting Agents

par

Matthew Di Lalla

Biologie Moléculaire

Faculté de Médecine

Mémoire présenté

en vue de l'obtention du grade de Maître en sciences (M.Sc.)

en Biologie Moléculaire

Option Génerale

Mai, 2020

Résumé

Les microtubules, composants clés du cytosquelette des cellules eucaryotes, sont des polymères de tubuline très dynamiques et impliqués dans une grande variété de processus cellulaires. Leur rôle essentiel dans le cycle cellulaire a fait d'eux une cible validée en thérapie anticancéreuse. Malgré l'efficacité clinique des agents ciblant les microtubules (ACM), les effets secondaires compliquent l'utilisation. Nous avons cherché à identifier des vulnérabilités génétiques qui peuvent être exploitées pour diminuer la dose requise tout en maintenant l'efficacité, et donc réduire les effets secondaires. En collaboration avec le laboratoire Tyers à l'IRIC, nous avons réalisé un criblage génétique basé sur la létalité synthétique avec des agents antiprolifératifs, dont les ACMs. Nous avons sélectionné les gènes dont l'extinction sensibilisait les cellules aux ACMs. J'ai confirmé que l'invalidation de chacun des gènes GNA13, SEPHS1, DLGAP5 et des gènes QRICH1, DLGAP5 sensibilisaient les cellules NALM6 au docétaxel et la vincristine respectivement. En revanche, aucune invalidation de ces gènes n'a augmenté la sensibilité au docétaxel dans les cellules U2OS.

En plus de son effet avec le docétaxel, le gène GNA13 s'est distingué être une cible particulièrement intéressante. En effet, la perte complète de GNA13 augmente considérablement la fréquence et la gravité d'erreurs de ségrégation des chromosomes dans les cellules U2OS. Cette augmentation n'a pas été rectifiée à la suite d'un traitement avec la molécule UMK57, connue pour réduire le taux d'erreurs de ségrégation des chromosomes. De manière intéressante, la perte complète de GNA13 augmente également la fréquence des erreurs de ségrégation des chromosomes dans les cellules RPE1, cellules non-cancéreuses et stables au niveau chromosomique. Cela suggère que la perte complète de GNA13 ne nécessite pas de transformation ni d'instabilité chromosomique, comme conditions préalables pour exacerber l'instabilité chromosomique.

L'ensemble de ces résultats ouvre une nouvelle voie de stratégies thérapeutiques anticancéreuses, à savoir, le traitement des cancers présentant une mutation des gènes QRICH1, DLGAP5, GNA13, et SEPHS1 avec de faibles doses d'ACMs. En particulier, GNA13 est fréquemment muté dans certains lymphomes. De plus, les résultats obtenus démontrent que la perte complète de GNA13 aggrave l'instabilité chromosomique et par conséquent, pourrait être

impliquée dans la cancérogenèse.

Mots clés : microtubules, cancer, instabilité chromosomique, mitose, létalité synthétique, docétaxel, vincristine, GNA13, QRICH1, DLGAP5, SEPHS1

Abstract

Microtubules, key components of the eukaryotic cytoskeleton, are highly dynamic polymers of tubulin implicated in a wide variety of cellular processes. Their essential roles in the cell cycle have made them a valid target in cancer therapy. Despite the clinical efficacy of microtubule targeting agents (MTA), their use is hampered by side effects. We sought to identify genetic vulnerabilities that can be exploited to decrease the required dose while maintaining efficacy, and therefore reduce side effects. In collaboration with the Tyers laboratory at IRIC, we carried out a genetic screen based on synthetic lethality with antiproliferative agents, including MTAs. We have selected genes whose knockout sensitized cells to MTAs. I have confirmed that the knockout of GNA13, SEPHS1, DLGAP5, and QRICH1, DLGAP5, sensitize NALM6 cells to docetaxel and vincristine respectively. However, no knockout of these genes increased the sensitivity to docetaxel in U2OS cells.

In addition to its effect with docetaxel, GNA13 stood out as being a particularly exciting target. GNA13 knockout increased the frequency and severity of chromosome segregation errors in U2OS cells. This increase was not corrected following treatment with UMK57, a molecule known to reduce the rate of chromosome segregation errors. Interestingly, the GNA13 knockout also increased the frequency of chromosome segregation errors in non-cancerous and chromosomally stable RPE1 cells. This suggests that GNA13 does not require transformation nor chromosomal instability as prerequisites for exacerbating chromosomal instability.

Overall, these results open up a new avenue of anticancer therapeutic strategies, namely, the treatment of cancers presenting mutations in QRICH1, DLGAP5, GNA13, and SEPHS1 with lower doses of MTAs. In particular, GNA13 is frequently mutated in certain lymphomas. In addition, the results obtained demonstrate that GNA13 knockout exacerbates chromosomal instability and, therefore, could be involved in carcinogenesis.

Key words: microtubules, cancer, chromosomal instability, mitosis, synthetic lethality, docetaxel, vincristine, GNA13, QRICH1, DLGAP5, SEPHS1

Table of Contents

Abbreviation List

17-AAG: 17-allylamino-17-demethoxy-geldanamycin

A-MT: astral microtubule

AICAR: 5-aminoimidazole-4-carboxamide riboside

APC/C: anaphase promoting complex/cyclosome

BRCA1: breast cancer type 1 susceptibility protein

BRCA2: breast cancer type 2 susceptibility protein

CB: chromosome bridge

CIN: chromosomal instability

CPC: chromosome passenger complex

CRISPR: Clustered regularly interspaced short palindromic repeats

DAPI: 4’,6-diamidino-2-phenylindole

DLBCL: diffuse large B cell lymphoma

DLGAP5: disks large-associated protein 5

DMEM: Dulbecco's modified Eagle's medium

DMSO: dimethyl sulfoxide

DSB: double strand break

eGFP: enhanced green fluorescent protein

FBS: Fetal Bovine Serum

FISH: fluorescence *in situ* hybridization

GC DLBCL: germinal center diffuse large B cell lymphoma

GNA13: G protein subunit alpha 13

GTP: guanine triphosphate

GEF: guanine exchange factor

H2B: histone 2B

Indel: insertion deletion mutation

Ip-MT: interpolar microtubule

K-MT: kinetochore microtubule

LC: lagging chromosome

LOF: loss-of-function

MAP: microtubule associated protein

MDR1: multi-drug resistance 1

MTA: Microtubule targeting agent

NEB: nuclear envelope breakdown

PAM: protospacer adjacent motif

PARP: poly (ADP-ribose) polymerase

PARPi: poly (ADP-ribose) polymerase inhibitor

PLK1: polo-like kinase 1

PCR: polymerase chain reaction

QRICH1: glutamine rich 1

R-CHOP: rituximab, cyclophosphamide, doxorubicin (hydroxydaunorubicin), vincristine (Oncovin®), and prednisone

RFP: red fluorescent protein

RNAi: RNA interference

RPE1: retinal pigmented epithelium 1 cell

RPMI: Roswell Park Memorial Institute 1640 Growth Medium

S&C: search & capture

SAC: Spindle assembly checkpoint

SD: standard deviation

SEM: standard error of the mean

SEPHS1: selenophosphatase synthetase 1

siRNA: short interfering RNA

sgRNA: single guide RNA

SSB: single strand break

STLC: *S*-trityl-L-cysteine

TACC3: transforming acidic coiled-coil containing protein 3

Topo IIα: topoisomerase IIα

U2OS: U-2 osteosarcoma cell

WT: wild-type

γ-TuRC: γ-tubulin ring complex

Table list

Figure list

Acknowledgements

First and foremost, I want to offer my most profound appreciation and gratitude to my supervisor, Dr. Benjamin Kwok, for granting me the opportunity to pursue my master studies under his supervision. His enthusiasm and dedication to science is inspiring, and I am incredibly thankful to have received his valuable time, encouragement, and guidance.

I would like to graciously thank members of the Kwok lab, both past and present, for our discussions, scientific and otherwise, their advice and technical assistance, and their comradery, all of which have made the lab an extraordinary and memorable place to work. I want to thank Dr. Benoit Barrette for teaching me the basics and assisting me at the start of my project. I want to also thank Dr. Lauralie Peronne for her time and guidance, which has helped me grow as a scientist.

I am deeply indebted to Dr. Julie Mantovani for her advice, support, and encouragement throughout my project. I whole-heartedly would like to thank Dr. Sylvain Meloche for his invaluable suggestions on my project, and for giving me a stronger sense of confidence as a scientist. I sincerely thank Dr. Mike Tyers and his team for our collaboration from which this project was based. My sincere thanks to Christian Charbonneau at IRIC's BioImaging platform for taking the time to train and assist me with all things microscopy. Being able to use the LSM880 was definitely a treat.

I am immensely thankful for my friends Johnny Daou, Shawna Wing, Savanna Smith, Gabriela Bernal Astrain, Vanessa Musacchio, Daniel Tiger, and Jeremy Kim, for their unwavering support and constant motivation, especially when I needed it most. I am also extremely grateful for my friend Dana Segal and our passionate late-night discussions about biology no one around us could follow. Finally, I extend my sincerest gratitude to my family for their unconditional love, support, and patience throughout this journey.

Chapter 1: Introduction

1.1 Mitosis (Overview)

Several scientists in the 19th century began describing the process by which cells divide; however, it was not until 1882 Walther Flemming coined the term "mitosis" (Flemming, 1879, 1965; McIntosh & Hays, 2016). Mitosis is the process by which a cell evenly separates its chromosomes between two daughter cells using a microtubule-based structure known as the mitotic spindle. It is by far the shortest phase of the cell cycle, and its progression is a tightly regulated process to ensure timely and error-free segregation of chromosomes. In preparation for mitosis, the cell duplicates its genome and its centrosome (Stearns, 2001; Takeda & Dutta, 2005). Mitosis has several stages, beginning with prophase (Fig. 1). During prophase, chromosomes begin to condense, and centrosomes separate while increasing microtubule nucleation (Gadde & Heald, 2004; Kuriyama & Borisy, 1981; Walczak et al., 2010). By prometaphase, the centrosomes arrive at opposite ends of the cell, and the nuclear envelope has broken down, releasing condensed chromosomes into the cytoplasm. Microtubules capture the free chromosomes, which then migrate to the spindle equator and biorient (Gadde & Heald, 2004; Walczak et al., 2010; Y. Zhang et al., 2018). Once all chromosomes align at the spindle equator, the cell reaches metaphase (Fig. 1). It is essential not only for all chromosomes to be correctly aligned at the spindle equator but also for each chromosome to form correct attachments to the mitotic spindle. At this stage, the spindle assembly checkpoint (SAC) senses the formation of erroneous attachments, which must be corrected to satisfy it and permit mitosis to progress. Erroneous attachments that persist through metaphase may result in incorrect chromosome segregation and aneuploidy (discussed in detail later). Once the SAC is satisfied, chromosome cohesion is relieved, and the dividing cell enters anaphase (Musacchio & Salmon, 2007; Salic et al., 2004). Anaphase has distinct two stages: anaphase A and anaphase B (Fig. 1). During anaphase A, chromosomes begin migrating towards the spindle poles while the spindle poles remain in place. Only in anaphase B do the spindle poles separate (Asbury, 2017; Scholey

et al., 2016; Walczak et al., 2010). Once chromosomes segregate to opposite poles, telophase begins: the nuclear envelope reassembles, chromosomes decondense, and furrow ingression begins to separate daughter cells begins (Fig. 1). Cytokinesis is the final step in which the spindle midbody, a structure of antiparallel microtubules, forms, and the cleavage furrow splits the two daughter cells (Chircop, 2014; Gadde & Heald, 2004).

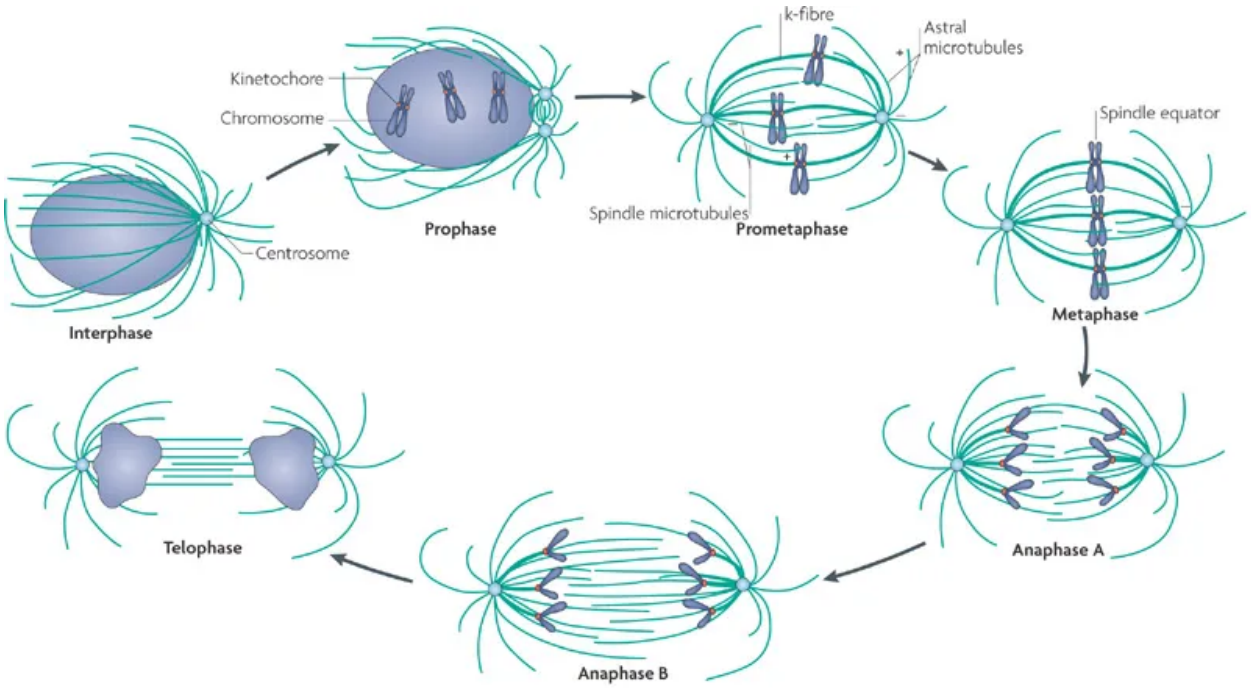

Figure 1. Stages of Mitosis. Mitosis has several stages. Duplication of the genome and the centrosome occurs in interphase in preparation for mitosis. In prophase, DNA condenses into chromosomes, and the duplicated centrosomes begin separating to opposite ends of the cell. By prometaphase, the mitotic spindle has formed, and the nuclear envelope has broken down. Once all the chromosomes correctly attach to the spindle and align along the spindle equator, the cell reaches metaphase. The separation of chromosomes occurs in anaphase. In anaphase A, chromosomes migrate towards the poles, while in anaphase B, the spindle poles separate further. Once separated at telophase, the chromosomes begin to decondense. The final stage is cytokinesis, in which the mitotic cell is cleaved into individual daughter cells (not depicted). Figure used with permission from Springer Nature, license number 4807680711420, (Walczak et al., 2010).

1.1.1 Microtubules

Microtubules are long, rigid, yet highly dynamic polymers that are involved in many cellular functions, such as intracellular trafficking, cell migration, and chromosome segregation during mitosis (Akhmanova & Steinmetz, 2015; T. Mitchison & Kirschner, 1984). They comprise of 13 protofilaments of αβ-tubulin heterodimers assembled into a hollow cylindrical structure with distinct plus- and minus-ends, with the plus-end being the more dynamic of the two. The minus-end commonly capped by the γ-tubulin ring complex (γ-TuRC) complex, which is also responsible for centrosomal microtubule nucleation (Fig. 2A) (Akhmanova & Steinmetz, 2015; Brouhard & Rice, 2018; Jiang & Akhmanova, 2011; Nogales & Wang, 2006). Both α- and β-tubulin bind one molecule of GTP each; however, only β-tubulin possesses GTPase activity (Horio et al., 2014). GTP-tubulin is incorporated at the microtubule plus-end, forming a stabilizing GTP cap. Once incorporated into the microtubule lattice, β-tubulin hydrolyzes GTP and remains within the lattice until released as GDP-tubulin when the microtubule experiences shrinkage (Fig. 2A) (Brouhard & Rice, 2018; Horio et al., 2014). Microtubules alternate between states of growth and shrinkage. Four rates impact microtubule dynamics: rate of growth, rate of shrinkage, catastrophe frequency (the abrupt switch from growth to shrinkage), and rescue frequency (the abrupt switch from shrinkage to growth) (Bowne-Anderson et al., 2013; Walker et al., 1987). The ability of microtubules to stochastically alternate between growth and shrinkage is called dynamic instability. It is a defining characteristic of microtubules and essential for its role in generating the force required to segregate chromosomes in mitosis (Fig. 2B) (Mary Ann Jordan & Wilson, 2004).

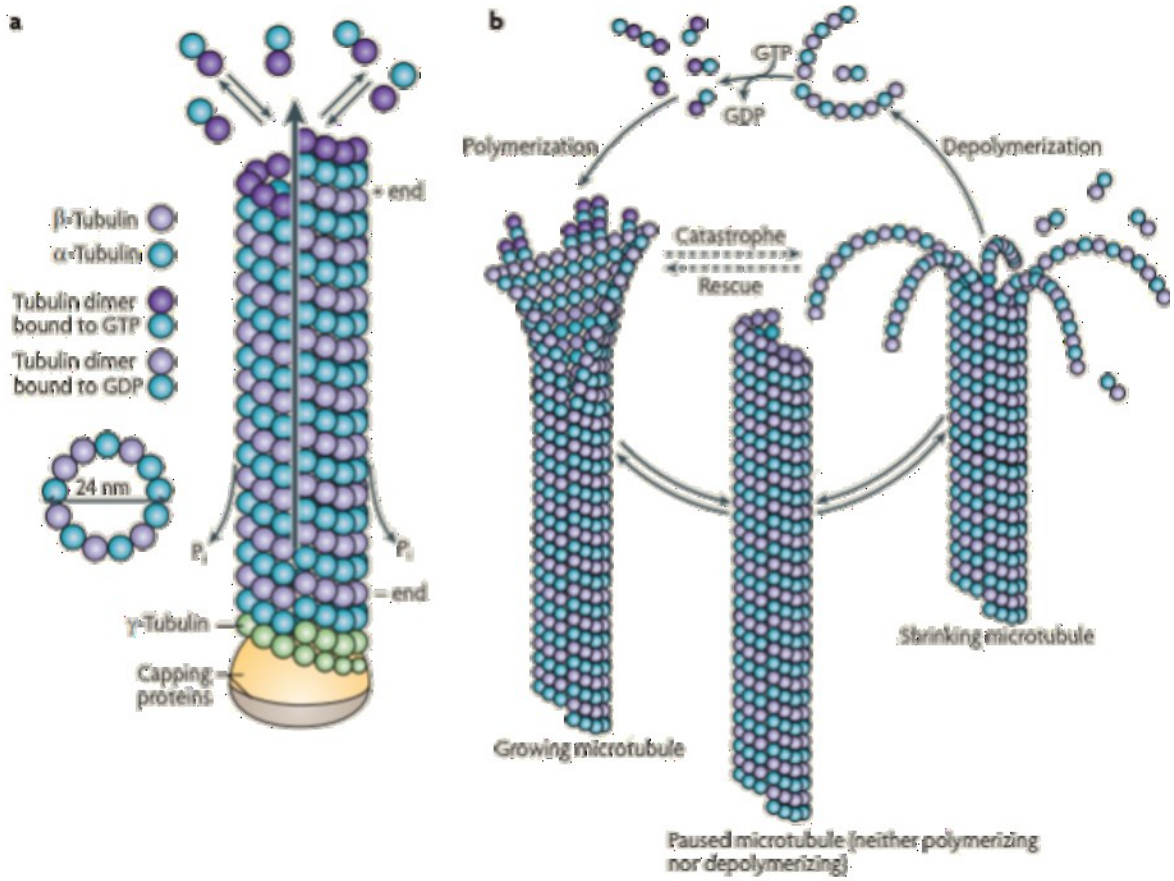

Figure 2. Microtubule structure and dynamic instability. (A) Microtubules are polymers of αβ-tubulin heterodimers that form hollow cylinders with distinct plus and minus ends. GTP-tubulin incorporates at the microtubule plus-end. Once incorporated into the lattice, GTP is hydrolyzed. The γ-TuRC complex caps the microtubule minus-end. (B) Dynamic instability is a defining characteristic of microtubules. Free tubulin exchanges GDP for GTP and is then incorporated into the growing plus-end of a microtubule (polymerization), forming the stabilizing GTP cap. Once the GTP cap is lost, the microtubule beings to disassemble (depolymerization). The rapid change from growth to shrinkage is called catastrophe, and the rapid change from shrinkage to growth is called rescue. Microtubules undergoing no growth or shrinkage are "paused." Figure used with permission from Springer Nature, license number 4807700592819, (Conde & Cáceres, 2009).

1.1.2 Microtubules of the mitotic spindle

The mitotic spindle is composed of microtubules arranged in a bipolar, antiparallel array, with the microtubule minus-ends oriented at the spindle poles and the microtubule plus-ends emanating outwards (Fig. 3A). Along with microtubule-associated proteins (MAPs), it is responsible for aligning and biorienting chromosomes along the spindle equator, and segregating chromosomes to each daughter cell. Centrosomes are the main microtubule-organizing centers during mitosis and nucleate the majority of microtubules. Both motor and non-motor MAPs are required to form and maintain a bipolar spindle and ensure proper chromosome congression. For example, the kinesin CENP-E transports chromosomes with free kinetochores to the spindle equator along spindle microtubules, while TACC3 and the microtubule plus-end polymerase ch-TOG ensure highly organized bipolar spindles are formed (Gergely et al., 2003; Heald & Khodjakov, 2015). There are three distinct types of spindle microtubules: (i) astral microtubules (a-MTs), (ii) interpolar microtubules (ip-MTs; also known as non-kinetochore microtubules), and (iii) kinetochore microtubules (k-MTs; Fig. 3A) (Mastronarde et al., 1993; Prosser & Pelletier, 2017).

A-MTs are nucleated by centrosomes and radiate their plus-ends outwards towards the cell cortex (Fig. 3A). The majority of a-MTs anchor the spindle to the cell cortex and are responsible for centrosome separation during early mitosis, and spindle positioning before anaphase. Dynein, a microtubule minus-end directed motor, is anchored to the cell cortex by dynactin and the NuMA-LGN-Gαi complex. This anchored complex generates the force that pulls the spindle via its minus-end directed movement towards the centrosome (Grill & Hyman, 2005; Laan et al., 2012; McNally, 2013; Okumura et al., 2018). Additionally, a small subset of a-MTs grow into the spindle midbody and assist chromosome congression by generating polar ejection force, a process by which they push chromosome arms towards the spindle equator with chromokinesins (kinesins that interact with chromosomes) such as Kid (Brouhard & Hunt, 2005; Levesque & Compton, 2001).

The second group of microtubules is known as ip-MTs. Ip-MTs form the bulk of the mitotic spindle and are the most dynamic of the three types of spindle microtubules (Zhai et al., 1995). They are responsible for spindle bipolarity, central spindle assembly, and chromosome congression to the spindle equator via chromokinesins and lateral interactions with kinetochores (Cai et al., 2009; Magidson et al., 2011; Vanneste et al., 2011; Wignall & Villeneuve, 2009). The bulk of ip-MTs are nucleated by the centrosomes, although some are nucleated along k-MTs. Ip-MTs extend towards the spindle midzone, with some extending beyond the midzone (Fig. 3A). These polar, overlapping ip-MTs are crosslinked by MAPs that generate poleward microtubule flux, such as the microtubule plus-end directed kinesin Eg5. Eg5 inhibition results in monopolar spindles as a result of failed centrosome separation (Khodjakov et al., 2003; Mastronarde et al., 1993; Miyamoto et al., 2004; Saxton & McIntosh, 1987).

The final type of spindle microtubules are the kinetochore microtubules (k-MTs). Bundles of about 20 k-MTs form kinetochore fibres (k-fibres; discussed below) and attach to chromosomes via association at kinetochores. The majority of these microtubules span the entire distance between centrosomes and kinetochores (Fig. 3A), although a small subset of k-MTs attach only at either the centrosome or the kinetochore. Once associated with the kinetochore, k-MT dynamics stabilize, but growth and shrinkage are not outright inhibited. Instead, microtubule dynamics become more tightly regulated to accomplish specific goals, such as correcting erroneous microtubule attachments (McDonald et al., 1992; Nixon et al., 2015; Prosser & Pelletier, 2017).

1.1.2.1 K-fibre formation

K-fibres link chromosomes to the spindle poles and are essential for chromosome segregation. The bulk of k-fibres are nucleated by the centrosomes and radiate outwards, randomly searching the cytoplasm for kinetochores by rapidly alternating between growth and shrinkage. Once a k-fibre plus-end “captures” a chromosome, the plus-end stabilizes. This is known as the search and capture (S&C) model of k-fibre formation. Centrosome-mediated

microtubule nucleation is very robust, and therefore the S&C method is believed to be the predominant method by which k-fibres form (Heald & Khodjakov, 2015; Kirschner & Mitchison, 1986; Prosser & Pelletier, 2017). However, there are two pitfalls to the S&C model being the only mechanism for k-fibre formation. First, mathematical modeling suggests that the S&C of microtubules alone is far too inefficient and would take far longer than the actual duration of mitosis (Wollman et al., 2005). Additionally, systems that lack centrosomes (naturally or experimentally) are capable of forming bipolar spindles (Khodjakov et al., 2000; Mahoney et al., 2006; Megraw et al., 2001). While centrosome-mediated k-fibre formation appears to be the predominant mechanism involved in cells containing centrosomes, chromosomes are not passive in spindle assembly and are actively involved in k-fibre formation.

K-fibres nucleated by chromosomes grow via plus-end polymerization at kinetochores; however, their growth is not directed towards the centrosome. Instead, the minus-end is captured by a-MTs and directed towards the spindle pole (Khodjakov et al., 2003; Maiato et al., 2004). There are two pathways involved in chromosome-mediated k-fibre formation: (i) the RAN-GTP pathway, and (ii) the chromosome passenger complex (CPC) pathway. Both these pathways produce gradients at the chromosomes that promote local microtubule assembly at the kinetochore. The RAN-GTP pathway forms a RAN-GTP and importin-β gradient around chromosomes, and is responsible for local microtubule nucleation and polymerization via the release of inhibition of spindle assembly factors (Kaláb et al., 2006; Prosser & Pelletier, 2017). The CPC (inner centromere protein [INCEP], survivin, borealin, and Aurora B kinase) creates an aurora B-generated phosphorylation gradient centered at centromeres that inhibits microtubule depolymerization via the inhibition of microtubule destabilizing proteins, such as KIF2C (also known as mitotic centromere-associated kinesin, MCAK) (Prosser & Pelletier, 2017; Ruchaud et al., 2007). It is crucial stable and correct attachments form between k-fibres and chromosomes, as defective chromosome capture and erroneous attachments may result in abnormal chromosome segregation.

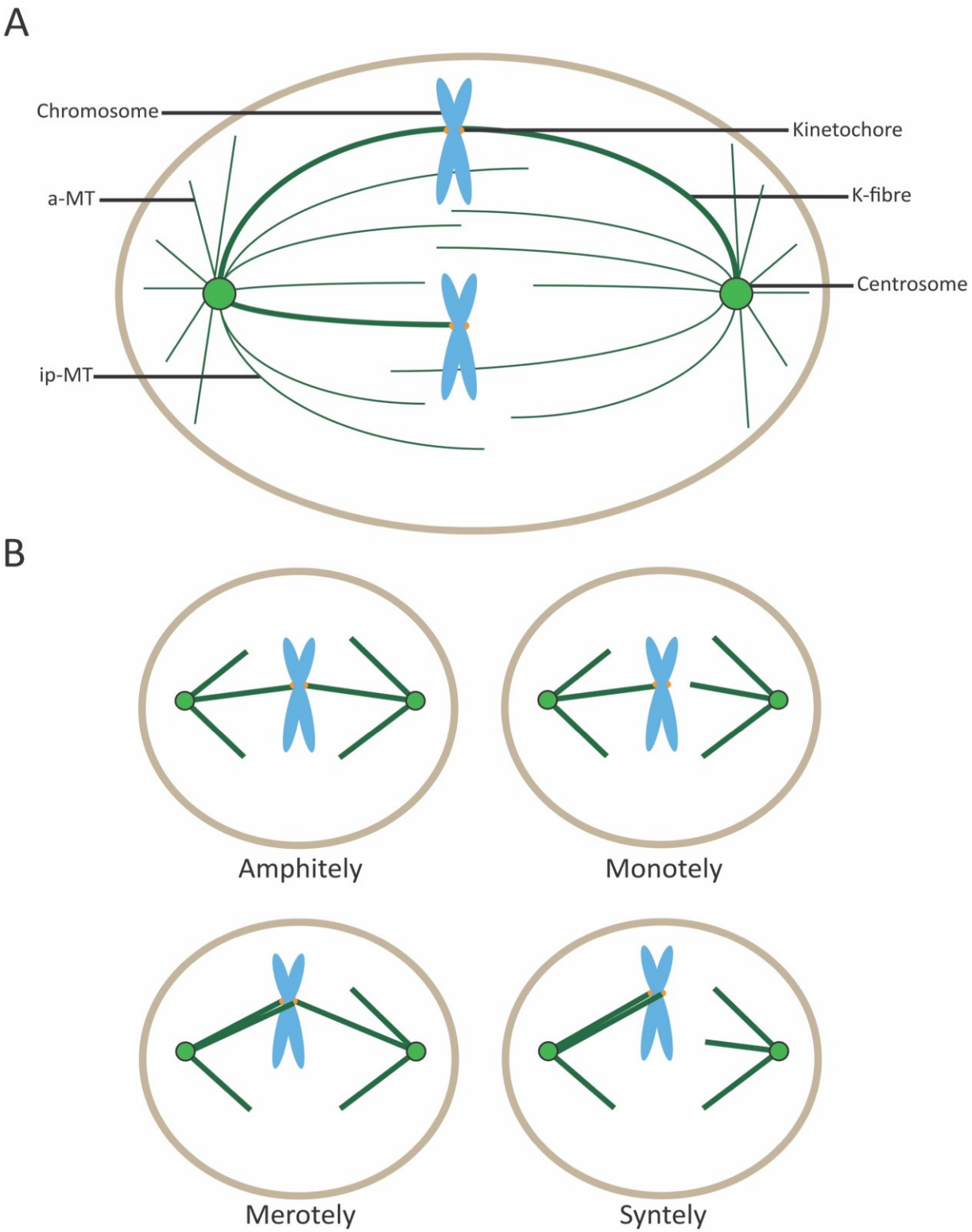
A
Chromosome
Kinetochore
a-MT
K-fibre
Centrosome
ip-MT
B
Amphitely
Monotely
Merotely
Syntely

Figure 3. The mitotic spindle and kinetochore attachments. (A) The mitotic spindle is a bipolar array of microtubules. Centrosomes, the principal microtubule-organizing centers during mitosis, nucleate the majority of spindle microtubules. There exist three types of microtubules that form the mitotic spindle. Astral microtubules (a-MTs) emanate from the centrosomes and anchor the spindle to the cell membrane. Interpolar microtubules (ip-MTs) extend to the spindle midzone and are crosslinked by MAPs to maintain spindle bipolarity and generate microtubule flux. Kinetochore microtubules form bundles called k-fibres. K-fibres are captured by chromosomes at the kinetochore to segregate chromosomes. (B) Types of microtubule attachment. A chromosome is correctly attached when sister chromatids orient towards opposite poles (amphitely). Erroneous attachments manifest in three ways. The chromosome attaches to only one spindle pole via one kinetochore (monotely). The chromosome biorients and attaches to opposite spindle poles, but one kinetochore is attached to both spindle poles (merotely). Finally, the chromosome is attached to only one spindle pole via both kinetochores (syntely).

1.1.3 Chromosomal instability and aneuploidy

Chromosomes must be equally divided between daughter cells, as abnormal chromosome segregation has drastic consequences. Cells containing multiples of the haploid number of chromosomes are euploid, while any deviation from the euploid state is aneuploid. Humans have 46 chromosomes, and deviation from that number is rarely tolerated (Mustaly & Ganem, 2015; Pfau & Amon, 2012). For example, aneuploidy is one of the leading causes of miscarriage in the first trimester of pregnancy, and most frequently manifests as a trisomy (a third copy of a chromosome present) of an autosome (a chromosome that is not a sex chromosome). Few trisomies are tolerable beyond the first trimester, with trisomy 21 (Down's Syndrome) the most common in humans (although trisomies 13 and 18 are also possible, but children do not survive to adulthood) (Hassold & Hunt, 2001; Robinson et al., 2001). If a cell can tolerate the result of an abnormal division, it is not without consequences.

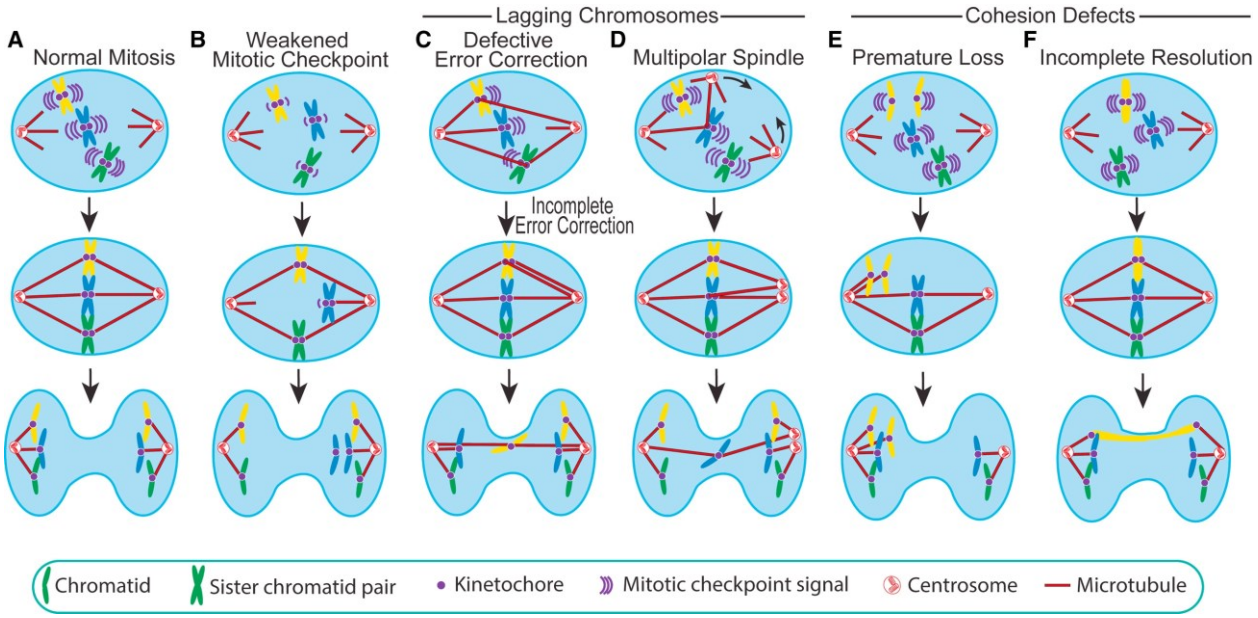

Figure 4. Mechanisms of chromosomal instability. (A) Normal mitosis in which chromosomes form amphitelic attachments with the mitotic spindle, biorient along the spindle equator, and segregate equally between daughter cells. (B) A mitosis in which the spindle assembly checkpoint is weakened and does not prevent anaphase onset before erroneous attachments are corrected, resulting in chromosome missegregation. Pictured above is an example of a monotelic attachment resulting in both sister chromatids segregating to the same daughter cell. (C and D) Mechanisms by which lagging chromosomes arise. (C) Defects in the machinery responsible for correcting erroneous attachments, or the inability to correct defects because of hyperstable attachments, allows incorrect attachments to persist until anaphase. Pictured above is a lagging chromosome from an uncorrected merotelic attachment. (D) Multipolar spindles increase the frequency of merotelic attachments. If centrosomes cluster for bipolar division, lagging chromosomes may arise if not corrected by anaphase. (E and F) Chromosomal instability produced by cohesion defects. (E) Premature loss of chromosome cohesion results in random segregation of sister chromatids. (F) If chromosome cohesion is not relieved by anaphase, sister chromatids remain entangled while being separated by the mitotic spindle. This manifests as a chromosome bridge, which, if not corrected by abscission, results in a DNA double-strand break. Figure used with permission from Elsevier, license number 4807670177482, (Funk et al., 2016).

Genomic instability is a hallmark of cancer, and one form of genomic instability is chromosomal instability (CIN). CIN refers to an increase in chromosome segregation error rate during mitosis, and defective chromosome segregation results in aneuploidy (Bolhaqueiro et al., 2019; Hanahan & Weinberg, 2011). While CIN and aneuploidy are both frequently observed in

cancer, these terms are not interchangeable. CIN is a means by which aneuploidy may arise; however, the presence of aneuploidy alone does not determine if a cell is chromosomally unstable. It is also important to note that CIN may be visible even though chromosomes segregate faithfully, and correct karyotype is maintained. Chromosome segregation errors observed at anaphase are readouts for CIN; however, it has been reported that chromosomes missegregate without any observable error as frequently as chromosomes that did visibly lag (Potapova et al., 2013; Thompson & Compton, 2008, 2011). CIN is not one homogenous cellular event, and there are multiple mechanisms as to how segregation errors arise.

1.1.3.1 Spindle assembly checkpoint defects

A chromosome is correctly attached to the mitotic spindle when kinetochores are oriented towards and attached to opposite spindle poles (amphitely). Erroneous attachments to the mitotic spindle include both kinetochores attaching to the same spindle pole (syntely), only one kinetochore attaching to only one spindle (monotely), and one kinetochore attached to the correct spindle while the other is attached to both (merotely) (Fig. 3B). The SAC, comprising of Mad1, Mad2, BubR1, Bub1, Bub3, and Mps1 in humans, is a safeguard mechanism that ensures erroneous attachment correction (except merotelic attachments which satisfy the SAC and are corrected via another mechanism) before anaphase. The primary target of the SAC complex is the anaphase-promoting complex/cyclosome (APC/C), a multi-subunit ubiquitin E3 ligase that regulates protein degradation by the 26S proteasome during mitosis. Chromosomes are held together by the cohesin complex until the cell is ready to proceed to anaphase. Once the SAC is satisfied, inhibition of the APC/C is relieved. The APC/C then ubiquitinates securin, which allows separase to cleave the cohesin complex subunit Rad21, freeing chromosomes for anaphase (Barbosa et al., 2011; Matsuura et al., 2006; Musacchio, 2015; Musacchio & Salmon, 2007).

A weakened SAC allows cells to enter anaphase before each chromosome is correctly attached to the mitotic spindle, resulting in abnormal segregation of chromosomes (Fig. 4B) (Musacchio, 2015; Thompson et al., 2010). An example of weakened SAC signaling is mosaic

variegated aneuploidy disorder, a rare disorder caused by mutations in the SAC gene BUB1B (encoding BubR1). People with this disease display growth retardation, microcephaly, premature chromatid separation, and monosomy/trisomy mosaicism. The increase in CIN results in a high degree of aneuploidy, with patients experiencing high rates of childhood cancer (Matsuura et al., 2006; Pfau & Amon, 2012; Thompson et al., 2010). Additionally, Bub1 insufficiency is capable of fueling tumorigenesis via increased chromosome missegregation (Baker et al., 2009). While these results support the notion that the SAC is paramount in ensuring correct chromosome segregation, mutations in SAC genes are uncommon in cancer, even those with elevated CIN. Rather, altered SAC gene expression results in increased CIN and aneuploidy (Barbosa et al., 2011; Holland & Cleveland, 2012; Tighe et al., 2001).

1.1.3.2 Lagging chromosomes

Lagging chromosomes (LC) are the most common form of CIN observed (Thompson & Compton, 2008). They arise when a single chromatid lags behind the rest of the segregating masses of chromatin (Fig. 4C) (Funk et al., 2016). Most kinetochores form merotelic attachments early in mitosis but correct them before anaphase (Cimini et al., 2003). Merotelic attachments do not activate the SAC because microtubule occupancy at kinetochores is sensed as equivalent to that of amphitelic attachments, thus satisfying the SAC. The majority of kinetochores with merotelic attachments form more attachments to the correct spindle pole, and chromatids ultimately segregate to the correct daughter cell (Cimini et al., 2001, 2004). However, a LC entrapped in the cleavage furrow may undergo a double-strand break (DSB) if not corrected before completion of cytokinesis. DSB repair occurs via non-homologous end-joining; however, this encourages chromosomal rearrangements and contributes to a cycle of break-fusion-break events (Janssen et al., 2011).

Merotelic attachments depend on their rate of formation and their rate of correction (Thompson et al., 2010), and CIN cancer cells possess reduced error correction capacity and hyperstable k-MTs (Bakhoum, Genovese, et al., 2009; Ferreira et al., 2020; Mustaly & Ganem,

2015). Aurora B is enriched at merotelic attachments and is responsible for recruiting the error correction machinery. For example, it is responsible for both recruiting and regulating the kinesin-13 KIF2C, a microtubule depolymerase. Centromeric KIF2C increases k-MT turnover to correct merotelic attachments. Phosphorylation of S196 by Aurora B then inhibits its activity, stabilizing the k-MT (Andrews et al., 2004; Knowlton et al., 2006; Lan et al., 2004). K-MT turnover decreases and the occurrence of LCs increases in KIF2C-deficient cells, while KIF2C overexpression or treatment with the KIF2C agonist UMK57 increases k-MT turnover and decreases LC formation (Bakhoum, Thompson, et al., 2009; Orr et al., 2016).

LCs may also arise in mitotic cells with more than two centrosomes. In addition to the main spindle, the additional centrosome(s) also form stable kinetochore attachments. This results in an increase in merotelic attachments during the multipolar intermediate that persists through anaphase (Fig. 4D). While cells with more than two centrosomes can undergo a multipolar anaphase, it is exceedingly rare and usually results in cell death due to severe chromosome gains/losses. Instead, cells have mechanisms in place to cluster extra centrosomes and ensure a bipolar division occurs. One example is the minus-end directed kinesin KIFC1, which is commonly overexpressed in cancers. KIFC1 depletion abrogates extra centrosome clustering, resulting in multipolar anaphase (Funk et al., 2016; Kwon et al., 2008; Quintyne et al., 2005; Silkworth et al., 2009; Zasadil et al., 2014).

1.1.3.3 Cohesion defects

Although less common than LCs, chromosome cohesion defects are additional sources of chromosome segregation errors. Cohesion defects may arise in two ways. The first is by premature loss of chromosome cohesion before anaphase (Fig. 4E) (Funk et al., 2016; Mustaly & Ganem, 2015; Thompson et al., 2010). Cells must maintain proper chromosome cohesion throughout mitosis to ensure correct chromosome segregation at anaphase. Chromosome cohesion is maintained by DNA catenations (DNA entanglements), and the cohesin complex (Díaz-Martínez et al., 2007). The cohesin complex comprises of four core components Smc1a,

Smc3, Rad21, and either Stag1 or Stag2. Cohesin is loaded onto DNA before S phase and remains bound until prophase, when the bulk of it is removed by Wap1, Aurora B, and Polo-like kinase 1 (PLK1) phosphorylation (cleavage-independent; prophase pathway). The remaining cohesin is primarily located at centromeres and telomeres, and protected by a complex of Shugosin and protein phosphatase 2A. Once chromosomes properly align at the spindle equator and the SAC is satisfied, separase cleaves Rad21 just before anaphase onset (cleavage dependant; separase pathway) (Dai et al., 2006; Nakajima et al., 2007; Peters et al., 2008). Cohesin-complex genes are rarely mutated, even in cancer (Peters et al., 2008). Rather, mechanisms maintaining chromosome cohesion are perturbed. Examples include premature cleavage of cohesin by separase via loss of inhibition from securin, and the loss of inhibitory phosphorylation by the cyclin dependant kinase CDK1 (Chiang et al., 2011; Stemmann et al., 2001). If chromosome cohesion is lost before anaphase, sister chromatids randomly segregate because they do not biorient at the spindle equator and randomly attach to spindle poles (Funk et al., 2016).

The second cohesion defect is the result of incomplete resolution of chromosome cohesion at anaphase (Fig. 4F). Genome replication during S phase inherently produces DNA catenations. DNA topoisomerase IIα (Topo IIα) is responsible for DNA decatenation before anaphase by passing one DNA strand through a transient DSB of another strand, with centromeres and telomeres being exceptions. Only once cohesin is cleaved by separase is Topo IIα capable of completing DNA decatenation and relieving cohesion (L. H. C. Wang et al., 2010). Incomplete resolution of chromosome cohesion, either by incomplete DNA decatenation or incomplete cohesin removal before anaphase, results in the formation of a chromosome bridge (CB), a distinguishable bridge of DNA that arises during anaphase that stretches between both DNA masses of a dividing cell. If unresolved, CBs can break via tension generated by the spindle poles, or cleavage by the cleavage furrow at cytokinesis, resulting in DNA DSB. Like with LCs, CBs experiencing a DSB may undergo structural rearrangements, fueling a cycle of break-fusion-break events (Funk et al., 2016; J. H. Lee & Berger, 2019; Pampalona et al., 2016). Other possible outcomes include cleavage furrow regression to allow enough time to correct the bridge, or complete cleavage furrow regression and tetraploidization (Ganem & Pellman, 2012; Janssen et

al., 2011; Pampalona et al., 2016).

1.1.3.4 Clinical relevance of CIN & aneuploidy

CIN and aneuploidy are quite common in cancer and drive tumorigenesis. CIN is observed in 44% of solid cancers and 14% of hematopoietic cancers, while aneuploidy is found in over 85% of solid cancers and over 70% of hematopoietic cancers (Ben-David & Amon, 2020; Taylor et al., 2018; Zasadil et al., 2013). The gain or loss of just a fraction of a chromosome may result in a change in copy number of dozens to thousands of genes (Ben-David & Amon, 2020; Kuukasjärvi et al., 1997). Paradoxically, CIN and aneuploidy confer an overall growth penalty to the cell. Elevated CIN negatively impacts proliferation but does not inhibit tumor cell initiation (Godek et al., 2016; Zasadil et al., 2016), while severe segregation defects results in cell death (Zasadil et al., 2014). This suggests that although CIN and aneuploidy are rather slow processes, they can act both oncogenically and as tumor suppressors. Their oncogenic potential depends on what has been gained or lost by the cell, as well as the context in which they occur, as no single chromosome gain or loss universally promotes tumorigenesis. Cell type heavily influences aneuploidy patterns. For example, chromosome arm 13q is frequently gained in colorectal adenocarcinoma, but frequently lost in lung squamous cell carcinoma. Cell type selects aneuploidies that confer advantageous karyotypes, as chromosomes gained frequently encode proliferation-promoting genes, and chromosomes lost encode anti-proliferative genes (Ben-David & Amon, 2020). Mentioned earlier, Bub1 deficient mice exhibited an increased incidence of aneuploidy and loss of tumor suppressor heterozygosity. However, this was in a cell type-specific manner, as loss of p53 heterozygosity lead to increased incidence of lymphoma, while loss of APC heterozygosity promoted colonic tumors (Baker et al., 2009). CIN and aneuploidy not only have the potential to induce cancer, but also to influence treatment outcome.

Tumors exhibiting CIN or aneuploidy are also associated with poor patient prognosis and worse overall survival (Bakhoum et al., 2011; C. M. Choi et al., 2009; Choma et al., 2001; Heilig et al., 2010; Hieronymus et al., 2018; Stopsack et al., 2019). This is because CIN and aneuploidy are

drivers of intratumor heterogeneity and clonal evolution. Upon selective pressure, clones that have acquired advantageous karyotypes survive and proliferate in a Darwinian “survival of the fittest” (Fig. 5). This is commonly observed in cancer, for example, by conferring an advantageous karyotype to a new microenvironment (metastasis), or conferring drug resistance (Ben-David & Amon, 2020; Duesberg et al., 2000). Clinically this results in poor treatment outcome as a result of drug-resistant cancer (Choma et al., 2001; Dagogo-Jack & Shaw, 2018; A. J. X. Lee et al., 2011; Sansregret et al., 2018). This has prompted researchers to attempt exploiting aneuploidy itself as a therapeutic target. Swanton and colleagues have demonstrated that CIN breast cancer cells were resistant to paclitaxel but sensitive to carboplatin (Swanton et al., 2009). Additionally, aneuploidy elicits cellular stress because of metabolic imbalances. Tang and colleagues identified the HSP90 protein folding inhibitor 17-allylamino-17-demethoxy-geldanamycin (17-AAG), the autophagy inhibitor chloroquine, and the metabolic stress-inducing agent 5-aminoimidazole-4-carboxamide riboside (AICAR), exacerbate proteotoxic and metabolic stress in aneuploid mouse embryonic fibroblasts. Additionally, 17-AAG and AICAR inhibited proliferation of CIN colorectal cancer cell lines, but not those with near euploid karyotypes (Tang et al., 2011). Although progress has been made, there are still many unknowns about processes driving CIN and aneuploidy and how they may be exploited to benefit patients.

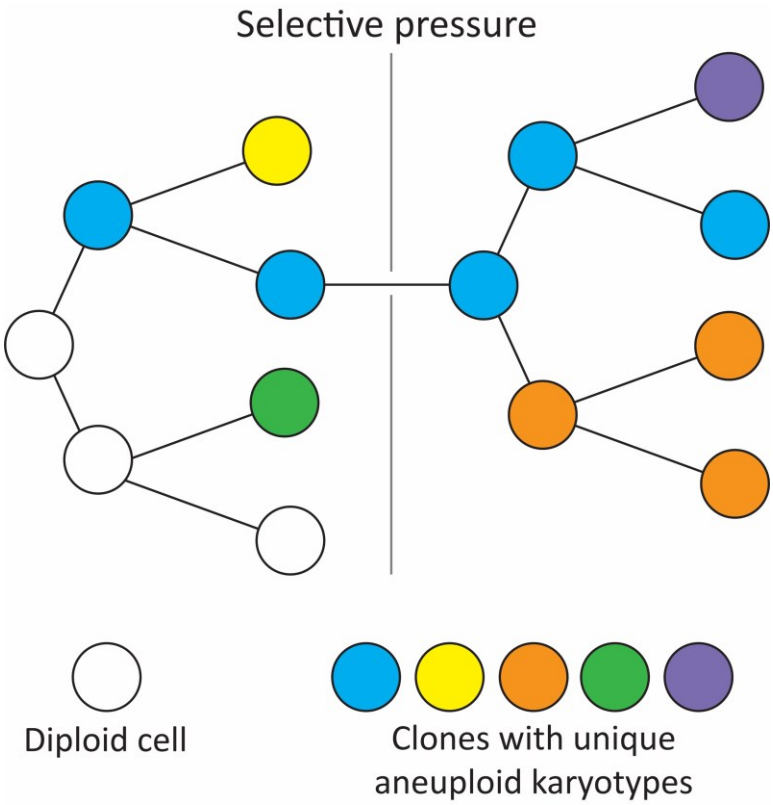

Figure 5. Clonal evolution and adaptive resistance. Over time, diploid cells will become aneuploid due to the gain or loss of chromosomes. If not lethal, these unique clones will continue to propagate until selective pressure, such as drug treatment, is applied. Clones sensitive to the selective pressure are terminated; however, clones that have randomly acquired advantageous karyotypes survive and continue to evolve.

1.2 Microtubule targeting agents

Microtubules are involved in many cellular processes and are a successful target in cancer treatment. Colchicine was the first microtubule targeting agent (MTA) discovered, but its use is limited to niche autoimmune diseases (Steinmetz & Prota, 2018). The discovery of Vinca alkaloids in the 1950s (Noble et al., 1958) and paclitaxel in the 1970s (Schiff et al., 1979) revolutionized cancer treatment. Several MTAs are now listed on the World Health Organization's (WHO) List of Essential Medicines (World Health Organization (WHO), 2019). As successful as they are clinically, they are far from perfect. Because MTAs are cytotoxic, toxicity remains a persistent challenge. To attempt to overcome these challenges, analogs of existing molecules, as well as novel

compounds, are presently being explored (Dumontet & Jordan, 2010; Steinmetz & Prota, 2018).

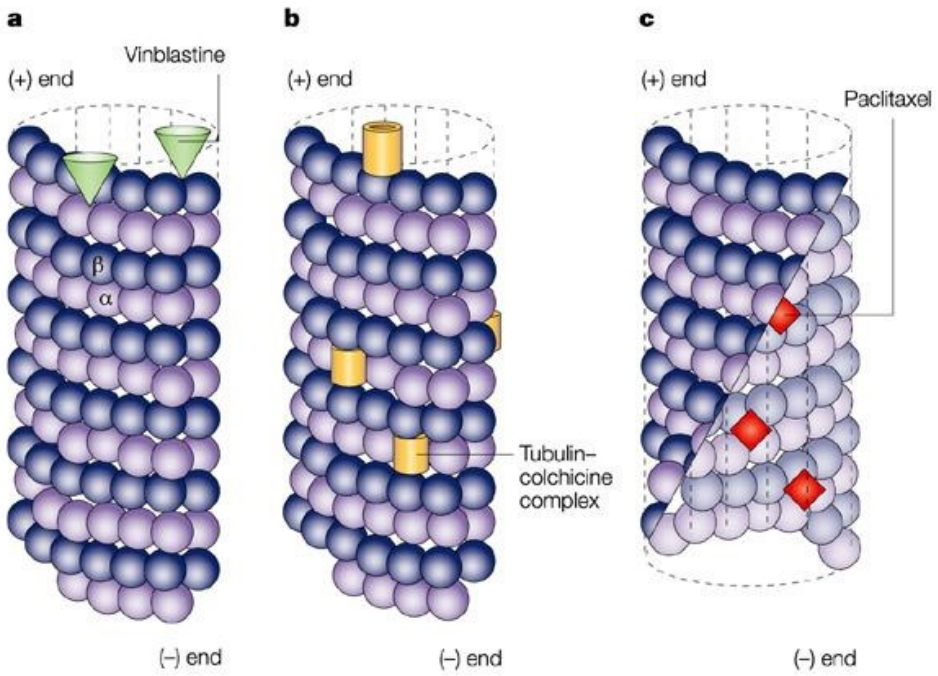

Figure 6. Main binding sites of microtubule targeting agents. (A) The Vinca alkaloid binding site. Vinca alkaloids bind at the microtubule plus end suppresses microtubule dynamics by generating a wedge between longitudinal tubulin dimers. Pictured is the Vinca alkaloid vinblastine. (B) The colchicine binding site. Compounds binding the colchicine site form complexes with free tubulin, which are then incorporated into the microtubule to suppress microtubule dynamics. Pictured is the formation of tubulin-colchicine complex incorporated within the microtubule lattice. (C) The taxane binding site. The taxane binding site is located on the luminal face of microtubules. Compounds binding this site bind polymerized microtubules and stabilize them. Pictured is the binding of paclitaxel. Figure used with permission from Springer Nature, license number 4807700592819, (Mary Ann Jordan & Wilson, 2004).

MTAs have also proven to be powerful tools in studying microtubule dynamics and the cellular processes they partake in, as they are reversible and enable dose-dependent studies. MTAs are capable of severely altering microtubule dynamics at very low stoichiometries with tubulin, making them substoichiometric poisons. At low concentrations, MTAs slow dynamic instability, and induce microtubule stabilization (Mary Ann Jordan & Wilson, 2004). However,

MTAs are broadly classified based on their effect on microtubule dynamics at high concentrations as either microtubule stabilizers or microtubule destabilizers (Kavallaris, 2010). While there exists several unique MTA bindings sites on tubulin, only the three most commonly targeted sites will be discussed in detail: (i) the Vinca alkaloid binding site, (ii) the colchicine binding site, and (iii) the taxane binding site (Fig. 6).

1.2.1 Vinca alkaloid binding site

The Vinca alkaloid binding site is named after the class of compounds first found to bind it. The Vinca alkaloids are a class of terpene alkaloids produced by the Madagascar periwinkle (*Catharanthus roseaus,* [*C. roseaus*]). In the 1950s, Canadian scientists Robert Noble and Charles Beer at the University of Western Ontario were exploring the therapeutic benefits of *C. roseaus* extract and discovered it acts as a myelosuppressive. This observation led them to believe it would be beneficial in treating hematological cancers. In 1958, they successfully isolated vinblastine and vincristine from extracts, and by partnering with Eli Lily, a new way to treat cancer was discovered (Mary Ann Jordan & Wilson, 2004; Noble et al., 1958). Since their discovery, semi-synthetic analogs have been generated, such as vindesine and vinorelbine, also used clinically. Additionally, novel natural products, such as the cryptophycins discovered in cyanobacteria, and the dolastatins discovered in sea slugs, are actively being researched (Bennouna et al., 2008; Gregory & Smith, 2000; Pettit et al., 1998; C. D. Smith et al., 1994).

One Vinca alkaloid binding site per tubulin dimer is located within the β-tubulin subunit at the tubulin inter-dimer interface. Vinca alkaloids are composed of two moieties, the catharanthine moiety and the vindoline moiety, both of which are required for binding. Binding at the plus-end prevents the curved-to-straight conformational change required to form microtubules. Due to binding occurring at the inter-dimer interface and a curved conformation, Vinca alkaloids induce the formation of helical tubulin aggregates, but at concentrations far beyond what is necessary to completely depolymerize microtubules (Gigant et al., 2005; Mary Ann Jordan et al., 1991). At low doses, Vinca alkaloids do not depolymerize microtubules. Rather,

they impede microtubule dynamics by decreasing the rate and duration of microtubule growth at the plus-end (Fig. 6A). Only at high doses are they capable of depolymerizing microtubules. For example, Jordan and colleagues reported vincristine and vinblastine completely depolymerize microtubules at 100nM in HeLa cells, but severely suppress mitotic progression by accumulating cells in a metaphase-like state at much lower concentrations (IC_{50} values of 2.7nM and 0.8nM, respectively) (Mary Ann Jordan et al., 1991; Mary Ann Jordan & Wilson, 2004).

The Vinca alkaloids were first approved for hematological cancers; however, their use has since expanded to include solid cancers (Dumontet & Jordan, 2010). For example, vinblastine is also used to treat germ cell cancers in both males and females, and vincristine to treat neuroblastoma and nephroblastoma (Martino et al., 2018; World Health Organization (WHO), 2019). The production of semi-synthetic analogs has expanded the repertoire of Vinca alkaloids used clinically, such as vindesine to treat hematological cancers and lung cancer, vinflunine to treat bladder cancer, and vinorelbine to treat metastatic breast cancer and non-small cell lung carcinoma. Vincristine, vinblastine, and vinorelbine are listed as essential medicines by the WHO (Dumontet & Jordan, 2010; World Health Organization (WHO), 2019).

1.2.2 Colchicine binding site

Colchicine was first extracted by the French chemists Pierre Pelletier and Joseph Caventou in 1820 from the plant *Colchicum autumnale*. While being the first MTA discovered, it is not used to treat cancer because of toxicity-related side effects. Instead, it is used to treat inflammatory diseases like gout, familial Mediterranean fever, pericarditis, and Behçet's disease (Lu et al., 2012; Slobodnick et al., 2015). While there is great structural diversity among ligands for the colchicine binding site, toxicity remains a challenge for many. For example, nocodazole is another well-known drug that binds the colchicine site, but it has not been explored for clinical use due to severe toxicity. However, nocodazole remains one of the most commonly used MTAs to study microtubule dynamics and mitosis *in vitro* (Attia, 2013; Bates & Eastman, 2017; Blajeski et al.,

2002; Brabander & Borgers, 1973). However, some colchicine binding site ligands show promise and are being explored in clinical trials, such as the combretastatins (Lu et al., 2012).

Drugs that bind the colchicine site are microtubule destabilizers. There is one binding site per tubulin dimer located on the β-tubulin subunit at the intra-dimer interface. Binding induces conformational changes in both α- and β-tubulin subunits, hindering the tubulin dimer from undergoing the curved-to-straight conformational change required to form microtubules (Ravelli et al., 2004; Steinmetz & Prota, 2018). Colchicine does not directly bind the microtubule plus-end; rather, it binds free tubulin heterodimers slowly to form poorly reversible colchicine-tubulin complexes, which are then incorporated into the polymerized microtubule (Fig. 6B). At low concentrations, the incorporation of colchicine-tubulin complexes impairs polymerization efficiency but does not halt polymerization altogether. Only at high concentrations do these complexes prevent polymerization and induce microtubule disassembly. Instead, microtubule dynamics are severely altered but not wholly suppressed (M. A. Jordan, 2002; Mary Ann Jordan & Wilson, 2004; Margolis & Wilson, 1977; Vandecandelaere et al., 1997).

Isolated from the African Bushwillow tree (*Combretum caffrum*), the combretastatins are structurally similar class of compounds that also bind the colchicine binding site. Of the natural combretastatins, combretastatin A4 is the most potent with regard to tubulin-binding and cytotoxicity, but has poor stability *in vivo*. More stable analogs are being explored predominantly as anti-vasculature agents to treat solid tumors (Gaspari et al., 2017; Mary Ann Jordan & Wilson, 2004; Lu et al., 2012). Solid tumors are limited in their growth capacity by the existing network of blood vessels that supply them with nutrients and oxygen. Tumors are capable of overcoming this by producing new blood vessels, a process called angiogenesis (Nishida et al., 2006). Tumor vasculature is abnormal compared to healthy vasculature, and therefore sensitive to MTAs. While antiangiogenic drugs are already in use clinically, such as inhibitors of vascular endothelial growth factor and matrix metalloproteinases, combretastatins are being explored to target the vasculature directly. The rapid shutdown of the tumor vasculature ultimately results in hypoxia-induced cell death (Shi et al., 2016; Tozer et al., 2002; Vasudev & Reynolds, 2014).

1.2.3 Taxane binding site

Drugs that bind the taxane binding site are microtubule stabilizers. These drugs inhibit dynamic instability by preventing microtubule depolymerization, and at high doses, by promoting microtubule polymerization (Winefield et al., 2008). There is one taxane binding site per tubulin heterodimer within the β-tubulin subunit, which is located on the luminal side of polymerized microtubules (Mary Ann Jordan & Wilson, 2004; Nogales et al., 1995). Taxanes were the first class of molecules identified to bind this site, but the list has grown to include epothilones, and more recently zamponolide, dactylolide, and taccalonolides (Dumontet & Jordan, 2010; Field et al., 2012; Y. Wang et al., 2017).

Taxanes are diterpene molecules initially discovered in trees. Paclitaxel (commonly known by its brand name Taxol®) was extracted from the Pacific yew tree (*Taxus brevifolia)* in the 1960s by Monroe Wall and Mansukh Wani (Wani et al., 1971). In 1979, its antiproliferative effect discovered by Susan Horwitz's lab. They demonstrated paclitaxel possessed antitumor activity and promoted microtubule polymerization, a novel mechanism because only microtubule destabilizers were known at the time (colchicine, Vinca alkaloids) (Schiff et al., 1979; Wall & Wani, 1995). Substoichiometric binding of paclitaxel is sufficient to impede mitotic progression by stabilizing microtubules without inducing polymerization (Derry et al., 1995; Mary Ann Jordan et al., 1996). The mechanism by which paclitaxel stabilizes microtubules is still a matter of debate; it is suggested that it stabilizes the microtubule lattice by inducing internal rearrangements of the tubulin dimer to modulate conformational strain and longitudinal contacts within the microtubule (Alushin et al., 2014). Paclitaxel is a highly successful MTA clinically and is used to treat breast and ovarian cancers, non-small cell lung carcinoma, and Kaposi's sarcoma (Dumontet & Jordan, 2010; Mary Ann Jordan & Wilson, 2004). Due to the success of paclitaxel and the initial scarcity of raw material to extract it from, docetaxel was developed as a semi-synthetic alternative using the European yew (*Taxus baccata*) (Yared & Tkaczuk, 2012). It found success clinically treating head and neck, prostate, lung, brain, and stomach cancers. Both paclitaxel and docetaxel are listed as essential by the WHO (World Health Organization (WHO), 2019). More

recently, carbazitaxel, a semi-synthetic drug derived from docetaxel, was approved for metastatic hormone-resistant prostate cancer (Dumontet & Jordan, 2010; Mary Ann Jordan & Wilson, 2004; Yared & Tkaczuk, 2012).

In addition to taxanes, the epothilones are another class of MTAs that also bind the taxane binding site that has achieved clinical success. Epothilones are 16-membered macrolides with potent antiproliferative effects discovered in the myxobacterium *Sporangium cellulosum* (Bollag et al., 1995; Gerth et al., 1996; Höfle et al., 1996). While they also bind the taxane site, they bind it somewhat differently. Taxanes and epothilones were initially believed to share a common pharmacophore (Giannakakou et al., 2000). It has been demonstrated that each bind the taxane binding site differently, but both stabilize microtubules via bridging of the M-loop and helix H7 adjacent to the nucleotide-binding site (Nettles et al., 2004). Epothilones are of particular interest in cancers that are taxane-resistant. Two mechanisms by which taxane resistance occurs are mutation of the binding site, and upregulation of the multi-drug resistance gene MDR1. Epothilones are not substrates for MDR1 and are insensitive to paclitaxel-resistant mutations. One epothilone has already completed clinical trials. Ixabepilone is the first and only epothilone to be approved by the Food and Drug Administration, and is now used to treat paclitaxel-resistant metastatic breast cancer (Conlin et al., 2007; J. J. Lee & Swain, 2008).

1.2.4 Mechanism of action of microtubule targeting agents *in vivo*

While the effects of MTAs on microtubule dynamics are well characterized, the mechanism by which MTAs kills cancer cells *in vivo* is less well understood. It is believed that by altering microtubule dynamics during mitosis, MTAs disrupt the mitotic spindle, and unattached kinetochores activate the SAC. Prolonged mitotic arrest activates downstream apoptotic machinery, resulting in cell death (Mary Ann Jordan et al., 1991, 1996; T. J. Mitchison, 2012; Musacchio, 2015; Yamada & Gorbsky, 2006). Although recent research now suggests that MTA-

induced apoptosis is a far more complex process that we do not understand entirely, and work exploring the multifaceted effect of paclitaxel highlights this complexity. Paclitaxel accumulates within cells *in vitro,* and *in vivo*, even though it is cleared from the circulation (Mori et al., 2006; Weaver, 2014). Clinically relevant cellular concentrations of paclitaxel do not induce apoptosis via the mechanism mentioned above. Rather, clinically relevant paclitaxel concentrations induce multipolar spindle formation and division *in vitro* and *in vivo*. Daughter cells become intolerably aneuploid and undergo apoptosis (Zasadil et al., 2014). Additionally, approximately 80% of cells in mice harboring cancer xenografts treated with paclitaxel undergo apoptosis without ever entering mitosis (T. J. Mitchison, 2012; Orth et al., 2011). It has also been postulated that the immune system may also be involved. Paclitaxel induces the expression of pro-inflammatory cytokines, and in patients treated with paclitaxel, leukocyte recruitment correlated with cell death and better response. However, whether paclitaxel-induced leukocyte recruitment is actively involved, or merely the clean-up response to remove dead cells is unknown (Demaria et al., 2001; Javeed et al., 2009; T. J. Mitchison, 2012). Paclitaxel is also capable of directly binding Bcl-2 to induce apoptosis via the intrinsic apoptotic pathway (Ferlini et al., 2009). While there are still many unknowns as to how MTAs induce cell death *in vivo*, they are nonetheless effective in doing so.

1.2.5 Side effects of microtubule targeting agents

"All things are poison and nothing is without poison; only the dose makes a thing not a poison" (Paracelsus & Band 2, 1965). Although variations exist between translations, this forms the basic tenet of pharmacology: the dose makes the poison. As successful as they are, MTAs, like any drug, are not without side effects. However, MTAs have narrow therapeutic indices (dose at which toxic effects occur over the therapeutic dose). Side effects range from inconvenient to severe, restricting the maximum dose administered to patients. Furthermore, MTAs are administered intravenously, and therefore act systemically without discriminating between healthy and cancerous cells. MTAs are toxic to rapidly dividing cells found in the bone marrow, hair follicles, and the gastrointestinal tract. Dose-limiting side effects common to MTAs include

gastrointestinal distress (nausea, vomiting, diarrhea), alopecia (hair loss), and myelosuppression (bone marrow suppression resulting in decreased red blood cells, white blood cells, and platelets) (Mukhtar et al., 2014; Yared & Tkaczuk, 2012).

While MTAs elicit side effects because of their impact on rapidly dividing cells, they are not the only side effects. MTAs frequently cause peripheral neuropathy, which commonly manifests as a loss of sensory function, but impaired motor function is also possible. In most cases, MTA-induced neuropathy is only partially reversible, but is irreversible in severe cases. Microtubules are essential for healthy neuronal function, but MTAs alter microtubule dynamics. Both microtubule stabilizers and destabilizers cause peripheral neuropathy, but the mechanisms are poorly understood. MTAs are reported to alter microtubule flux, demyelinate neurons, cause axonal atrophy, impair signal responsiveness, and impair neuronal arborization (neuronal end-branching). Axonal flow may be impaired by abnormal microtubule bundling, as microtubule destabilizers impair microtubule bundling, and microtubule stabilizers promote excessive bundling. Additionally, the microtubule stabilizers paclitaxel and ixabepilone impair kinesin-based (anterograde) axonal transport of mitochondria, but not dynein-based (retrograde) transport, in cultured human neuronal cells and mouse sciatic neurons. Vincristine also impairs kinesin-based transport but required significantly higher concentrations (Mary Ann Jordan & Wilson, 2004; Quasthoff & Hartung, 2002; J. A. Smith et al., 2016). Understanding how MTAs induce side effects and how to minimize them remains an active field of study.

Many efforts are being made to discover drugs with the same efficacy as MTAs but fewer side effects. Under the pretense that MTAs exert their antitumoral effect by inhibiting mitosis, mitotic inhibitors were developed. However, mitotic inhibitors against Eg5, PLK1, and aurora kinases have demonstrated poor efficacy towards cancer while exhibiting strong myelosuppressive activity. Their lack of efficacy further suggests that mitosis is likely not the only target of MTAs in cancer (Komlodi-Pasztor et al., 2011; T. J. Mitchison, 2012). Another approach to decrease side effects is increasing specificity by targeting the drug to the tumor. Nanoparticle albumin-bound paclitaxel (Abraxane®) has improved outcomes while eliciting less severe

neutropenia and slightly lower incidence of sensory neuropathy than paclitaxel. It is already approved for breast cancer and is undergoing clinical trials for lung, ovarian, and pancreatic cancers. Other MTA formulations, such as liposomal vincristine, and are under investigation to overcome dose-limiting toxicities (Dumontet & Jordan, 2010; Yared & Tkaczuk, 2012). While these methods may one day prove successful at reducing dose-limiting toxicities, another means to accomplish this is by exploiting genetic vulnerabilities the cancer already possesses to decrease the dose required to patients.

1.3 Synthetic lethality

Cancer drugs are inherently toxic and do not discriminate between healthy and cancerous cells, and therefore, have narrow therapeutic indices. To more effectively treat cancer while minimizing side effects, the therapeutic index must be widened. This is achievable by exploiting genetic differences between cancerous and healthy cells (Cleeland et al., 2012; Kaelin, 2005; Reddy & Kaelin, 2002).

In 1922, Calvin Bridges noted when crossing *Drosophila melanogaster* that mutations in genes that are non-lethal individually were lethal in combination. However, only in 1946 did Theodore Dobzhansky describe the phenomenon using the term “synthetic lethality” (Bridges, 1922; Dobzhansky, 1946). Synthetic lethality describes two simultaneous perturbations occurring in a cell that ultimately leads to cell death. There are two categories of synthetic lethality. The first is genetic synthetic lethality. Genetic synthetic lethality describes loss-of-function (LOF) mutations in two non-essential genes simultaneously that results in cell death, whereas mutations in either of the genes individually results in a viable cell. This is commonly observed with genes involved in the same cellular process or that have redundant functions. The second category is chemical synthetic lethality. There are two types of chemical synthetic lethality based on the combination of interactions present, and in which drug treatment induces a LOF phenotype. The first is a gene-drug interaction, in which the combination of a LOF mutation and a sublethal dose of a drug (as all drugs are lethal with a high enough dose) is lethal. In this case,

the LOF mutation sensitizes the cell to a lower dose of the drug, whereas a cell harboring the wild-type (WT) allele would remain viable. The second is a drug-drug interaction. In this case, the simultaneous inhibition of two pathways via two sublethal drug treatments induces cell death (Dhanjal et al., 2017; Kaelin, 2005; Nijman, 2011).

The first (and so far, best) example of drugs exploiting pre-existing mutations in cancer is the discovery of poly-(ADP-ribose) polymerase (PARP) inhibitors for the treatment of cancers harboring breast cancer type 1 (BRCA1) and breast cancer type 2 (BRCA2) mutations. BRCA1 and BRCA2 are genes involved in DNA DSB repair. BRCA1 and BRCA2 mutations increase the risk of developing cancer and are frequently found in familial breast and ovarian cancers. Sites of DNA single-strand breaks (SSB) recruit PARP1/2 to PARylate other proteins and signal DNA repair machinery recruitment. The SSB is then repaired via base excision repair; however, PARP inhibition results in the formation of a DSB. Cancer cells lacking functional BRCA1 and BRCA2 are incapable of repairing these newly formed DSBs. When treated with PARPi, they undergo cell cycle arrest and cell death. Healthy cells are spared because they are heterozygous for BRCA1/2, and therefore have functional DNA repair machinery. Olaparib was the first PARPi approved to treat BRCA-mutated ovarian cancers, but the class has since expanded with several PARPi gaining approval. Another PARPi, talazoparib, recently gained approval for BRCA-mutated breast cancer. Clinical trials using PARPi to treat other cancers, such as prostate and pancreatic cancer, are ongoing (Drew, 2015; Exman et al., 2019; Farmer et al., 2005; Lord & Ashworth, 2017). So, while it is feasible to exploit naturally occurring mutations to treat cancer while sparing healthy cells, these vulnerabilities need to be identified first.

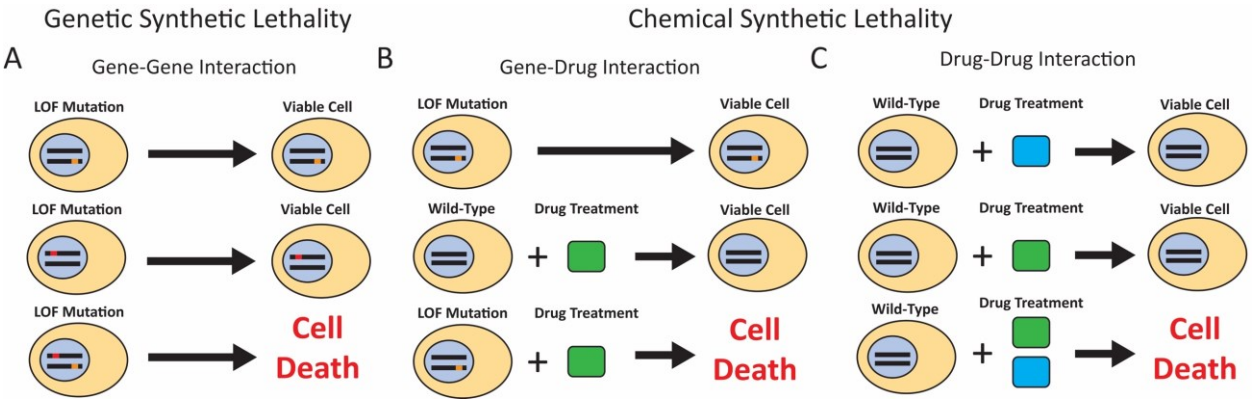

Figure 7. Overview of synthetic lethality. Synthetic lethality occurs upon the simultaneous perturbation of two cellular events, resulting in cell death. (A) Genetic synthetic lethality. A LOF mutation in one gene alone still results in a viable cell, but the simultaneous loss of another gene results in cell death. (B-C) Chemical synthetic lethality occurs in two ways. (B) The first is the result of a gene-drug interaction. A LOF mutation sensitizes a cell to a sublethal dose of a drug. (C) The second form of chemical synthetic lethality is a drug-drug interaction. The sublethal treatment of two different drugs separately results in viable cells. The combination of both drugs results in synthetic lethality, with the sublethal dose of one drug sensitizing the cell to sublethal dose of a second drug.

1.3.1 High throughput screening

The concept of drug screening is not new. In the early 1900s, Paul Ehrlich systematically screened hundreds of compounds to find a "magic bullet" against *Treponema pallidum*, the pathogen responsible for syphilis. His discovery of arsphenamine not only revolutionized syphilis treatment, but also the drug discovery process (Ehrlich, 1911; Wuster & Madan Babu, 2008). However, his work was very low throughput. As technology progressed, so did the screening process. High throughput screening has been around since the 1980s, but without the technology to silence or edit genes, it was limited to screening chemical libraries and different cell lines (Dhanjal et al., 2017; Pereira & Williams, 2007). The discovery of RNA interference (RNAi) technology provided scientists with a method to silence gene expression that was amenable to high throughput screening to probe gene-gene and gene-drug interactions (Nijman, 2011). First, Dicer cleaves long double-stranded RNA into short interfering RNA. The RNA-induced silencing

complex (RISC) then uses the newly formed siRNA to silence genes by guiding the sequence-specific degradation of the complementary RNA transcript and repressing translation, thereby inhibiting translation without directly editing the genome (Pratt & MacRae, 2009; Stewart et al., 2003). However, there are disadvantages such as incomplete and temporary target knockdown and off-target effects due to the binding and destruction of other mRNAs. These challenges were partially overcome with the discovery of the CRISPR/Cas9 system (Dhanjal et al., 2017; A. Lin et al., 2019; Shalem et al., 2015).

1.3.2 CRISPR/Cas9

Discovered as part of adaptive bacterial immunity (Jinek et al., 2012), the clustered regularly interspaced short palindromic repeats (CRISPR) and the CRISPR associated nuclease Cas9 system has allowed for specific, efficient, stable, and simple genome editing. Cas9 edits the genome by generating a DSB at a targeted site, which is repaired via non-homologous end-joining. This generates random insertion or deletion (indel) mutations that frequently cause frameshifts in the coding sequence. Gene expression ceases because of early stop codons or unstable mRNA transcripts. Cas9 uses a single guide RNA (sgRNA) that is specific to a 20-nucleotide sequence region of the genome and is flanked by a 3-nucleotide protospacer adjacent motif (PAM). *Streptococcus pyogenes* Cas9 is the most commonly used in human cells because its PAM sequence, 5'-NGG, is frequently found in the human genome (Ran et al., 2013; Shalem et al., 2015). By generating a genome-wide library of sgRNAs contained within a lentiviral vector, it is possible to probe the entire genome with unprecedented ease, prompting its rapid adaptation to large-scale functional genomic knockout and synthetic lethal screens. Pooled formats are preferred for large-scale projects because they are much cheaper and less labor-intensive than arrayed formats; however, they have drawbacks as well. Because they are performed at the population level, rare phenotypes are more likely to be missed, and phenotypes must be validated individually. They have nonetheless proven invaluable in deciphering gene-phenotype relationships (Agrotis & Ketteler, 2015; Kim et al., 2018; Koike-Yusa et al., 2014; Shalem et al., 2015; T. Wang et al., 2014).

1.3.3 Genome-wide chemogenomic screen

Recently, the Tyers laboratory at IRIC published the results of a genome-wide CRISPR/Cas9 screen evaluating gene essentiality in the pre-B acute lymphocytic leukemia line NALM6 (Bertomeu et al., 2017). NALM6 cells were used because they are (i) suspension cells, facilitating their use in high throughput screening, (ii) are p53 WT (Davies et al., 2011), and (iii) are pseudodiploid (Bertomeu et al., 2017; Ghandi et al., 2019). By using a cell line that is pseudodiploid, gene copy number variation does not need to be taken into consideration, as using cell lines with genomic amplifications are more sensitive to CRISPR/Cas9 cutting toxicity, resulting in false positives (Aguirre et al., 2016; Meyers et al., 2017). In collaboration and using the same genome-wide knockout library of doxycycline-inducible Cas9 NALM6 cells, we performed a pooled genetic screen to identify synthetic lethal combinations using a library of antiproliferative drugs, including several MTAs (Fig. 8). All MTAs included in the screen target the three main binding sites on tubulin, and the majority are used clinically. Enrichment or depletion of sgRNAs from the pool was measured using Illumina® next-generation sequencing after 8 days of sublethal MTA treatment. From this, hits were narrowed to those exhibiting bias towards MTAs, and further narrowed down to five genes exhibiting synthetic lethality with MTAs for validation.

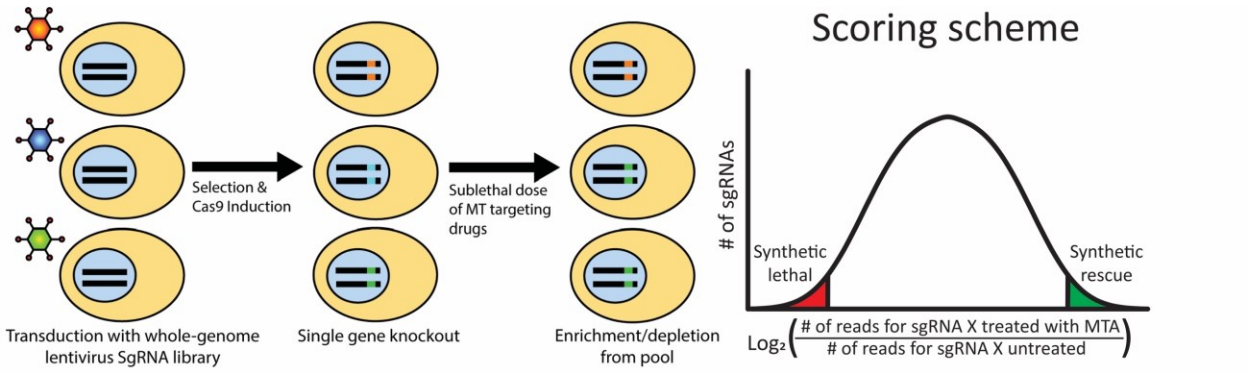

Figure 8. Overview of the synthetic lethal screen. Doxycycline-inducible Cas9 NALM6 cells were transduced with pooled lentivirus containing the extended knockout library of sgRNAs at a multiplicity of infection of ~0.5, followed by selection, Cas9 induction, and treatment with either DMSO or sublethal doses of MTAs for 8 days. Enrichment or depletion from the pool was

determined by measuring changes in sgRNA frequencies between treated and untreated pools using next-generation sequencing. The screen and hit scoring were performed by the Tyers laboratory.

1.3.4 Selected targets

1.3.4.1 QRICH1

Glutamine Rich 1 (QRICH1) emerged as the hit with the most synthetic lethal combinations with MTAs from the screen. QRICH1 has three domains: the caspase activation recruitment (CARD) domain, a glutamine-rich domain, and domain of unknown function 3504 (DUF3504) (Ververi et al., 2018). DUF3504 is suggested to be reminiscent of a yeast *crypton* using tyrosine recombinase that lost its catalytic ability, but may still bind DNA to regulate gene transcription (Kojima & Jurka, 2011; Lui et al., 2019). To date, QRICH1 has no known functions; however, LOF mutations appear to cause neurodevelopmental delay, and chondrodysplasia causing abnormal growth plate morphology and reduced linear growth (Lui et al., 2019; McRae et al., 2017; Ververi et al., 2018). Additionally, the presence of a CARD domain suggests a role in apoptosis and/or inflammation (Bouchier-Hayes & Martin, 2002). QRICH1 is expressed in all tissues (Fagerberg et al., 2014), and LOF mutations are found in various cancers (Lawrence et al., 2014).

1.3.4.2 GNA13

GNA13 (G protein subunit alpha 13) is a Gα protein of the G12/13 family that signals through a variety of G-protein coupled receptors (GPCRs) in conjunction with the $\beta\gamma$ heterodimer. Upon ligand binding and receptor activation, the Gα undergoes a conformational change and exchanges GDP for GTP. The Gα subunit then dissociates from the $\beta\gamma$ subunit to signal downstream effectors, usually guanine exchange factors (GEFs). Of GNA13's signaling pathways, the GNA13-GEF-RhoA signaling pathway is the best characterized. GNA13 is expressed in nearly

all tissues in humans (Fagerberg et al., 2014; Spicher et al., 1994) and is implicated in a number of cellular processes such as actin cytoskeleton reorganization, gene transcription, cell migration and invasion, cell growth and proliferation, and cellular transformation (Bar-Shavit et al., 2016; Engel et al., 2008; Juneja & Casey, 2009; Kelly et al., 2007; Suzuki et al., 2009; Syrovatkina et al., 2016; Syrovatkina & Huang, 2019; Tan et al., 2006). GNA13 is upregulated in many solid tumors where it acts as an oncogene, including breast (Kelly et al., 2006; S. A. Rasheed et al., 2015; Teo et al., 2016), prostate (S A K Rasheed et al., 2013), gastric (Jia Xing Zhang et al., 2016), colorectal (J. X. Zhang et al., 2014; Z. Zhang et al., 2018), pancreatic (Gardner et al., 2013; Hu et al., 2015), liver (Xu et al., 2016), and head and neck cancer, where it also promotes resistance to multiple cancer drugs (Suhail Ahmed Kabeer Rasheed et al., 2018).

In contrast to solid cancers, GNA13 acts as a tumor suppressor in two specific subtypes of germinal center B-cell lymphomas: germinal center diffuse large B-cell lymphoma (GC DLBCL) and Burkitt lymphoma. GNA13 is one of the most frequently mutated genes in GC DLBCL and Burkitt lymphoma, with LOF mutations found in 15-30% of cases (Lawrence et al., 2014; Lohr et al., 2012; Love et al., 2012; J. Zhang et al., 2013). LOF mutations in GNA13 in germinal B cells impairs affinity selection after somatic hypermutation of the immunoglobulin genes, promotes cell survival, proliferation, and prevents restriction to the germinal center of secondary lymphoid tissues via the lack of inhibition of the AKT pathway by RhoA (Healy et al., 2016; Muppidi et al., 2014; O'Hayre et al., 2016).

1.4.3.3 SEPHS1

Selenophosphatase synthetase 1 (SEPHS1, also known as: selenide, water dikinase 1) is an enzyme involved in the selenocysteine biosynthesis pathway. The exact role for SEPHS1 in this pathway is unknown, but it is presently believed to be involved in selenium recycling and not *de novo* selenophosphate synthesis (for which SEPHS2 is responsible) (Oudouhou et al., 2017; Tamura et al., 2004). Selenium is required in trace amounts to maintain proper physiological functions. Selenophosphate is required for the production of selenocysteine,

which is incorporated into selenoproteins. Most notable are the glutathione peroxidases and thioredoxin reductases, proteins involved in redox homeostasis (Labunskyy et al., 2014). SEPHS1 knockout cells demonstrate decreased levels of proteins responsible for redox metabolism and are more sensitive to oxidative stress, suggesting SEPHS1 is involved redox homeostasis (M. O. Lee & Cho, 2019; Morey et al., 2003; Tobe et al., 2016). SEPHS1 expression is upregulated in rapidly dividing cells, such as *Drosophila melanogaster* embryos (Alsina et al., 1998), human oocytes, and embryonic stem cells (Assou et al., 2009; M. O. Lee & Cho, 2019), while SEPHS1 knockout is embryonic lethal in *Drosophila melanogaster* and mice (Alsina et al., 1998; Tobe et al., 2016). SEPHS1 may be required to modulate oxidative stress in cancer cells, as it is upregulated in a variety of cancers and suggested to have a role in rectal carcinogenesis (S. Y. Choi et al., 2011; Fagerberg et al., 2014; Gorrini et al., 2013). SEPHS1 mutations are found in various cancers but are not associated with any specific cancer type (Lawrence et al., 2014).

1.4.3.4 TACC3

Transforming acidic coiled-coil containing protein 3 (TACC3) is a MAP that regulates microtubule dynamics and mitotic spindle assembly downstream of Aurora A phosphorylation (Lioutas & Vernos, 2013). TACC3 promotes centrosomal microtubule nucleation by stabilizing γ-TuRC assembly (Singh et al., 2014) and acentrosomal microtubule nucleation near the kinetochores to facilitate chromosome-mediated k-fibre formation (Fu et al., 2013). TACC3 is recruited to the spindle and forms a complex with the clathrin heavy chain (CHC) and ch-TOG to stabilize k-fibres by forming inter-microtubule bridges (Booth et al., 2011). Depletion of TACC3 results in abnormal spindle assembly, microtubule destabilization, and chromosome misalignment (Fu et al., 2010, 2013; C. H. Lin et al., 2010; Leonid Schneider et al., 2007). Upregulation has been observed in several cancers and is associated with poorer prognosis in soft tissue sarcoma (Matsuda et al., 2017), prostate cancer (Li et al., 2017), cholangiocarcinoma (He et al., 2016), colorectal (Du et al., 2016), esophageal squamous cell carcinoma (Huang et al., 2015), osteosarcoma (Matsuda et al., 2018). TACC3 mutations are found in various cancers but not associated with any specific cancer type (Lawrence et al., 2014).

1.4.3.5 DLGAP5

Disks large-associated protein 5 (DLGAP5; also known as discs large homolog 7 (DLG7); hepatoma upregulated protein, HURP) is a MAP frequently upregulated in hepatocellular carcinoma (hence the name) (Liao et al., 2013). DLGAP5 stabilizes microtubules and promotes microtubule bundling both *in vitro* and *in vivo* (Santarella et al., 2007; Wong & Fang, 2006). During mitosis, it localizes to microtubules in proximity to kinetochores in a RAN-GTP dependent gradient and is involved in proper chromosome congression at the metaphase plate. DLGAP5 is reported to directly interact with TACC3 to form stable lateral kinetochore attachments in prometaphase (Y. Zhang et al., 2018), and is also involved in centrosome clustering in mouse oocytes and human cancer cells with supernumerary centrosomes (Breuer et al., 2010). DLGAP5 depletion decreases interkinetochore tension and k-fibre stability, impairing chromosome alignment along the spindle equator (Silljé et al., 2006; Wong & Fang, 2006), and impairs cell migration in colorectal, lung, and liver cancer cell lines (Branchi et al., 2019; Liao et al., 2013; Q. Wang et al., 2018). DLGAP5 upregulation has been reported in prostate (Gomez et al., 2013), lung (Q. Wang et al., 2018), and colorectal cancers (Branchi et al., 2019) and is associated with worse clinical outcome. DLGAP5 mutations are found in various cancers but are not associated with any specific cancer type (Lawrence et al., 2014).

Rational & hypothesis

Microtubules are essential in many cellular processes and have proven to be a successful target in cancer treatment using MTAs. As successful as MTAs are, their use is severely restricted by their narrow therapeutic index. Efforts to decrease dose-related side effects are already underway but so far have yielded limited improvements. Synthetic lethality occurs when the simultaneous perturbation of two cellular events results in cell death; therefore, exploiting existing mutations within cancer makes it possible to use a lower dose to elicit the same therapeutic effect. This concept has already proven successful clinically with PARPi to treat BRCA1/2 mutated cancers. However, these vulnerabilities must be elucidated from the thousands of genes within the human genome. High throughput screening, combined with genome-editing technologies, has dramatically accelerated the identification of these synthetic lethal relationships. A pooled synthetic lethal chemogenomic screen performed in collaboration with the Tyers lab identified dozens of hits demonstrating bias towards MTAs in NALM6 cells. Of them, five were selected for validation to confirm they are indeed true hits, and if they hold in other cell lines. **If the selected targets are true synthetic lethal hits, then individual gene knockouts will exhibit increased sensitivity towards MTAs.** Because these hits were obtained with MTAs, we also hypothesize the knockout may affect mitosis. Using U2OS cells, another cancerous cell line that is also ideal for microscopy, the hits will be evaluated for cell-type dependency and any effect on mitosis can be observed. This project aims to uncover novel synthetic lethal combinations with MTAs that may be exploited in the future to treat cancer with lower doses of MTAs to decrease side effects while maintaining efficacy.

Objectives

1. Validate synthetic lethal hits of interest using individual gene knockouts in NALM6 cells.
2. Validate synthetic lethal hits using individual gene knockouts in U2OS cells.
3. Observe the effect of the knockout on mitosis in U2OS cells.

Chapter 2 - Methods & materials

2.1 Cell culture

NALM6 cell lines were cultured in Roswell Park Memorial Institute 1640 media (RPMI 1640; Wisent 350-000CL) supplemented with 10% heat-inactivated fetal bovine serum (FBS) (Wisent) and 1% penicillin-streptomycin (Gibco 15140-122). HEK293T, U2OS, and RPE1 cells were cultured in Dulbecco's Modified Eagle Medium (DMEM) (Wisent 319-005-CL) supplemented with 10% heat-inactivated FBS (Wisent) and 1% penicillin-streptomycin (Gibco 15140-122). All cell lines were cultured at 37°C and 5% CO_2. U2OS and RPE1 cells stably express enhanced green fluorescent protein-tagged histone 2B (H2B-eGFP) and red fluorescent protein-tagged α-tubulin (α-tubulin-RFP).

2.2 Lentivirus production and transduction

Knockout lines were generated using CRISPR-Cas9 gene-editing technology. SgRNAs designed by the Tyers lab (Appendix II) were cloned into lentiCRIPSR V2 (a gift from Feng Zhang via the Addgene repository, Addgene #52961) (Sanjana et al., 2014). HEK293T cells were transfected with 0.375μg of both packaging plasmids pRSV-Rev (Addgene #12253) and pMDLG/pRRE (Addgene #12251) (Dull et al., 1998), 0.75μg of the envelope plasmid pCMV-VSV-G (Addgene #8454) (Stewart et al., 2003), and 1.5μg of the lentiCRIPSR V2-SgRNA construct using 9μL of TransIT®-LT1 Transfection Reagent (Mirus, MIR 2300). The media was replaced with fresh, complete DMEM 18 hours post-transfection. Viral supernatant was harvested 48 hours post-transfection and filtered through a 0.45μm filter. 1mL of lentivirus was incubated with 4μg of polybrene (Sigma-Aldrich, TR-1003-G at room) temperature for 20 minutes and added to cells containing 3mL of complete media. The supernatant was removed 18 hours post-transduction, and the cells were expanded for 48 hours before selection with complete media containing 2μg/mL (NALM6, U2OS) or 10 μg/mL (RPE1) puromycin (Wisent). Genomic DNA was extracted 6

days post-selection using DNAzol (Invitrogen 10503027). Exons targeted by sgRNAs were amplified by polymerase chain reaction (PCR) and sequenced by Sanger sequencing. Three sgRNAs were evaluated per target in U2OS cells (QRICH1, GNA13, SEPHS1) or NALM6 cells (TACC3, DLGAP5). Knockout efficiency was evaluated by TIDE (tracking of indels by decomposition) analysis using the freely available online webtool (https://tide.deskgen.com) (Brinkman et al., 2014). Chromatograms were generated using SeqMan Pro (DNASTAR, Madison, WI). The sgRNAs with the highest knockout efficiency were used to generate knockouts in other cell lines. Clonal lines were generated from knockout populations, and knockout efficiency validated the same way.

2.3 Preparation of cell lysates and immunoblots

Cells were collected and washed once with cold phosphate-buffered saline. Cells were then lysed with lysis buffer containing 150mM NaOH, 10mM tris pH 7.5, 0.1% sodium dodecyl sulfate, 0.1% Triton X, 1mM dithiothreitol, and 10μg/mL of protease inhibitors leupeptin, pepstatin A, chymostatin. Samples were immediately homogenized by passing the lysates through a 21-gauge syringe 25 times. Lysates were centrifuged at 13.2k rpm for 15 minutes at 4°C. The supernatants were collected and boiled with Laemmli buffer at 85°C for 5 minutes. Protein concentration was determined using the bicinchoninic acid protein assay kit as described except suggested volumes were halved (Sigma Aldrich, BCA1 & B9643). 10μg of total lysate were resolved by SDS-PAGE on 10% polyacrylamide. Proteins were transferred to Immobilon-P polyvinylidene fluoride membrane (Millipore IPVH00010). The membrane was blocked in tris-buffered saline containing 0.1% Tween-20 and 5% (w/v) milk protein for 2 hours at room temperature. Once blocked, the membrane was incubated with antibody diluted in tris-buffered saline containing 0.1% Tween-20 containing 5% milk protein, 0.02% sodium azide, and primary antibody at room temperature for one hour. The membranes were then washed in tris-buffered saline containing 0.1% Tween-20, and incubated with secondary antibody for one hour at room temperature. Signals were revealed using Amersham ECL Start western blotting detection reagent (GE Healthcare RPN3243) and Amersham Hyperfilm ECL (GE Healthcare 28906839).

Antibodies and respective dilutions used: rabbit anti-GNA13, 1:2000 (Abcam ab128900); rabbit anti-KIF2C, 1:20000 (Abcam ab187652); DM1 mouse monoclonal anti-α-tubulin, 1:50000 (Thermo Fisher 62204); HRP-conjugated goat anti-rabbit IgG H&L, 1:10000 (Abcam 6721) or HRP-conjugated goat anti-mouse IgG H&L, 1:10000 (Abcam 6789).

2.4 Viability assays

The alamarBlue® cell viability assay was used to measure IC_{50}. Optimum seeding density was predetermined for each cell line, and cells were seeded in triplicate in solid black, flat-bottom 96-well plates (Costar). NALM6 cells were seeded and treated the same day. Adherent cell lines were seeded and treated the following day. Cells were treated for 72 hours with either 0.1% DMSO alone, or titrated docetaxel or vincristine and constant 0.1% DMSO (final volume 200μL). 20μL 0.1% (wt/v) resazurin (Sigma Aldrich R7017-5G) in 0.9x PBS (Wisent) was added, and plates incubated for 4 hours at 37°C, 5% CO_2. Fluorescence was measured using an Infinite 200 plate reader (Tecan Group Ltd., Switzerland) using the following conditions: excitation: 530nm; emission: 580nm: gain: 65; height: 22000μm. The same assay was used to measure proliferation under the same conditions. Cells were seeded at optimal seeding density in triplicate and measured each day for 5 days. Day 1 for NALM6 cells refers to the same day as seeding, while day 1 for adherent cells refers to the day following seeding. Results were exported into Microsoft Excel (Redmond, WA) and plotted using KaleidaGraph (Synergy Software, Reading, PA). Student's t-tests were performed in Microsoft Excel.

2.5 Confocal time-lapse microscopy

U2OS and RPE1 cells were seeded on 35mm four-compartment imaging dishes (Ibidi 80416) 1-3 days before imaging. Overnight live cell imaging was performed using a Zeiss spinning disk confocal microscope Axio Observer system with a 40X Plan-Apochromat/1.4 oil objective (Zeiss, Oberkochen, Germany), at 37°C, 5% CO_2. Images were acquired at 2μm intervals over an 18μm range (10 stacks), at 10-minute intervals. For experiments involving UMK57 treatment,

cells were treated with 150nM UMK57 or 0.15% DMSO alone and immediately imaged overnight under the same conditions. Image processing was performed using Zen Blue Software (Zeiss). Images represent maximum-intensity projections of z-stacks. Student's two-tailed t-tests performed in Microsoft Excel (Redmond, WA). Fisher's exact two-tailed tests performed in Matlab (Natick, MA). 2x3 Fisher's exact two-tailed tests performed in Matlab using a script created by Giuseppe Cardillo and published on GitHub (Cardillo, 2007).

2.6 Cell fixation and confocal microscopy

U2OS cells were grown on 18mm^2 glass coverslips for 2-3 days to ~75% confluency. Mitotic cells were accumulated by treating them with 5μM *S*-trityl-L-cysteine (STLC) for 4 hours. Cells were gently washed twice with 1x PBS (Wisent) and once with complete DMEM. Cells were fixed in methanol at -20°C for 6 minutes and washed twice with 37°C 1x PBS (Wisent). Coverslips were mounted on glass slides using mounting media containing Antifade and 4',6-diamidino-2-phenylindole (DAPI; Vector Shield H-1200), and sealed with clear, quick-dry nail polish. Slides were imaged using a Zeiss LSM880 AxioObserver system with a 40X EC Plan-Neofluar/1.3 oil objective and Zen Black software (Zeiss, Oberkochen, Germany). Images were acquired at 1μm intervals covering a range of 18-20μm. Image processing was performed using Zen Blue software (Zeiss). Images represent maximum-intensity projections of z-stacks. Fisher's exact two-tailed test performed in Matlab (Natick, MA). 2x3 Fisher's exact two-tailed test performed in Matlab using a script created by Giuseppe Cardillo and published on GitHub (Cardillo, 2007).

Chapter 3 – Results

3.1 Validation of synthetic lethal hits in NALM6 Cells

In order to validate the hits from the screen, clonal knockout lines were generated. Clonal lines are advantageous in that the knockout is stable. The freely available webtool TIDE (https://tide.deskgen.com) is capable of accurately estimating knockout efficiency off indel formation and was therefore used to assess the knockout clones generated (Brinkman et al., 2014). Clones with a knockout efficiency >90% and with only 1 or 2 indels (determined by TIDE) were deemed to be complete knockout clones. In NALM6 cells, several unique clones were confirmed by TIDE for GNA13, SEPHS1, and DLGAP5. Three were used to validate the hits with MTAs (Fig. 9). Several clones were validated for QRICH1 and TACC3; however, indel distribution and sequencing revealed that the clones were identical. Therefore, only one clone of each QRICH1 and TACC3 was included in the viability assays (Fig. 9).

To measure any changes in sensitivity towards MTA treatment, the alamarBlue® cell viability assay, a non-toxic assay commonly used to measure drug sensitivity, was used (Rampersad, 2012). Hits were validated with one microtubule stabilizer, docetaxel, and one microtubule destabilizer, vincristine. We expect that the knockout lines will be more sensitize cells to MTA treatment than the empty vector control (hereinafter referred to as control). We tested the response to 3 days of MTA treatment by measuring the change in IC_{50} values. Cell viability was assessed as a measure of viable cells treated with docetaxel or vincristine as a percentage of the DMSO treated cells. The results are summarized in Figure 10 and Table 1. WT cells were included and compared against the control to verify that lentiviral transduction and the expression of the Cas9 containing vector alone does not alter the response towards MTA treatment. There is little difference in IC_{50} between the WT and the control for both docetaxel and vincristine (Fig. 10A-B, Table 2), confirming that the approach used did not alter the results obtained when validating the hits.

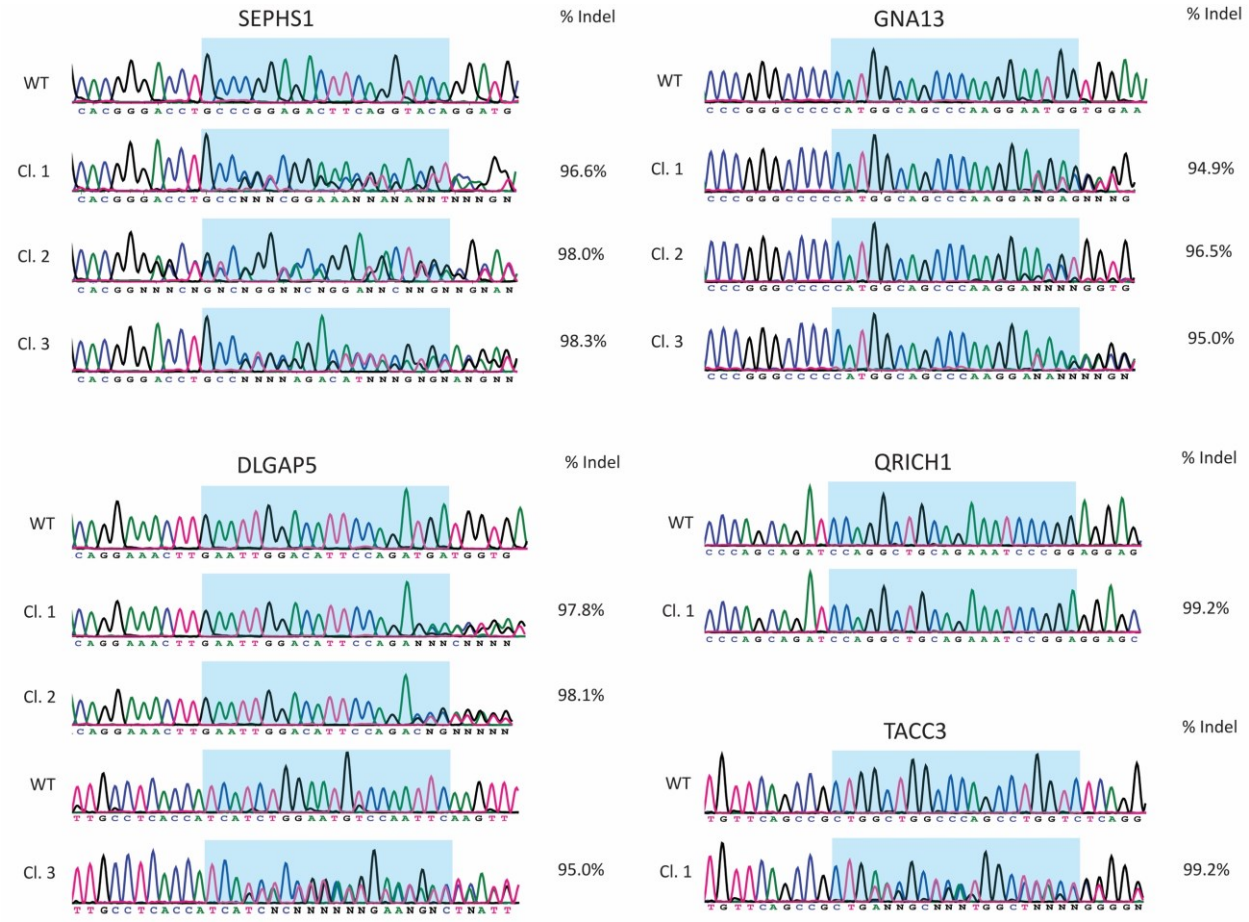

Figure 9. Chromatograms of NALM6 knockout clones. Genomic DNA was purified from the indicated NALM6 line, the targeted exon amplified by PCR, and sequenced by Sanger sequencing. Knockout efficiency was measured as the percent of indel formation against the respective WT sequence using TIDE. The highlighted region indicates the 20-nucleotide sequence recognized by the sgRNA. Note: all DLGAP5 knockout clones were generated with the same sgRNA, but clone 3 was sequenced with the reverse primer.

The majority of hits assayed demonstrated increased sensitivity to docetaxel treatment as measured by a decrease in IC_{50} compared to control cells. Two of the hits, QRICH1 and TACC3, did not significantly alter the response to docetaxel treatment, but QRICH1 knockout did increase sensitivity and approached significance (Fig. 10C-D, Table 1). Three hits, GNA13, SEPHS1, and DLGAP5, did exhibit significant overall increases sensitivity towards docetaxel (Fig. 10E-G, Table 1). However, the response to docetaxel treatment was not uniform between clones. Only two of three clones demonstrated a significant increase in sensitivity towards docetaxel, although the clones that did not exhibit a significant change in sensitivity did exhibit some change to varying

degrees. GNA13 clone 2 exhibited a minor increase in sensitivity, while SEPHS1 clone 1 and DLGAP5 clone 3 exhibited more moderate increases (Fig 10E-G, Table 1).

Fewer hits demonstrated increased sensitivity to vincristine than docetaxel. QRICH1 knockout elicited one of the most substantial increases observed, while TACC3 knockout elicited an increase in sensitivity that approached significance (Fig. 10H-I, Table 1). Although minor changes in sensitivity were observed, GNA13 knockout did not elicit any significant change overall (Fig. 10J, Table 1). SEPHS1 knockout clones exhibited mixed results. Clones 1 and 3 displayed minor but insignificant changes in sensitivity, while clone 2 a significant increase in sensitivity. The overall result was insignificant (Fig. 10K, Table 1). DLGAP5 elicited the most substantial overall change in IC_{50}, although results varied between clones. Clone 1 exhibited a significant increase in sensitivity, clone 2 approached significance, and Clone 3, although not significant, did exhibit a modest increase in sensitivity (Fig. 10J, Table 1).

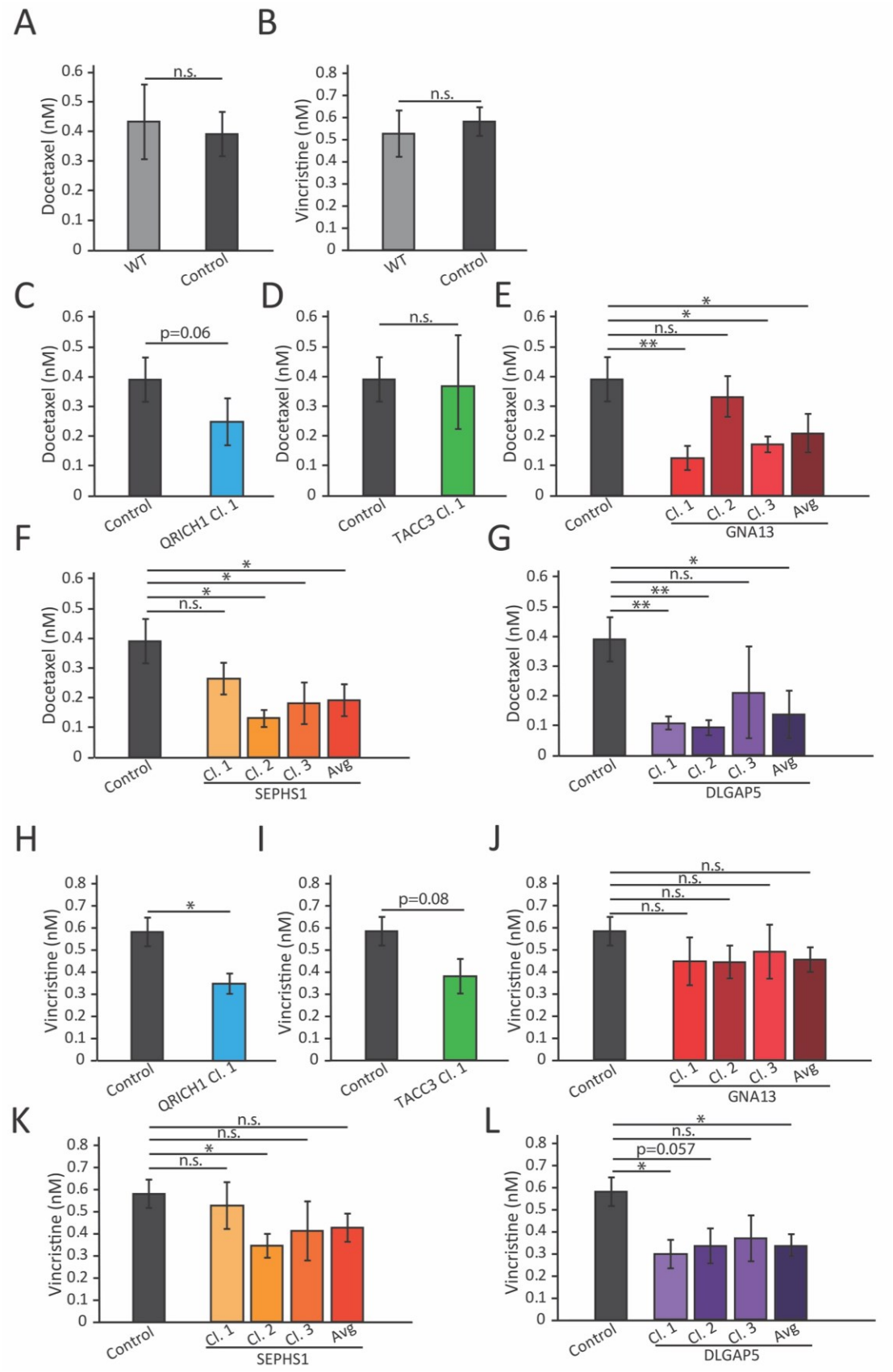
A
B
Docetaxel (nM)
Vincristine (nM)
n.s.
WT
Control
C
D
E
p=0.06
QRICH1 Cl. 1
TACC3 Cl. 1
*
**
Cl. 1
Cl. 2
Cl. 3
Avg
GNA13
F
G
SEPHS1
DLGAP5
H
I
J
K
L
p=0.08
p=0.057

Figure 10. Mean IC_{50} values of NALM6 lines treated with docetaxel or vincristine. Mean IC_{50} values obtained for WT and control cells with (A) docetaxel and (B) vincristine. (C-G) Mean docetaxel IC_{50} values of knockout clones for (C) QRICH1, (D) TACC3, (E) GNA13, (F) SEPHS1, (G) DLGAP5. (H-L) Mean vincristine IC_{50} values of knockout clones for (H) QRICH1, (I) TACC3, (J) GNA13, (K) SEPHS1, and (L) DLGAP5. Error bars represent the SEM of at least three independent experiments. n.s., $p>0.10$; *$p<0.05$; **$p<0.01$, using Student's t-test.

Drug	Line		IC_{50} (nM)	Sensitivity fold change against control
Docetaxel	Control		0.39±0.08	1.00
	WT		0.44±0.15	0.90
	QRICH1 Clone 1		0.25±0.03	1.56
	TACC3 Clone 1		0.38±0.16	1.02
	GNA13	Clone 1	0.13±0.04	3.11
		Clone 2	0.33±0.07	1.18
		Clone 3	0.17±0.03	2.26
		Average	0.21±0.06	1.86
	SEPHS1	Clone 1	0.26±0.05	1.48
		Clone 2	0.13±0.03	2.97
		Clone 3	0.18±0.07	2.15
		Average	0.19±0.05	2.03
	DLGAP5	Clone 1	0.12±0.03	3.25
		Clone 2	0.10±0.03	3.80
		Clone 3	0.24±0.18	1.66
		Average	0.15±0.09	2.56
Vincristine	Control		0.59±0.07	1.00
	WT		0.53±0.10	1.10
	QRICH1 Clone 1		0.35±0.05	1.70
	TACC3 Clone 1		0.38±0.08	1.54
	GNA13	Clone 1	0.45±0.12	1.30

		Clone 2	0.45±0.08	1.32
		Clone 3	0.50±0.13	1.18
		Average	0.46±0.06	1.27
	SEPHS1	Clone 1	0.53±0.11	1.12
		Clone 2	0.35±0.06	1.67
		Clone 3	0.41±0.14	1.42
		Average	0.43±0.07	1.36
	DLGAP5	Clone 1	0.30±0.07	1.94
		Clone 2	0.34±0.08	1.74
		Clone 3	0.38±0.11	1.56
		Average	0.34±0.05	1.73

Table 1. Mean IC_{50} values and fold-change in sensitivity of NALM6 lines treated with docetaxel or vincristine. Mean IC_{50} values ± SEM of at least three independent experiments. Fold change was calculated as an increase in sensitivity compared to the control.

3.2 Validation of synthetic lethal hits in U2OS Cells

Although several hits exhibited significant shifts in IC_{50} towards MTAs, determining if these hits are dependent on cellular context remains to be determined. U2OS cells were chosen because they are another cancer cell line that is also ideal for microscopy experiments because they are flat. Fewer clones were assayed because fewer were confirmed by TIDE analysis. Two knockout clones were confirmed for both GNA13 and DLGAP5, while only one was confirmed for both SEPHS1 and TACC3 (Fig. 11). After multiple attempts, I was ultimately unsuccessful at generating any QRICH1 knockout clones in U2OS cells. Hits were only assayed with docetaxel in U2OS cells because the hits for which I have knockouts exhibited increased sensitivity in NALM6 cells, with the exception of TACC3. However, TACC3 was included because synthetic lethality has been reported with paclitaxel in HeLa cells (Schmidt et al., 2010; L. Schneider et al., 2008).

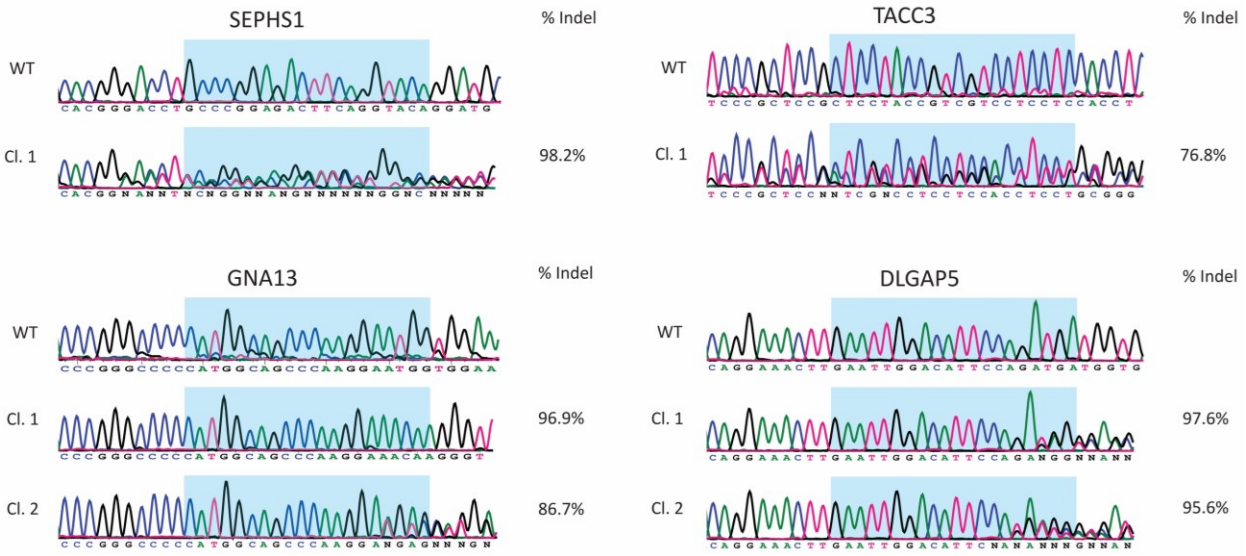

Figure 11. Chromatograms of U2OS knockout clones. Genomic DNA was purified from the indicated U2OS line, and the targeted exon amplified by PCR. Knockout efficiency was measured as the percent of indel formation against the respective WT sequence using TIDE analysis. The highlighted region indicates the 20-nucleotide sequence recognized by the sgRNA.

The alamarBlue® viability assay was again used to validate the hits with docetaxel. Statistical tests were performed against the WT, which had a very similar IC_{50} to the control but smaller SEM (Fig. 12A). The results are summarized in Figure 12 and Table 2. Fewer hits demonstrated increased sensitivity towards docetaxel in U2OS cells. SEPHS1 exhibited little change in sensitivity, while TACC3 exhibited a more modest but still insignificant increase in sensitivity (Fig. 12B-C, Table 2). Similarly, GNA13 knockout clones were not significantly more sensitive towards docetaxel, but there was variation in the response between the two clones. Clone 1 exhibited almost no change in sensitivity compared to WT cells, while clone 2 exhibited a moderate increase in sensitivity (Fig. 12D, Table 2). Of the lines assayed, DLGAP5 knockout clones exhibited most substantial shifts in IC_{50}. Clone 1 exhibited a near significant increase in sensitivity to docetaxel compared to WT cells, while clone 2 exhibited a significant increase in sensitivity. The average of the two clones also approached significance (Fig. 12E, Table 2).

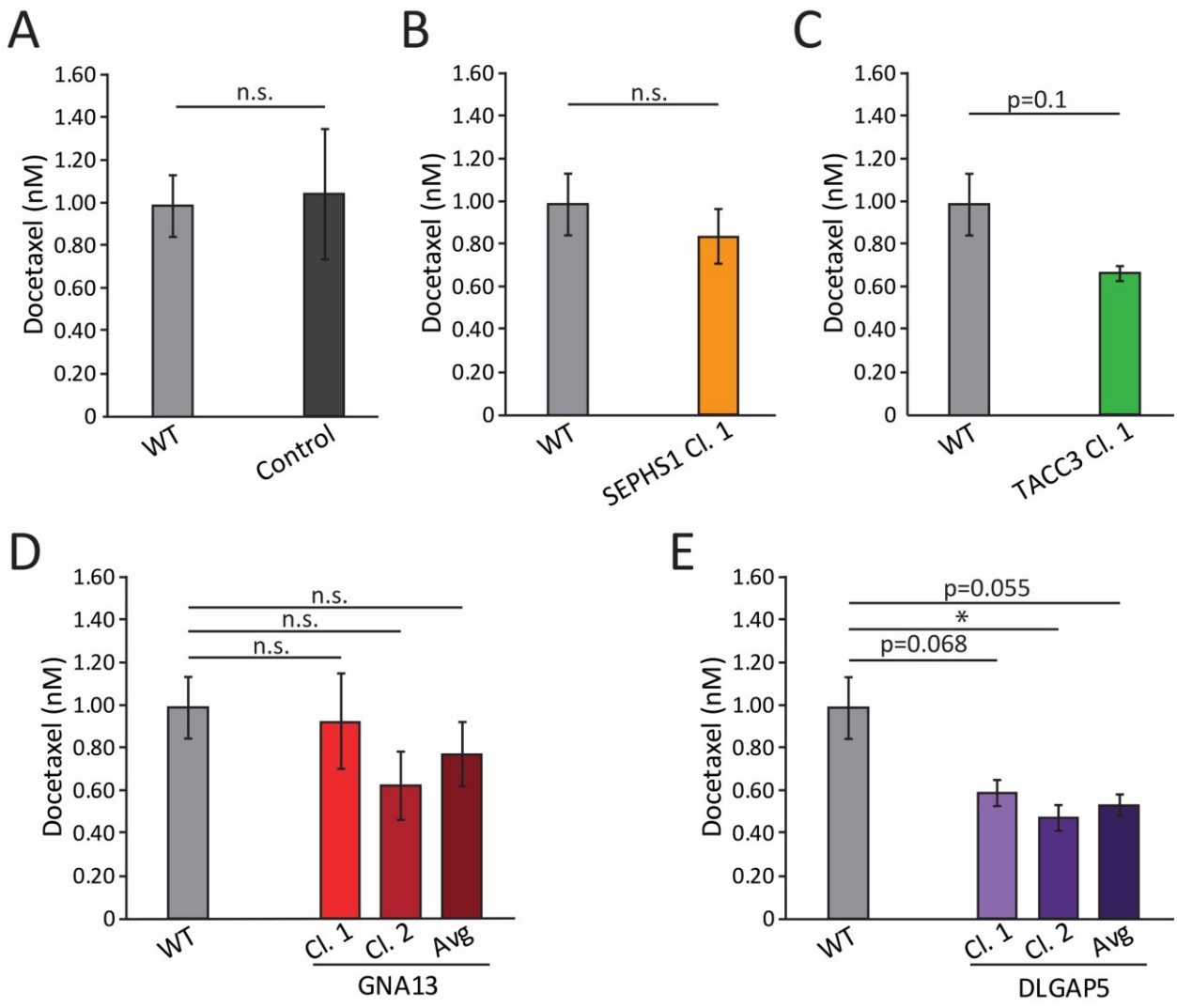

Figure 12. Mean IC_{50} values of U2OS lines treated with docetaxel. Mean IC_{50} values obtained for docetaxel in U2OS cells using the alamarBlue® viability assay. (A) IC_{50} values obtained for WT and control cells. (B-E) IC_{50} values obtained for (B) SEPHS1 clone 1, (C) TACC3 clone 1, (D) GNA13 clones 1-2, and (E) DLGAP5 clones 1-2. Error bars represent the SEM of at least three independent experiments. n.s., $p>0.10$; *$p<0.05$, using Student's t-test.

Line	IC_{50} (nM)	Sensitivity fold change against WT
WT	0.98±0.14	1.00
Control	1.04±0.30	0.95
SEPHS1 Clone 1	0.83±0.22	1.18
TACC3 Clone 1	0.66±0.03	1.48

GNA13	Clone 1	0.91±0.22	1.08
	Clone 2	0.62±0.16	1.59
	Average	0.77±0.15	1.28
DLGAP5	Clone 1	0.58±0.06	1.68
	Clone 2	0.47±0.06	2.11
	Average	0.52±0.05	1.87

Table 2. Mean IC_{50} values and fold-change in sensitivity of U2OS lines treated with docetaxel. Mean IC_{50} values ± SEM of at least three independent experiments. Fold change was calculated as an increase in sensitivity compared to the WT.

3.3 Validation of GNA13 Knockout in NALM6 and U2OS Cells

Of the hits validated, GNA13 emerged as particularly interesting for two reasons. First, GNA13 knockout sensitized NALM6 cells to docetaxel, but not vincristine. This is intriguing because GNA13 is frequently mutated in germinal center lymphomas, for which vincristine is commonly used to treat patients. Secondly, GNA13 knockout was observed to increase CIN in U2OS and RPE1 cells (discussed in the following chapters). Clones verified by TIDE analysis were assumed to be complete knockouts, but this remained to be confirmed using additional methods. First, protein expression was assessed by immunoblot. Immunoblots for NALM6 and U2OS lines revealed that all clones are indeed complete knockouts (Fig. 13A, C). Second, proliferation was used as a readout for GNA13 knockout. Since GNA13 acts as an oncogene and is involved in the proliferation of solid cancers (Kelly et al., 2007), we expected that U2OS GNA13 knockout clones would proliferate more slowly. Conversely, we expected that NALM6 GNA13 knockout clones would proliferate more quickly because of its function as a tumor suppressor in germinal center B-cells (Muppidi et al., 2014). This was easily assessed using the alamarBlue® viability assay. Cells were seeded at predetermined optimal densities, and readings were taken each day for five days. Results were plotted relative to the first day. GNA13 knockout did not affect proliferation in NALM6 cells but did slow proliferation in U2OS cells (Fig. 13B, D). Both U2OS clones proliferated more slowly, consistent with observations made while culturing the lines, but only clone 2

exhibited a significant decrease compared to control cells. These results suggest that using proliferation as a readout to confirm GNA13 knockout is valid, but only for solid cancer cell lines.

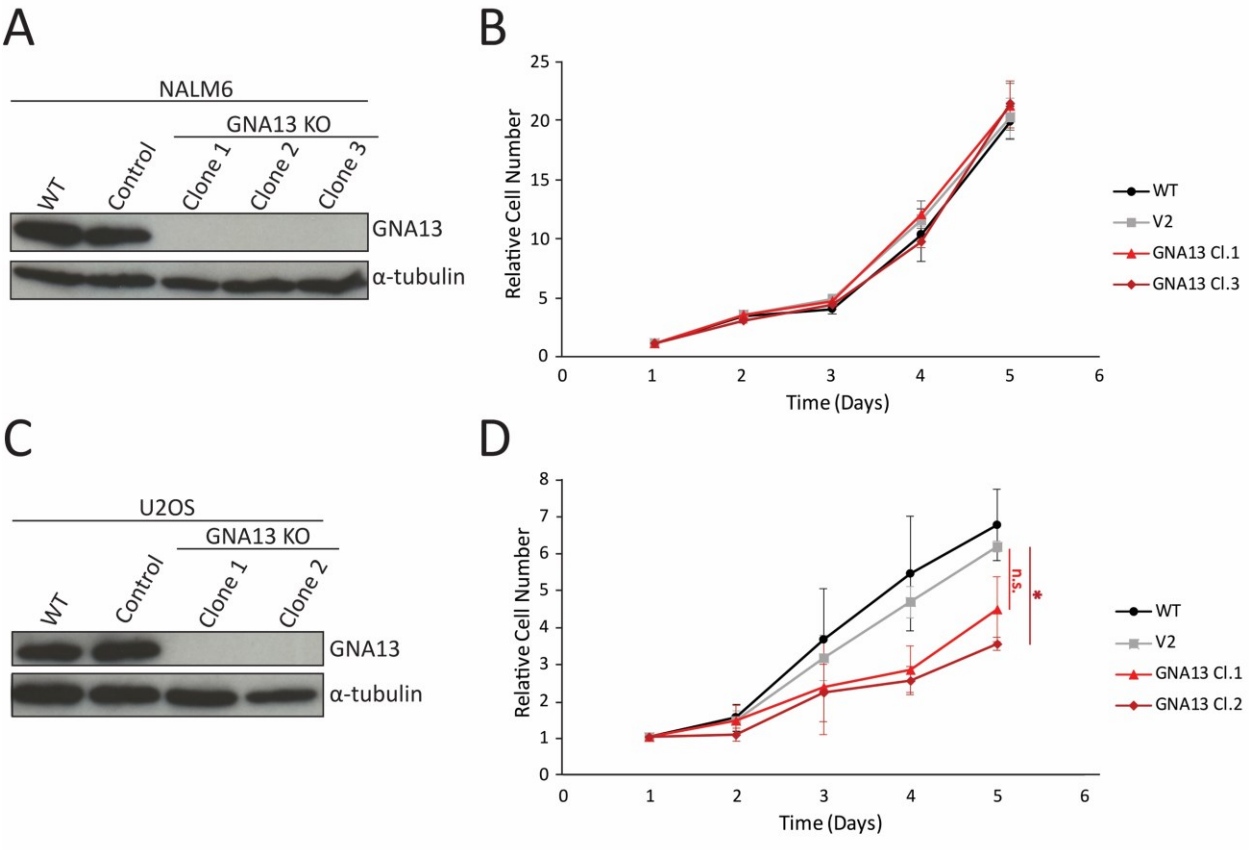

Figure 13. Validation of GNA13 knockout in NALM6 and U2OS cells. (A) Immunoblot of NALM6 WT, control, and GNA13 knockout clones 1-3. α-tubulin used as the loading control. (B) Growth rate of NALM6 WT, control, and GNA13 knockout clones 1 and 3. Results plotted as cell number relative to day 1. Graph shows mean±SEM of three independent experiments. (C) Immunoblot of U2OS WT, control, and GNA13 knockout clones 1-2. α-tubulin used as the loading control. (D) Growth rate of U2OS WT, control, and GNA13 knockout clones 1 and 2. Results plotted as cell number relative to day 1. Graph shows mean±SEM of three independent experiments. n.s., $p>0.05$; *$p<0.05$, using Student's t-test.

3.4 GNA13 knockout increases anaphase chromosome segregation error rate in U2OS cells

Even though GNA13 demonstrated synthetic lethality with docetaxel only in NALM6 cells,

we continued to pursue it because of a fascinating and unexpected phenotype observed in U2OS cells unrelated to synthetic lethality; GNA13 knockout drastically increased anaphase chromosome segregation error rate. Two GNA13 knockout clones were validated in U2OS cells, but only clone 2 was amenable to live-cell microscopy because it expresses H2B-eGFP, while clone 1 does not. Confocal time-lapse microscopy revealed that GNA13 knockout clone 2 had 74.5±2.5% of anaphases with segregation

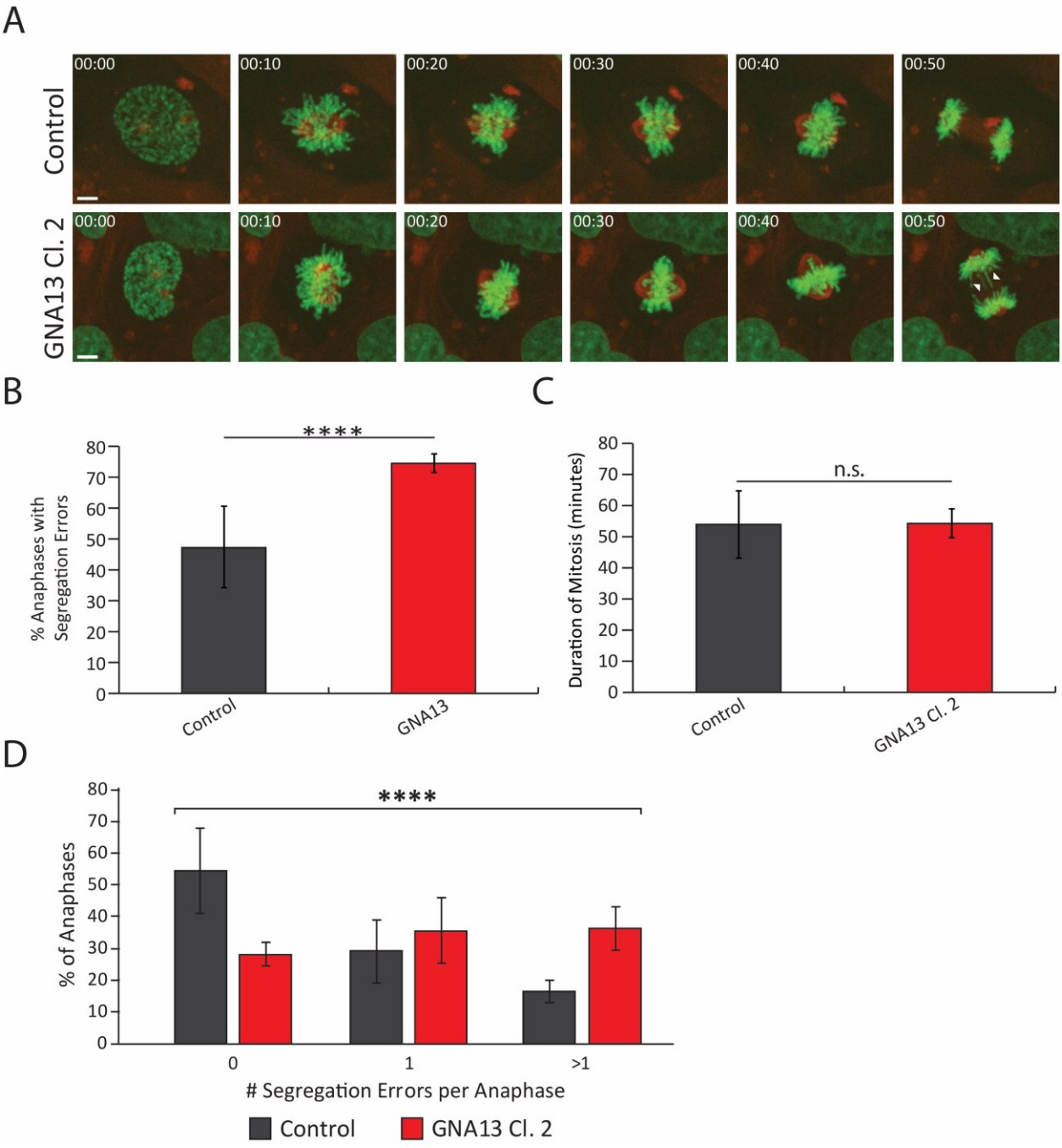

Figure 14. GNA13 knockout increases anaphase segregation error rate without altering mitotic progression in U2OS cells. (A) Representative images illustrating the different stages of mitosis of control and GNA13 knockout clone 2 U2OS cells stably expressing H2B-eGFP (green) and α-tubulin-RFP (red). Arrowheads indicate lagging chromosomes. Time is hours:minutes. Scale bar=5μm. (B) Percentage of anaphases with segregation errors (all errors) in control and GNA13 knockout clone 2 cells. Control: n=106 anaphases; GNA13 clone 2: n=105 anaphases. Error bars represent the SD of three independent experiments. ****p<0.001, using Fisher's exact two-tailed test. (C) The duration of mitosis measured from NEB to anaphase of control and GNA13 knockout clone 2. Control: n=106; GNA13 clone 2: n=105. Error bars represent the SD of three independent experiments. n.s., p>0.05 using two-tailed Student's t-test. (D) Percentage of anaphases with the indicated number of segregation errors (LCs and CBs only) per anaphase in control and GNA13 knockout clone 2 cells. Control: n=104; GNA13 clone 2: n=103. Error bars represent the SD from three independent experiments. ****p<0.001, using

errors, compared to 56.2±13.2% of anaphases in control cells (mean±SD; Fig. 14A-B). This increase in segregation error rate was not accompanied by any change in the duration of mitosis, as measured from NEB to anaphase, with both completing mitosis in 54 minutes (Fig. 14C). Strikingly, GNA13 not only increased the total number of anaphases with segregation errors, but also increased the severity as measured by the number of errors per anaphase (LCs and CBs only), approximately halving the number of error-free anaphases and more than doubling the number of anaphases with more than one error (Fig. 14D).

Observing an increase in anaphase chromosome segregation error rate in GNA13 knockout cells was fascinating, but the increase has only observed in one clone thus far. We reasoned that if GNA13 knockout does increase anaphase chromosome segregation error rate, then the same phenotype should be observed in clone 1. Cells were grown on glass coverslips, arrested in a monopolar prometaphase-like state with the Eg5 inhibitor STLC (Skoufias et al., 2006) for 4 hours. STLC was washed out, and after 2 hours, cells were fixed, and the DNA was stained with DAPI. DNA staining overcame the problem of clone 1 lacking H2B-eGFP. The same phenotype was observed: GNA13 knockout clone 1 had an average of 64.0±5.9% of anaphases with segregation errors, a drastic increase compared to the 44.2±7.3 of WT cells (mean±SD; Fig. 15A-B). Consistent with clone 2, there was also a significant increase in the number of segregation

errors per anaphase. There were far fewer cells with error-free anaphases, a comparable number with 1 error per anaphase, and far more with >1 error per anaphase (Fig. 15C). This pattern is consistent with the previous result. These results confirm the phenotype observed in clone 2, and suggest that GNA13 knockout not only increases anaphase chromosome segregation error rate globally, but also the severity of anaphase chromosome segregation errors in U2OS cells.

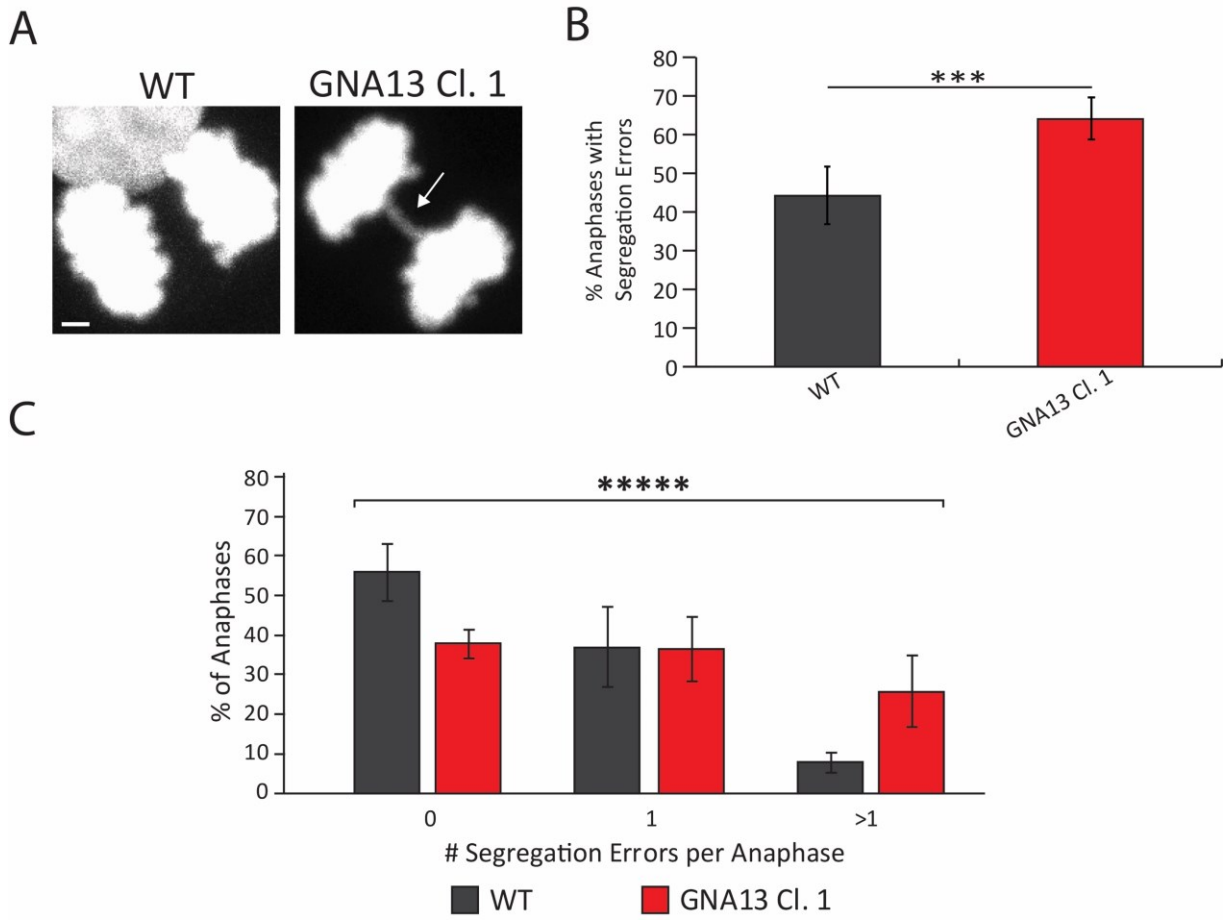

Figure 15. U2OS GNA13 knockout clone 1 exhibits increased anaphase chromosome segregation error rate. (A) Representative images of WT and GNA13 knockout clone 1. Cells were treated with STLC for 4 hours to arrest at prometaphase. STLC was removed, and after 2 hours, cells were fixed, and DNA stained with DAPI. Arrow indicates a chromosome bridge. Scale bar=2μm. (B) Percentage of anaphases with segregation errors (all errors) in WT and GNA13 knockout clone 1. WT: n=152 anaphases; GNA13 clone 1: n=150 anaphases. Error bars represent the SD of three independent experiments. ***p<0.005, using Fisher's exact two-tailed test. (C) Percentage of anaphases with the indicated number of segregation errors (LCs and CBs only) per anaphase in WT and GNA13 knockout clone 1. WT: n=152 anaphases; GNA13 clone 1: n=148 anaphases. Error bars represent the SD of three independent experiments. *****p<0.0001 , using Fisher's exact two-tailed test (Cardillo, 2007).

3.5 UMK57 does not reduce chromosome segregation error rates in GNA13 knockout U2OS cells

GNA13 knockout increasing anaphase chromosome segregation error rate in U2OS cells was a novel and unanticipated observation. Next, we wanted to determine if this increase could be reduced. We have previously reported UMK57, a KIF2C agonist that partially rescues CIN in chromosomally unstable cell lines (Orr et al., 2016). We hypothesized that if GNA13 knockout increases anaphase chromosome segregation error rate in a KIF2C dependant mechanism, then we should observe a decrease by treating cells with UMK57. WT cells were used out of convenience, as many control cells had lost the expression of H2B-eGFP with time. Cells were treated with DMSO or 150nM UMK57 and immediately imaged overnight. WT cells experienced a significant decrease in the percentage of anaphases with segregation errors when treated with UMK57, decreasing from 45.8±2.4% to 36.7±4.6% (mean±SD, Fig. 16A-B). However, this was not observed in GNA13 knockout clone 2, with 60.8±3.9% of DMSO-treated and 67.7±15.6% of UMK57-treated cells experiencing segregation errors (mean±SD, Fig. 16A-B). Additionally, the difference between DMSO treated WT and GNA13 knockout cells remained significant (Fig. 16A), consistent with prior experiments. UMK57 treatment had no effect on the mitotic progression of both lines (Fig. 16C). There was a minor but insignificant decrease in the number of errors per anaphase between DMSO and UMK57 treated WT cells ($p=0.069$), but no change in between DMSO and UMK57 treated GNA13 knockout cells (Fig. 16D). An immunoblot was performed to verify that these results are not due to the absence of KIF2C. The immunoblot revealed that KIF2C is expressed in both U2OS WT and GNA13 knockout clone 2. Control and GNA13 clone 1 were also included and express KIF2C (Fig. 16E). These results suggest that the observed increase in anaphase chromosome segregation error rate in U2OS GNA13 knockout cells likely occurs via a KIF2C independent mechanism.

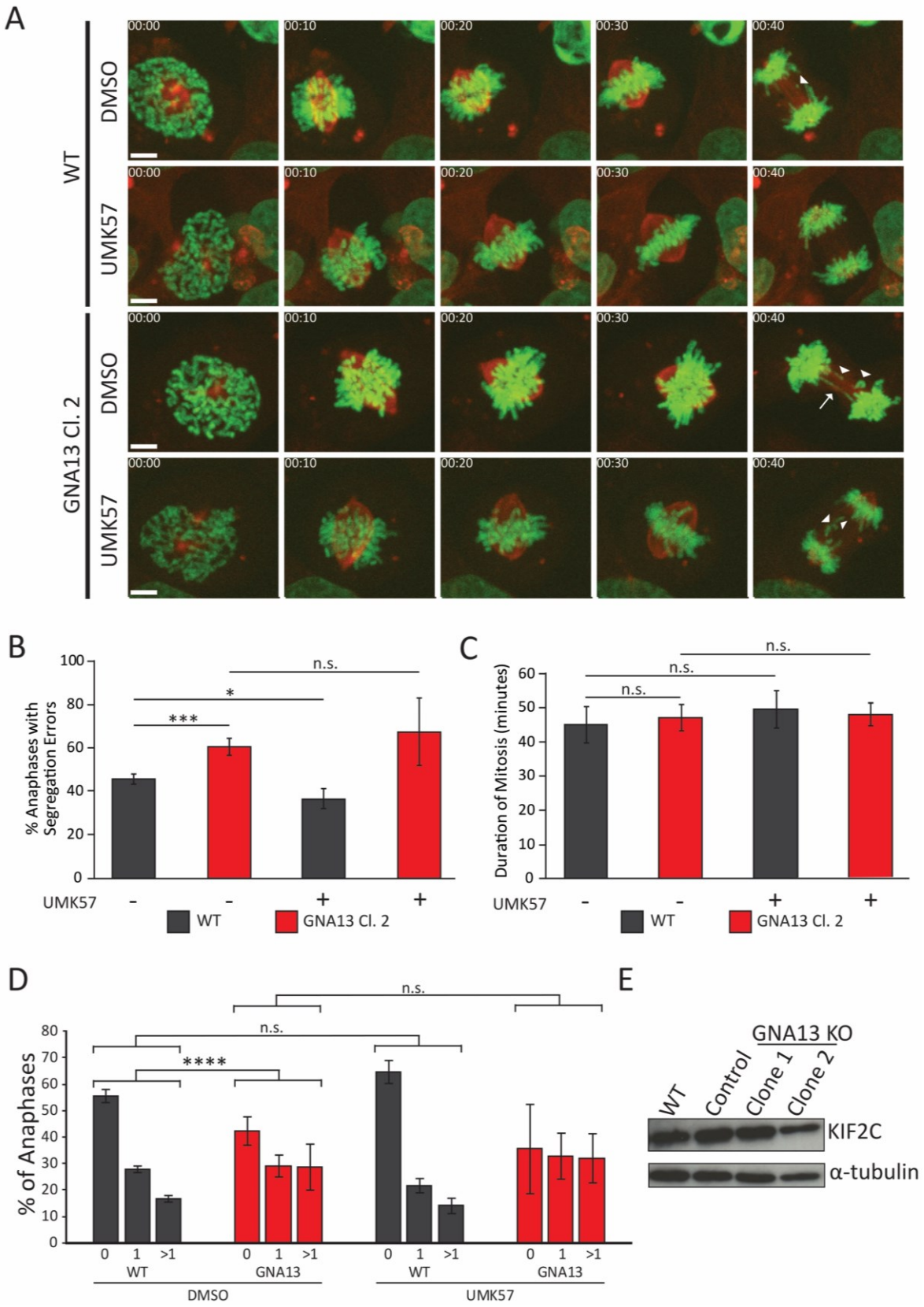
A
WT
GNA13 Cl. 2
DMSO
UMK57
00:00
00:10
00:20
00:30
00:40
B
% Anaphases with Segregation Errors
n.s.
*
***
UMK57
WT
GNA13 Cl. 2
C
Duration of Mitosis (minutes)
n.s.
D
% of Anaphases
****
0
1
>1
WT
GNA13
DMSO
UMK57
E
GNA13 KO
WT
Control
Clone 1
Clone 2
KIF2C
α-tubulin

Figure 16. GNA13 knockout-induced anaphase chromosome segregation errors are not rescued by UMK57. (A) Representative images illustrating the different stages of mitosis of WT and GNA13 knockout clone 2 U2OS cells stably expressing H2B-eGFP (green) and α-tubulin-RFP (red) after treatment with DMSO or UMK57. Time is hours:minutes. Arrowheads indicate lagging chromosomes, and the arrow indicates a chromosome bridge. Scale bar = 5μm. (B) Percentage of anaphases with segregation errors (all errors) in WT and GNA13 knockout clone 2 after treatment with DMSO or UMK57. WT DMSO: n=312 anaphases; WT UMK57: n=345 anaphases; GNA13 clone 2 DMSO: n=303 anaphases; GNA13 clone 2 UMK57: n=214 anaphases. Error bars represent the SD of three independent experiments. n.s., $p>0.05$; *$p<0.05$; ***$p<0.005$ using Fisher's exact two-tailed test. (C) Duration of mitosis from NEB to anaphase of WT and GNA13 knockout clone 2 after treatment with DMSO or UMK57. WT DMSO: n=304 mitoses; WT UMK57: n=329 mitoses; GNA13 clone 2 DMSO: n=293 mitoses; GNA13 clone 2 UMK57: n=201 mitoses. Error bars represent the SD of three independent experiments. n.s., $p>0.05$ using Student's two-tailed t-test. (D) Percentage of anaphases with the indicated number of segregation errors (LCs and CBs only) per anaphase in WT and GNA13 knockout clone 2 treated with DMSO or UMK57. WT DMSO: n=306 anaphases; WT UMK57: n=341 anaphases; GNA13 clone 2 DMSO: n=297 anaphases; GNA13 clone 2 UMK57: n=207 anaphases. Error bars represent the SD of three independent experiments. n.s., $p>0.05$ ****$p<0.001$, using Fisher's exact two-tailed test (Cardillo, 2007). (E) Immunoblot of U2OS WT, control, and GNA13 knockout clones for KIF2C. α-tubulin used as the loading control.

3.6 GNA13 knockout increases anaphase chromosome segregation error rate in RPE1 cells

While the observed increase in anaphase chromosome segregation error rate is interesting, it was observed in a chromosomally unstable, transformed cell line. Next, we wanted to know if this phenotype is unique to that context. RPE1 cells are immortalized non-transformed, diploid, and chromosomally stable cells also ideal for microscopy. We hypothesized that if GNA13 knockout increases anaphase chromosome segregation error rate in U2OS cells, it will do the same in RPE1 cells. Three clones validated by TIDE analysis were verified by immunoblot to be complete GNA13 knockouts (Fig. 17A-B). Since GNA13 is involved in proliferation, and GNA13 knockout slowed proliferation in U2OS cells (Fig. 13D), we hypothesized that GNA13 knockout in RPE1 cells will have the same effect. The alamarBlue® viability assay was again used to measure

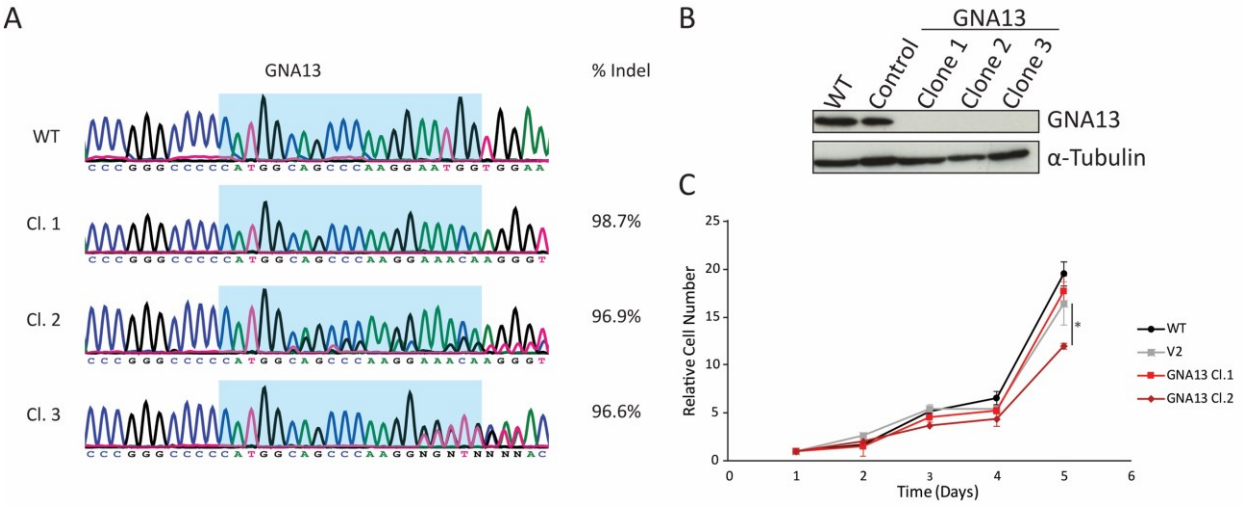

Figure 17. Validation of GNA13 knockout in RPE1 cells. (A) Chromatograms of RPE1 lines. Genomic DNA was purified from the indicated RPE1 line, the targeted exon amplified by PCR, and sequenced by Sanger sequencing. Knockout efficiency was measured as the percent of indel formation against the respective WT sequence using TIDE analysis. The highlighted region indicates the 20-nucleotide sequence recognized by the sgRNA. (B) Immunoblot of RPE1 WT, control, and GNA13 knockout clones 1-3. α-tubulin was used as the loading control. (C) Growth rate assay of RPE1 WT, control, and GNA13 knockout clones 1 and 2. Results plotted as cell number relative to day 1. Graph shows mean$\pm$SEM of three independent experiments. n.s., $p>0.05$; *$p<0.05$, using Student's t-test.

the proliferation of WT and control cells, and the knockout clones imaged: clones 1 and 2. Clone 1 demonstrated proliferation comparable to both WT and control cells, while clone 2 proliferates at a significantly slower rate (Fig. 17C). While the effect of GNA13 knockout was inconsistent between clones, they were nonetheless validated to be complete knockout.

With the clones validated, we sought to confirm the phenotype previously observed in U2OS cells. By using RPE1 cells stably expressing H2B-eGFP and a-tubulin-RFP, it was possible to observe the effect of GNA13 knockout on mitosis via confocal time-lapse microscopy. Only clones 1 and 2 were imaged because clone 3 does not express either H2B-eGFP or a-tubulin-RFP. GNA13 knockout drastically increased the percentage of anaphases with segregation errors compared to the control. Control cells had 3.6±0.2% of anaphases with segregation errors compared to 7.2±0.7% for GNA13 clone 2 (mean±SD). Clone 1 was even more striking as the error rate was

more than double that of control cells, with 9.0±0.6% of anaphases experiencing segregation errors (Fig. 18A-B). Consistent with U2OS cells, GNA13 knockout had no significant impact on mitotic progression in RPE1 cells, with all three lines completing mitosis within 35-40 minutes (Fig. 18A, C). These results demonstrate GNA13 knockout-induced anaphase chromosome segregation error rate is not unique to transformed, chromosomally unstable cell lines.

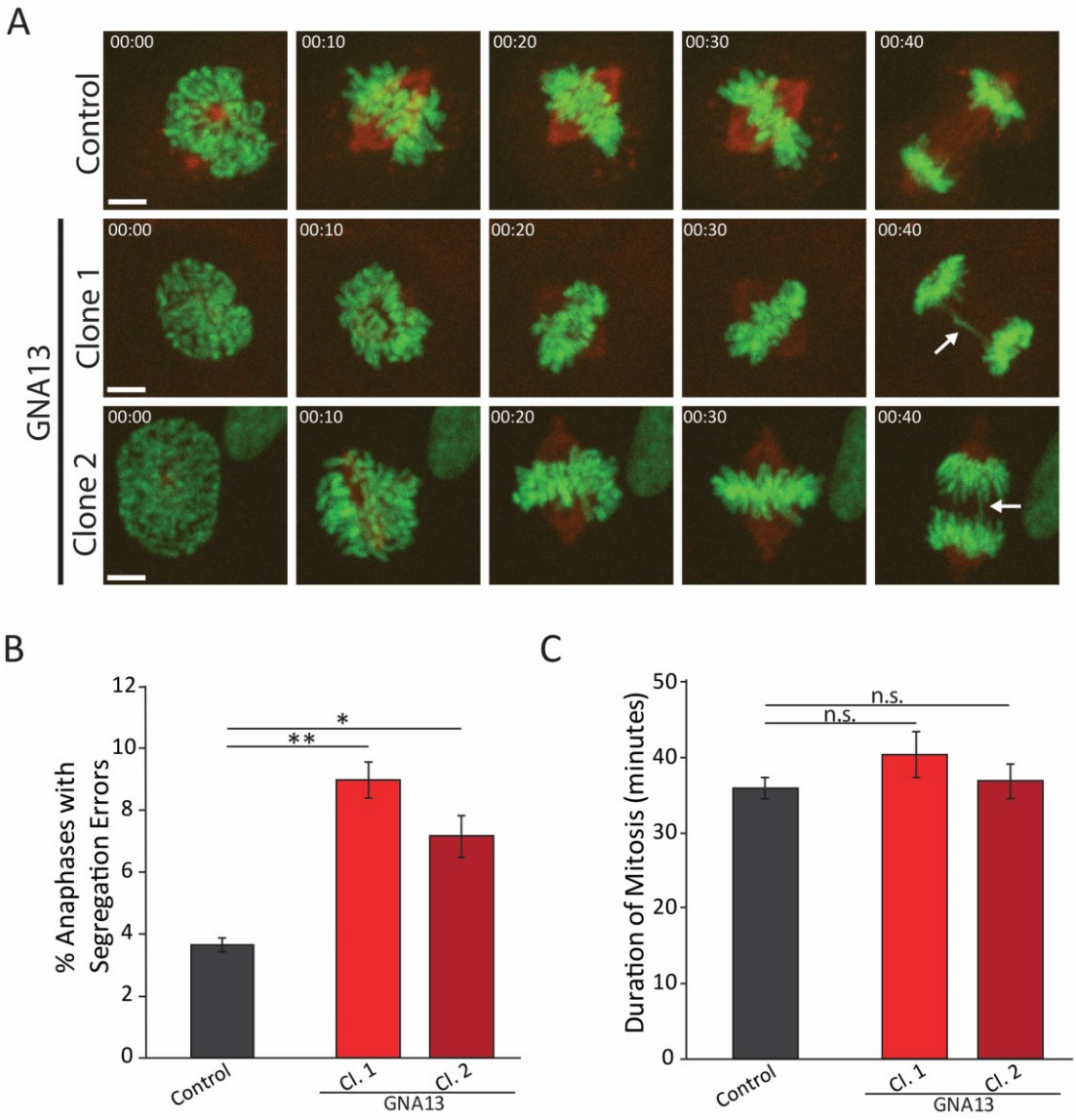

Figure 18. GNA13 knockout exacerbates CIN in the chromosomally stable RPE1 cells. (A) Representative images illustrating the different stages of mitosis of control and GNA13 knockout RPE1 cells stably expressing H2B-eGFP (green) and α-tubulin-RFP (red). Time is hours:minutes. Arrow indicates a chromosome bridge. Scale bar = 5μm. (B) Percentage of anaphases with segregation errors in control and GNA13 knockout clones 1 and 2. Mean values $\pm$ SD of three independent experiments. Control: n=356 anaphases; GNA13 clone 1: n=219 anaphases; GNA13 clone 2: n=328 anaphase. *p<0.05; **p<0.01 using Fisher's exact two-tailed test. (C) Duration of mitosis from NEB to anaphase of control and GNA13 knockout clones 1 and 2. Mean values $\pm$ SD of three independent experiments. Control: n=350 mitoses; GNA13 clone 1: n=209 mitoses; GNA13 clone 2: n=306 mitoses. n.s., p>0.05 using Student's two-tailed t-test.

Chapter 4 – Discussion

4.1 Validation of synthetic lethal hits in NALM6 and U2OS Cells

Several hits from the chemogenomic screen were successfully validated with docetaxel and vincristine using clonal knockout lines and the alamarBlue® viability assay. A hit was considered validated if the decrease in IC_{50} was statistically significant for hits with one clone. Hits with three knockout clones tested were considered validated if: (i) 2/3 clones exhibited a significant decrease in IC_{50} compared to control cells, and (ii) the overall average IC_{50} of the three clones is significantly lower than that of control cells. Satisfying these conditions in NALM6 cells are GNA13, SEPHS1, and DLGAP5 with docetaxel, and QRICH1 and DLGAP5 with vincristine (Fig. 10).

Likewise, a hit was considered validated in U2OS cells if the decrease in IC_{50} was statistically significant for hits with one clone. For those with two clones, a hit was considered validated if both exhibited a significant decrease in IC_{50}. However, none of the clones satisfied these conditions. Although DLGAP5 knockout does sensitize the cell to docetaxel treatment as the average of the two clones approached significance, only one of the two clones exhibited a significant change in sensitivity (Fig. 12E). Therefore, we can deduce that DLGAP5 knockout is likely synthetic lethal with docetaxel in U2OS cells as well, but this cannot be concluded confidently from these data. Supporting the results obtained for DLGAP5 in both NALM6 and U2OS cells, DLGAP5 knockdown is reported to be synthetic lethal with docetaxel in androgen-sensitive prostate cancer cells (Hewit et al., 2018). This demonstrates that the methodology used is robust.

More hits are likely synthetic lethal than what the results suggest but were not validated for a few possible reasons. Some hits did exhibit increased sensitivity towards MTAs that approached significance, and likely would have reached significance if more replicates were

performed. For example, in NALM6 cells, QRICH1 knockout increased the sensitivity to docetaxel 1.56-fold (p=0.06), and TACC3 knockout increased the sensitivity towards vincristine 1.54-fold (p=0.08).

Another possible explanation as to why some hits were not validated, and why there are differences in MTA response between clones, is that some clones are knockout at the genomic level but may still express a functional gene product. Knockout efficiency measured by TIDE analysis does not guarantee complete knockout of the target because cells can overcome Cas9-induced frameshift mutations. There are several mechanisms by which this may occur. For example, by generating an in-frame indel that produces a still-functional protein, or by in-frame skipping of the edited exon to produce a partially functional protein. This is known as knockout evasion and it is actually a fairly common phenomenon (Makino et al., 2016; Smits et al., 2019). For example, several NALM6 GNA13 knockout clones were confirmed by TIDE analysis, but some still expressed protein, albeit at decreased levels (Fig. S1A). This offers one possibility as to why, for example, SEPHS1 clone 1 exhibited little change in sensitivity towards docetaxel and vincristine in NALM6 cells. This was also observed in U2OS cells. U2OS cells have four copies of GNA13. A third GNA13 knockout clone validated by TIDE analysis to have a knockout efficiency similar to clone 2 (≈85%) had four unique indels, suggesting each copy of GNA13 was mutated, but it still expressed GNA13 (Fig. S1B). Additionally, the U2OS TACC3 clone is likely not a complete knockout, simply because it contains one unedited copy of the gene. TIDE estimated a knockout efficiency of ≈75% and identified three indels. This indicates 3 out of 4 copies contain indels, but U2OS cells are supposed to have only two copies of TACC3 (Bruhn et al., 2014). There are two possibilities as to why this is. First, this line may be a population of two clones, one of which is heterozygous for TACC3. For this to be true, both clones must proliferate at near-identical rates because TIDE analysis revealed a knockout efficiency per indel of ≈25%, suggesting they are present in approximately equal proportions. This is unlikely as TACC3 knockdown impedes proliferation (Guo & Liu, 2018). A more likely explanation is the acquisition of two additional copies of TACC3, only one of which was edited by Cas9. This is possible because U2OS cells are chromosomally unstable. Therefore, a 1.48-fold increase in sensitivity towards docetaxel for a

knockout line that is likely not a complete knockout is quite drastic.

Another possibility is the presence of genetic differences between clones. Clonal cell lines are powerful tools in elucidating gene function and gene-drug relationships. However, clonal lines are generated from diverse populations, and one limitation of working with clones is heterogeneity between them. Therefore, by utilizing multiple unique clones when possible to validate hits, the likelihood that the observed phenotype is an artifact of clonal selection is reduced (Giuliano et al., 2018; A. Lin et al., 2017). This offers another explanation as to why variation in MTA response was observed between clones. GNA13 knockout was synthetic lethal with docetaxel in NALM6 cells, and all three clones were verified by immunoblot (Fig. 12A); however, clone 2 exhibited little change in sensitivity towards docetaxel compared to clones 1 and 3 (Fig, 10E, Table 1). SEPHS1 knockout was also synthetic lethal with docetaxel in NALM6 cells, but only two of the three clones demonstrated a statistically significant increase in sensitivity. Clone 1 demonstrated a minor change in sensitivity towards docetaxel. Interestingly, the same clone also demonstrated very little change in sensitivity towards vincristine, suggesting that this clone may have some aberration conferring resistance to MTAs (Fig. 10F, K, Table 1).

Interestingly, SEPHS1 was validated with docetaxel in NALM6 cells, but not U2OS cells (Fig. 10F, 12B). Assuming the clone is a complete knockout, then another explanation as to why this is the case is SEPHS1 exerts cell type dependant functions. U2OS cells were chosen because they are another cancer cell line that is amenable to microscopy experiments; however, osteosarcoma is not the same as acute lymphoblastic leukemia. Therefore, we could reason that other leukemic cell lines harboring SEPHS1 LOF mutations would likely be more sensitive to docetaxel, but not necessarily all adherent cell lines.

GNA13 emerged as a hit with both docetaxel and vincristine in the screen; however, it was only validated with docetaxel (Fig. 10E, J). GNA13 knockout may be synthetic lethal with vincristine in NALM6 cells, but to a much lesser extent than docetaxel. This would explain why it emerged as a hit in the screen but exhibited only minor increases in sensitivity here (Table 1). Of

the two replicates performed with docetaxel in the screen, GNA13 ranked #1 and #2, respectively, compared to ranking #62 with vincristine. As a comparison, DLGAP5 ranked #25 and #119 with docetaxel, and #5 with vincristine. Consistent with the screen, GNA13 knockout NALM6 cells were more sensitive to docetaxel than vincristine, and DLGAP5 knockout NALM6 cells were more sensitive to vincristine than GNA13 knockout cells. However, our results suggest that DLGAP5 knockout NALM6 cells are more sensitive to docetaxel than vincristine, and that they are more sensitive to docetaxel than GNA13 knockout NALM6 cells. Rather than providing a concrete ranking for each synthetic lethal combination, the screen simply identifies synthetic lethal hits that must be validated using additional methods.

Mutations in QRICH1, DLGAP5, GNA13, and SEPHS1 are found in various cancers (Lawrence et al., 2014). These results offer potential therapeutic strategies by treating cancers harboring mutations within these genes with lower doses of MTAs, reducing side effects associated with MTA use. Additionally, SEPHS1 is an enzyme, and therefore, "druggable." By developing SEPHS1 inhibitors, it would also be possible to treat cancers overexpressing SEPHS1 in combination with docetaxel. The most interesting among these genes is GNA13, which is frequently mutated in specific subsets of aggressive lymphomas.

4.2 GNA13 and germinal center lymphomas

The goal of the project was to validate hits from a genetic synthetic lethal screen, which could then be exploited to treat cancer using lower doses of MTAs. Synthetic lethality was not observed with vincristine in GNA13 knockout in NALM6 cells but was observed with docetaxel (Fig. 10J E). This result is interesting for two reasons. First, GNA13 is heavily implicated in GC DLBCL and Burkitt lymphoma, two aggressive subtypes of non-Hodgkin's lymphoma. GNA13 LOF mutations are found in 15-30% of GC DLBCL and Burkitt lymphoma cases, making it one of the most commonly mutated genes (Lawrence et al., 2014; Lohr et al., 2012; Love et al., 2012; J. Zhang et al., 2013). DLBCL accounts for 28% of all lymphomas, while Burkitt lymphoma accounts for less than 5% of all cases and is more common in children (30% of cases) than adults (<1% of

cases) (Kalisz et al., 2019). Secondly, the standard treatment regimen for GC DLBCL and Burkitt lymphoma uses vincristine (in combination with rituximab, cyclophosphamide, doxorubicin, and prednisone; R-CHOP). However, R-CHOP is only effective in about 50% of DLBCL and adult Burkitt lymphoma cases (Graham B.S., 2020; Jacobson & Lacasce, 2017; Linch, 2012; Lyon-sud & Lyon, 2016; Zayac & Olszewski, 2020). This raises the possibility of exploiting naturally occurring mutations within a unique subset of patients not by decreasing MTA dose, but by making treatment more effective by swapping the MTA used.

Clinical trials exploring the use of paclitaxel and docetaxel in patients with non-Hodgkin's lymphoma who have either not or only partially responded to initial treatment or have relapsed, has yielded some success, with 25-69% of patients responding positively to treatment. However, non-Hodgkin's lymphoma is a very heterogeneous disease (Armitage et al., 2017), and the majority of these studies did not distinguish between lymphoma subtypes. One study did distinguish DLBCL cases from others, but did not distinguish between germinal or non-germinal center origin. Most importantly, none of the studies specified if patients with Burkitt lymphoma were included. However, it is possible none, or extremely few, were included because adult cases are rare (Nieto et al., 2005; Rizzieri et al., 2004; Westin et al., 2014; Younes et al., 1995, 1997; Zayac & Olszewski, 2020; Zekri et al., 2003). These trials demonstrate that taxane use to treat non-Hodgkin's lymphoma is possible and is worth exploring in greater detail.

Although there is potential to exploit naturally occurring GNA13 mutations in these lymphomas, the results obtained in NALM6 cells must be validated in the appropriate cell lines. NALM6 is not a germinal center lymphoma cell line, but still of B cell origin. Therefore, we hypothesize that GNA13 knockout would elicit a more considerable increase in sensitivity towards docetaxel than vincristine in GC DLBCL and Burkitt lymphoma GNA13 knockout cell lines. The advantage of probing this hypothesis in these types of lymphomas is that not only can GNA13 knockout cell lines be generated, but cell lines already harboring LOF mutations (e.g., Raji) can be rescued with WT GNA13 and assayed as well. If docetaxel does prove to be more effective than vincristine, it may eventually lead to a more effective first line treatment for a subset of

patients with germinal center lymphomas for which present therapy is often ineffective.

4.3 GNA13 knockout impedes proliferation in a cell context dependant manner

Although all GNA13 knockout clones were validated by immunoblot, we wanted to validate the knockout another way. The role of GNA13 on proliferation is well documented in solid cancers, and to a lesser extent, hematological cancers. In solid cancers, GNA13 acts as an oncogene, and upregulation promotes proliferation (Worzfeld et al., 2008; Jia Xing Zhang et al., 2016; Z. Zhang et al., 2018). This suggested that proliferation rate could be used as another measure of GNA13 knockout. Consistent with the literature, GNA13 knockout did markedly impede proliferation in U2OS cells, albeit to slightly different degrees. Clone 1 did proliferate more slowly, but only clone 2 proliferated significantly slower than control cells (Fig. 13D). The difference between control and clone 1 would likely have been significant if the assay was performed over a more extended period. Although increasing CIN can negatively affect proliferation (Godek et al., 2016), we can rule out that possibility in this context because aneuploid cell lines are adapted to proliferating in an aneuploid state and can proliferate even if CIN is exacerbated (Thompson & Compton, 2008).

Although RPE1 cells are non-transformed, we still expected GNA13 knockout to impede proliferation. However, the results were inconsistent between the two clones assayed. Clone 1 proliferated at a comparable rate to both WT and control cells, while clone 2 exhibited a significant decrease (Fig. 17C). There is the possibility GNA13 knockout has no effect on proliferation in RPE1 cells, but clone 1 has gained a pro-proliferative karyotype because of chromosome missegregation. However, the opposite may also be true; GNA13 has no effect on proliferation in RPE1 cells, but clone 2 is aneuploid and therefore bears a growth penalty or a disadvantageous karyotype. This result alone does not suggest that measuring the growth rate to validate GNA13 knockout in RPE1 cells was inappropriate, but rather, variation exists between the clones, and that the third clone should be assayed to confirm whether GNA13 knockout

impedes proliferation or not.

Opposite to its oncogenic role in solid cancers, GNA13 acts as a tumor suppressor in germinal center lymphomas, and LOF mutations promote germinal center B cell proliferation (Healy et al., 2016; Muppidi et al., 2014). Therefore, we hypothesized that GNA13 knockout would increase proliferation. However, GNA13 knockout did not affect proliferation in NALM6 cells (Fig. 13B). GNA13 knockout may only elicit its pro-proliferative effect on transformed B cells *in vivo*. Expression of WT GNA13 in Raji cells, a Burkitt lymphoma cell line containing LOF mutations in GNA13, did not affect proliferation *in vitro*, but did significantly impair proliferation in mouse xenograft models (O'Hayre et al., 2016). It has also been suggested that GNA13 knockout alone does not promote B cell proliferation. In mouse models, Healy and colleagues reported that the proportion of germinal center B cells from spleens of GNA13 knockout mice were significantly larger than those of GNA13 WT mice. Rather than promote proliferation of germinal center B cells, they suggest that GNA13 knockout inhibits affinity selection-mediated apoptosis, as germinal center B cells from GNA13 knockout mice have lower levels apoptotic marker active caspase-3. They also observed lower levels of the proliferation marker Ki67 in germinal center B cells of lymph nodes (Healy et al., 2016). Therefore, the role of GNA13 in B cell proliferation may be more complex than solid cancers, and using proliferation as a method of validating GNA13 knockout in NALM6 cells was ultimately inappropriate. These results suggest that GNA13 not only exerts context-dependent functions on proliferation between solid and hematological cancers, but that its effect on the proliferation of B cells is not straightforward.

This underlines one major caveat to using proliferation as method to validate gene knockout: proliferation is influenced by many factors. So, while using proliferation as a readout to validate GNA13 knockout in solid cancer cell lines can be done more confidently than hematopoietic cancers because it has been better documented, it still does not guarantee GNA13 knockout will impede proliferation in all solid cancer cell lines and exceptions have been reported (S. A. Rasheed et al., 2015; Xu et al., 2016). Therefore, measuring something downstream of GNA13 that is influenced by fewer other factors and that is more direct would be an optimal

method to validate GNA13 knockout, such as RhoA. A common method to measure RhoA activation is the glutathione S-transferase-Rhotekin-Rho binding domain (GST-Rhotekin-RBD) pulldown assay. Rhotekin binds RhoA-GTP only, which is used as a readout for activation of upstream mediators of RhoA, such as GNA13 (O'Hayre et al., 2016; Tan et al., 2006). This assay provides a more consistent readout between different cell lines because GNA13-RhoA signaling is well documented across many cell types, as opposed to the cell-type specific role of GNA13 on proliferation.

4.4 GNA13 knockout increases anaphase chromosome segregation error rate in U2OS and RPE1 cells

U2OS cells are a chromosomally unstable cell line ideal for microscopy. Upon imaging U2OS GNA13 knockout cells we observed an increase in anaphase chromosome segregation errors, which was unexpected and intriguing. Both U2OS GNA13 knockout clones demonstrated significantly higher rates of segregation errors, as well as an increase in the number of segregation errors per anaphase, compared to either WT or control cells (Fig. 14, 15). GNA13 knockout-induced segregation errors was not unique to U2OS cells and was observed in the chromosomally stable RPE1 cell line. GNA13 knockout approximately doubled the percentage of anaphases with segregation errors compared to control cells (Fig. 18B). Additionally, GNA13 knockout had minimal effect on mitotic duration in both U2OS and RPE1 cells (Fig. 14C, 18C). CIN is associated with a weakened SAC (Swanton et al., 2006), but RPE1 cells have a robust SAC. This suggests that either the SAC is not activated, or that it is surpassed entirely. It is unlikely that this phenotype is an artifact of clonal selection because it was observed in four clones between two cell lines. However, to be certain that the phenotype observed is truly a result of GNA13 knockout, rescue experiments should be performed by expressing GNA13 cDNA containing silent mutations in the sgRNA binding sequence and the PAM. Overall, these results strongly suggest GNA13 knockout impairs chromosome segregation and does not require pre-existing CIN or cellular transformation as prerequisites.

While it is commonplace to use anaphase segregation errors as a readout for CIN, there is one caveat to doing this: it does not necessarily represent actual missegregation events. It is likely that an increase in CIN, as measured by anaphase segregation error rate, also results in an increase in actual chromosome missegregation events and aneuploidy, but this is not guaranteed. It is possible the role GNA13 plays in chromosome segregation is subtle, and therefore impairs chromosome segregation without increasing nondisjunction. It is very tempting to suggest there is an increase in CIN simply because GNA13 knockout increases anaphase chromosome segregation error rate, but this suggestion is premature. Therefore, additional methods, such as fluorescence *in situ* hybridization (FISH) or karyotyping, are required to determine not only if GNA13 knockout does truly increase CIN, but also to what extent it does so (Nicholson & Cimini, 2013; Selvarajah et al., 2006; Thompson & Compton, 2011).

Treatment with the KIF2C agonist UMK57 (Orr et al., 2016) decreased the segregation error rate in WT, but not GNA13 knockout U2OS cells (Fig. 16A). Immunoblot revealed that KIF2C is expressed in all U2OS cell lines, although expression appears slightly lower in clone 2 (Fig. 16D). It is unlikely that this is the cause of increased anaphase segregation error rate in GNA13 knockout U2OS cells because UMK57-treated and DMSO-treated cells had comparable rates (Fig. 16A). However, aurora B expression should be verified, as high levels of aurora B hyper-stabilizes k-MT attachments (Orr et al., 2016). Although GNA13 knockout has not been reported to alter Aurora B expression in other contexts (Nakano et al., 2019; Teo et al., 2016), it should be verified in U2OS cells because GNA13-mediated processes are highly dependent on cellular context (Suzuki et al., 2009). This does suggest, however, that GNA13 knockout-induced anaphase chromosome segregation errors may occur in a KIC2C independent mechanism.

GNA13 transmits extracellular signals from many different GPCRs through a number of different pathways. The most well-studied pathway is the GNA13-GEF-RhoA pathway. GEFs promote RhoA GDP exchange for GTP upon GNA13 activation. However, one challenge of studying GNA13-mediatied signaling is the significant overlap with GNA12-mediated signaling as

they share many downstream effectors, including several GEFs specific for RhoA (Andreeva et al., 2007; Kelly et al., 2007; Suzuki et al., 2009). However, this overlap can be exploited to narrow down which downstream effectors are involved in chromosome segregation by repeating the same experiments with GNA12 knockouts. If GNA12 knockout U2OS or RPE1 cells also exhibit an increase in anaphase segregation errors, then the downstream effectors are common to both GNA12 and GNA13; if not, then the effector is unique to GNA13, and the pool of possible GNA13 effectors is drastically narrowed. This is plausible because some proteins downstream of GNA12/13 and RhoA have already been implicated in mitosis.

Bakal and colleagues reported the GEF-H1 animal homologue, Lfc, is required for correct chromosome segregation in Rat-2 cells, as Rat-2 cells injected with anti-Lfc antibodies were prone to chromosome segregation errors at anaphase. This occurred via RhoA and the formin mDia1 (also known as diaphanous homolog 1, DIAPH1) (Bakal et al., 2005). In mammals, there exists three diaphanous formins: mDia1 is activated specifically by RhoA, while mDia2 (also known as DIAPH2) and mDia3 (also known as DIAPH3) are activated by RhoA, Rac1, and Cdc42 (Lammers et al., 2008). mDia2 knockdown appeared to increase the severity of anaphase segregation errors in HT29 cells (Grueb et al., 2019). mDia3 knockdown has also been reported to impair chromosome segregation in HeLa and NIH 3T3 cells, although the authors suggest this occurs via a Cdc42-dependant mechanism (Yasuda et al., 2004). Therefore, the three diaphanous formins are the most tempting suspects downstream of GNA13, particularly mDia1 and mDia2.

There are a few experiments that can be done to validate a possible GNA13-RhoA-mDia1/2/3/ pathway. It is easy to suggest that expressing constitutively active mDia1/2/3, which have their Rho-binding and autoinhibitory domains deleted (Otomo et al., 2005), would rescue the phenotype in GNA13 knockout cells. However, expressing constitutively active mDia1 in WT Rat-2 cells, and mDia1 and mDia3 in HeLa and NIH 3T3 cells drastically increased chromosome segregation error rate at anaphase (Bakal et al., 2005; Yasuda et al., 2004). It is unknown if expressing constitutively active mDia2 would yield similar results, but it is plausible. Therefore, this approach may be counterproductive. While RhoA inhibition with C3 exoenzyme is possible,

it produces binucleated cells as a result of cytokinesis failure (Kato et al., 2001). Using RhoA mutants uncoupled from downstream effectors overcomes some of the challenges of exploring this pathway. Expression of RhoA T37Y/C20R, a RhoA mutant uncoupled from all downstream effectors, should increase chromosome segregation error rate in WT and GNA13 knockout cells. RhoA F39A is uncoupled from all effectors except mDia1-3, and RhoA G14V is constitutively active. If RhoA G14V/F39A expression in GNA13 knockout cells improves chromosome segregation error rate, then mDia1/2/3 are likely involved. Finally, expression of WT or constitutively active RhoA in GNA13 knockout cells should decrease chromosome segregation error rate at anaphase in GNA13 knockout cells (Bakal et al., 2005; Sahai et al., 1998). There also exist inhibitors that preferentially bind the FH2 domain of mDia1 and mDia2, but not mDia3, that can be used: small molecule inhibitor of formin homology 2 domains (SMIFH2), and 3-(2-amino-5-bromophenyl)-1H-quinoxalin-2-one (Gauvin et al., 2009; Rizvi et al., 2009). Although they do not distinguish between mDia1 and mDia2, they may be useful in determining if mDia1 or mDia2, rather than mDia3, are involved in GNA13-mediated chromosome segregation in U2OS and RPE1 cells. These results may provide mechanistic insight into a GNA13-RhoA-mDia pathway involved in error-free chromosome segregation.

4.5 Oncogenic potential of GNA13 knockout

Although GNA13 is more commonly found to be upregulated in solid cancers, data from TumorPortal (http://www.tumorportal.org/; Lawrence et al., 2014) and The Cancer Genome Atlas research network (https://www.cancer.gov/tcga) have identified mutations in primary solid tumor samples from a variety of cancer types. CIN is a common feature of cancer that has the potential to produce aneuploidy via chromosome missegregation events. Both CIN and aneuploidy are common features of cancer implicated in drug resistance and tumorigenesis (Ben-David & Amon, 2020; Choma et al., 2001; Dagogo-Jack & Shaw, 2018; Kuukasjärvi et al., 1997; A. J. X. Lee et al., 2011; Sansregret et al., 2018; Swanton et al., 2009). We investigated the role of GNA13 knockout on mitosis and found that GNA13 knockout exacerbates anaphase segregation error rate in both transformed U2OS and non-transformed RPE1 cells (Fig. 14, 15, 18). The latter

was surprising as RPE1 cells are chromosomally stable, with <5% of mitoses exhibiting segregation errors (Fig. 18B) (Thompson & Compton, 2008). This poses interesting questions. Does the increase in anaphase segregation error rate also result in aneuploidy? Could GNA13 knockout cells more easily develop drug resistance, and therefore promote transformation?

The observed increase in segregation errors would suggest that GNA13 knockout U2OS cells should be more sensitive to MTA treatment, which would further exacerbate CIN and produce highly aneuploid daughter cells incapable of surviving (Zasadil et al., 2014). However, U2OS GNA13 knockout clones did not exhibit significantly increased sensitivity towards docetaxel. Clone 2 did exhibit some shift in IC_{50}, but clone 1 exhibited no change. One explanation is that this clone has acquired some sort of resistance to docetaxel via CIN. This is not impossible as U2OS cells are chromosomally unstable, and this clone has already lost the expression of H2B-eGFP. The observed increase in anaphase chromosome segregation errors, as well as the difference in response towards docetaxel in U2OS cells, suggests that GNA13 knockout may induce oncogenic transformation and drug resistance via CIN.

The presence of CIN, as measured by anaphase segregation error rate, does not guarantee aneuploidy. Thompson and Compton reported nocodazole and monastrol (another Eg5 inhibitor) treated RPE1 cells did exhibit increased chromosome missegregation to become aneuploid, but the population did not maintain an aneuploid state. Aneuploidy confers a growth penalty, and reduced proliferative capacity selects against aneuploid cells, and the population converges back to a diploid karyotype (Thompson & Compton, 2008). However, it remains to be determined if the observed increase in anaphase segregation error rate in GNA13 knockout RPE1 cells also results in aneuploidy. This is possible by quantifying chromosome number from chromosome spreads. Coupling this with FISH to identify centromeres and telomeres would also allow for simultaneous identification of any structural abnormalities present, such as telomere fusions and dicentric chromosomes, which are capable of further exacerbating CIN via the break-fusion-break cycle (Janssen et al., 2011; Pampalona et al., 2016) and influencing karyotype evolution (Duesberg et al., 2000). If there is a difference in ploidy, numerically or structurally, compared to

control cells, GNA13 knockout cells can tolerate it because they propagate well in culture. It would also indicate the clonal lines will continue to evolve and become increasingly heterogeneous with time. Although it is possible aneuploid cells are still selected against because it confers a growth penalty, they may be selected for upon introduction of a selective pressure.

It is tempting to speculate that GNA13 knockout RPE1 cells would more easily develop drug resistance via the accumulation of abnormal karyotypes under selective pressure, which would suggest cellular transformation. Work by Duesberg and collogues eloquently demonstrated aneuploid Chinese hamster embryo cells acquired multi-drug resistance, unlike parental cells that did not develop resistant colonies to just single drug treatment (Duesberg et al., 2000). It would be interesting to explore if GNA13 knockout does produce drug-resistant clones under drug treatment, and ultimately influence cellular transformation of RPE1 cells. Testing this hypothesis could be done, not just with MTAs, but with several cancer drugs with different mechanisms of action to determine if multi-drug resistance arises, or if vulnerability to specific drugs arise. This would uncover a novel role for GNA13 in tumorigenesis via the induction of CIN.

To summarize, these results offer potential anticancer therapeutic strategies, namely, the treatment of cancers presenting mutations in QRICH1, DLGAP5, GNA13, and SEPHS1 with lower doses of MTAs. GNA13 is frequently mutated in germinal center lymphomas, and these results propose exploring the use of docetaxel, rather than vincristine, as a more effective treatment. These results also demonstrate that GNA13 knockout exacerbates anaphase chromosome segregation error rate in U2OS and RPE1 cells and may be involved in cancerous transformation.

Permissions

Figure	License Number	Source Publication	DOI
Figure 1	4807680711420	(Walczak et al., 2010)	10.1038/nrm2832
Figure 2	4807700592819	(Conde & Cáceres, 2009)	10.1038/nrn2631
Figure 4	4807670177482	(Funk et al., 2016)	10.1016/j.devcel.2016.10.023
Figure 6	4805220853376	(Mary Ann Jordan & Wilson, 2004)	10.1038/nrc1317

References

Agrotis, A., & Ketteler, R. (2015). A new age in functional genomics using CRISPR/Cas9 in arrayed library screening. *Frontiers in Genetics*, *6*, 300. https://doi.org/10.3389/fgene.2015.00300

Aguirre, A. J., Meyers, R. M., Weir, B. A., Vazquez, F., Zhang, C. Z., Ben-David, U., Cook, A., Ha, G., Harrington, W. F., Doshi, M. B., Kost-Alimova, M., Gill, S., Xu, H., Ali, L. D., Jiang, G., Pantel, S., Lee, Y., Goodale, A., Cherniack, A. D., … Hahn, W. C. (2016). Genomic copy number dictates a gene-independent cell response to CRISPR/Cas9 targeting. *Cancer Discovery*, *6*(8), 914–929. https://doi.org/10.1158/2159-8290.CD-16-0154

Akhmanova, A., & Steinmetz, M. O. (2015). Control of microtubule organization and dynamics: Two ends in the limelight. *Nature Reviews Molecular Cell Biology*, *16*(12), 711–726. https://doi.org/10.1038/nrm4084

Alsina, B., Serras, F., Baguñà, J., & Corominas, M. (1998). patufet, the gene encoding the Drosophila melanogaster homologue of selenophosphate synthetase, is involved in imaginal disc morphogenesis. *Molecular and General Genetics*, *257*(2), 113–123. https://doi.org/10.1007/s004380050630

Alushin, G. M., Lander, G. C., Kellogg, E. H., Zhang, R., Baker, D., & Nogales, E. (2014). High-Resolution microtubule structures reveal the structural transitions in αβ-tubulin upon GTP hydrolysis. *Cell*, *157*(5), 1117–1129. https://doi.org/10.1016/j.cell.2014.03.053

Andreeva, A. V., Kutuzov, M. A., & Voyno-Yasenetskaya, T. A. (2007). Scaffolding proteins in G-protein signaling. *Journal of Molecular Signaling*, *2*, 1–9. https://doi.org/10.1186/1750-2187-2-13

Andrews, P. D., Ovechkina, Y., Morrice, N., Wagenbach, M., Duncan, K., Wordeman, L., & Swedlow, J. R. (2004). Aurora B regulates MCAK at the mitotic centromere. *Developmental Cell*, *6*(2), 253–268. https://doi.org/10.1016/S1534-5807(04)00025-5

Armitage, J. O., Gascoyne, R. D., Lunning, M. A., & Cavalli, F. (2017). Non-Hodgkin lymphoma. *The Lancet*, *390*(10091), 298–310. https://doi.org/10.1016/S0140-6736(16)32407-2

Asbury, C. L. (2017). Anaphase a: Disassembling microtubules move chromosomes toward

spindle poles. *Biology*, *6*(1). https://doi.org/10.3390/biology6010015

Assou, S., Cerecedo, D., Tondeur, S., Pantesco, V., Hovatta, O., Klein, B., Hamamah, S., & De Vos, J. (2009). A gene expression signature shared by human mature oocytes and embryonic stem cells. *BMC Genomics*, *10*. https://doi.org/10.1186/1471-2164-10-10

Attia, S. M. (2013). Molecular cytogenetic evaluation of the mechanism of genotoxic potential of amsacrine and nocodazole in mouse bone marrow cells. *Journal of Applied Toxicology*, *33*(6), 426–433. https://doi.org/10.1002/jat.1753

Bakal, C. J., Finan, D., Larose, J., Wells, C. D., Gish, G., Kulkarni, S., Desepulveda, P., Wilde, A., & Rottapel, R. (2005). The Rho GTP exchange factor Lfc promotes spindle assembly in early mitosis. *Proceedings of the National Academy of Sciences of the United States of America*, *102*(27), 9529–9534. https://doi.org/10.1073/pnas.0504190102

Baker, D. J., Jin, F., Jeganathan, K. B., & van Deursen, J. M. (2009). Whole Chromosome Instability Caused by Bub1 Insufficiency Drives Tumorigenesis through Tumor Suppressor Gene Loss of Heterozygosity. *Cancer Cell*, *16*(6), 475–486. https://doi.org/10.1016/j.ccr.2009.10.023

Bakhoum, S. F., Danilova, O. V., Kaur, P., Levy, N. B., & Compton, D. A. (2011). Chromosomal instability substantiates poor prognosis in patients with diffuse large B-cell lymphoma. *Clinical Cancer Research*, *17*(24), 7704–7711. https://doi.org/10.1158/1078-0432.CCR-11-2049

Bakhoum, S. F., Genovese, G., & Compton, D. A. (2009). Deviant Kinetochore Microtubule Dynamics Underlie Chromosomal Instability. *Current Biology*, *19*(22), 1937–1942. https://doi.org/10.1016/j.cub.2009.09.055

Bakhoum, S. F., Thompson, S. L., Manning, A. L., & Compton, D. A. (2009). Genome stability is ensured by temporal control of kinetochore-microtubule dynamics. *Nature Cell Biology*, *11*(1), 27–35. https://doi.org/10.1038/ncb1809

Bar-Shavit, R., Maoz, M., Kancharla, A., Nag, J. K., Agranovich, D., Grisaru-Granovsky, S., & Uziely, B. (2016). G protein-coupled receptors in cancer. In *International Journal of Molecular Sciences* (Vol. 17, Issue 8). https://doi.org/10.3390/ijms17081320

Barbosa, J., Nascimento, A. V., Faria, J., Silva, P., & Bousbaa, H. (2011). The spindle assembly checkpoint: Perspectives in tumorigenesis and cancer therapy. *Frontiers in Biology*, *6*(2),

147–155. https://doi.org/10.1007/s11515-011-1122-x

Bates, D., & Eastman, A. (2017). Microtubule destabilising agents: far more than just antimitotic anticancer drugs. *British Journal of Clinical Pharmacology*, *83*(2), 255–268. https://doi.org/10.1111/bcp.13126

Ben-David, U., & Amon, A. (2020). Context is everything: aneuploidy in cancer. *Nature Reviews Genetics*, *21*(1), 44–62. https://doi.org/10.1038/s41576-019-0171-x

Bennouna, J., Delord, J. P., Campone, M., & Nguyen, L. (2008). Vinflunine: A new microtubule inhibitor agent. *Clinical Cancer Research*, *14*(6), 1625–1632. https://doi.org/10.1158/1078-0432.CCR-07-2219

Bertomeu, T., Coulombe-Huntington, J., Chatr-aryamontri, A., Bourdages, K., Coyaud, E., Raught, B., Xia, Y., & Tyers, M. (2017). A high resolution genome-wide CRISPR/Cas9 viability screen reveals structural features and contextual diversity of the human cell-essential proteome. *Molecular and Cellular Biology*. http://mcb.asm.org/content/early/2017/10/10/MCB.00302-17.abstract

Blajeski, A. L., Phan, V. A., Kottke, T. J., & Kaufmann, S. H. (2002). G1 and G2 cell-cycle arrest following microtubule depolymerization in human breast cancer cells. *The Journal of Clinical Investigation*, *110*(1), 91–99. https://doi.org/10.1172/JCI200213275.Introduction

Bolhaqueiro, A. C. F., Ponsioen, B., Bakker, B., Klaasen, S. J., Kucukkose, E., van Jaarsveld, R. H., Vivié, J., Verlaan-Klink, I., Hami, N., Spierings, D. C. J., Sasaki, N., Dutta, D., Boj, S. F., Vries, R. G. J., Lansdorp, P. M., van de Wetering, M., van Oudenaarden, A., Clevers, H., Kranenburg, O., … Kops, G. J. P. L. (2019). Ongoing chromosomal instability and karyotype evolution in human colorectal cancer organoids. *Nature Genetics*, *51*(5), 824–834. https://doi.org/10.1038/s41588-019-0399-6

Bollag, D. M., McQueney, P. A., Zhu, J., Hensens, O., Koupal, L., Liesch, J., Goetz, M., Lazarides, E., & Woods, C. M. (1995). Epothilones, a New Class of Microtubule-stabilizing Agents with a Taxol-like Mechanism of Action. *Cancer Research*, *55*(11), 2325 LP – 2333. http://cancerres.aacrjournals.org/content/55/11/2325.abstract

Booth, D. G., Hood, F. E., Prior, I. A., & Royle, S. J. (2011). A TACC3/ch-TOG/clathrin complex stabilises kinetochore fibres by inter-microtubule bridging. *EMBO Journal*, *30*(5), 906–919.

https://doi.org/10.1038/emboj.2011.15

Bouchier-Hayes, L., & Martin, S. J. (2002). CARD games in apoptosis and immunity. *EMBO Reports*, *3*(7), 616–621. https://doi.org/10.1093/embo-reports/kvf139

Bowne-Anderson, H., Zanic, M., Kauer, M., & Howard, J. (2013). Microtubule dynamic instability: A new model with coupled GTP hydrolysis and multistep catastrophe. *BioEssays*, *35*(5), 452–461. https://doi.org/10.1002/bies.201200131

Brabander, M. D. E., & Borgers, M. (1973). The formation of annulated lamellae induced by the disintegration of microtubules. *Cell*, *340*, 331–340.

Branchi, V., García, S. A., Radhakrishnan, P., Győrffy, B., Hissa, B., Schneider, M., Reißfelder, C., & Schölch, S. (2019). Prognostic value of DLGAP5 in colorectal cancer. *International Journal of Colorectal Disease*, *34*(8), 1455–1465. https://doi.org/10.1007/s00384-019-03339-6

Breuer, M., Kolano, A., Kwon, M., Li, C. C., Tsai, T. F., Pellman, D., Brunet, S., & Verlhac, M. H. (2010). HURP permits MTOC sorting for robust meiotic spindle bipolarity, similar to extra centrosome clustering in cancer cells. *Journal of Cell Biology*, *191*(7), 1251–1260. https://doi.org/10.1083/jcb.201005065

Bridges, C. B. (1922). The Origin of Variations in Sexual and Sex-Limited Characters. *The American Naturalist*, *56*(642), 51–63. https://doi.org/10.1086/279847

Brinkman, E. K., Chen, T., Amendola, M., & van Steensel, B. (2014). Easy quantitative assessment of genome editing by sequence trace decomposition. *Nucleic Acids Research*, *42*(22), e168–e168. http://dx.doi.org/10.1093/nar/gku936

Brouhard, G. J., & Hunt, A. J. (2005). Microtubule movements on the arms of mitotic chromosomes: Polar ejection forces quantified in vitro. *Proceedings of the National Academy of Sciences of the United States of America*, *102*(39), 13903–13908. https://doi.org/10.1073/pnas.0506017102

Brouhard, G. J., & Rice, L. M. (2018). Microtubule dynamics: an interplay of biochemistry and mechanics. *Nature Reviews Molecular Cell Biology*, *19*(7), 451–463. https://doi.org/10.1038/s41580-018-0009-y

Bruhn, C., Kroll, T., & Wang, Z.-Q. (2014). Systematic Characterization of Cell Cycle Phase-dependent Protein Dynamics and Pathway Activities by High-content Microscopy-assisted

Cell Cycle Phenotyping. *Genomics, Proteomics & Bioinformatics*, *12*(6), 255–265. https://doi.org/https://doi.org/10.1016/j.gpb.2014.10.004

Cai, S., O'Connell, C. B., Khodjakov, A., & Walczak, C. E. (2009). Chromosome congression in the absence of kinetochore fibres. *Nature Cell Biology*, *11*(7), 832–838. https://doi.org/10.1038/ncb1890

Cardillo, G. (2007). *MyFisher23: a very compact routine for Fisher's exact % test on 2x3 matrix*. https://github.com/dnafinder/myfisher23

Chiang, T., Schultz, R. M., & Lampson, M. A. (2011). Age-Dependent Susceptibility of Chromosome Cohesion to Premature Separase Activation in Mouse Oocytes1. *Biology of Reproduction*, *85*(6), 1279–1283. https://doi.org/10.1095/biolreprod.111.094094

Chircop, M. (2014). Rho GTPases as regulators of mitosis and cytokinesis in mammalian cells. *Small GTPases*, *5*(JUL). https://doi.org/10.4161/sgtp.29770

Choi, C. M., Seo, K. W., Jang, S. J., Oh, Y. M., Shim, T. S., Kim, W. S., Lee, D. S., & Lee, S. Do. (2009). Chromosomal instability is a risk factor for poor prognosis of adenocarcinoma of the lung: Fluorescence in situ hybridization analysis of paraffin-embedded tissue from Korean patients. *Lung Cancer*, *64*(1), 66–70. https://doi.org/10.1016/j.lungcan.2008.07.016

Choi, S. Y., Jang, J. H., & Kim, K. R. (2011). Analysis of differentially expressed genes in human rectal carcinoma using suppression subtractive hybridization. *Clinical and Experimental Medicine*, *11*(4), 219–226. https://doi.org/10.1007/s10238-010-0130-5

Choma, D., Daurès, J. P., Quantin, X., & Pujol, J. L. (2001). Aneuploidy and prognosis of non-small-cell lung cancer: A meta-analysis of published data. *British Journal of Cancer*, *85*(1), 14–22. https://doi.org/10.1054/bjoc.2001.1892

Cimini, D., Cameron, L. A., & Salmon, E. D. (2004). Anaphase Spindle Mechanics Prevent Mis-Segregation of Merotelically Oriented Chromosomes. *Current Biology*, *14*(23), 2149–2155. https://doi.org/https://doi.org/10.1016/j.cub.2004.11.029

Cimini, D., Howell, B., Maddox, P., Khodjakov, A., Degrassi, F., & Salmon, E. D. (2001). Merotelic kinetochore orientation is a major mechanism of aneuploidy in mitotic mammalian tissue cells. *Journal of Cell Biology*, *152*(3), 517–527. https://doi.org/10.1083/jcb.153.3.517

Cimini, D., Moree, B., Canman, J. C., & Salmon, E. D. (2003). Merotelic kinetochore orientation

occurs frequently during early mitosis in mammalian tissue cells and error correction is achieved by two different mechanisms. *Journal of Cell Science*, *116*(20), 4213–4225. https://doi.org/10.1242/jcs.00716

Cleeland, C. S., Allen, J. D., Roberts, S. A., Brell, J. M., Giralt, S. A., Khakoo, A. Y., Kirch, R. A., Kwitkowski, V. E., Liao, Z., & Skillings, J. (2012). Reducing the toxicity of cancer therapy: Recognizing needs, taking action. *Nature Reviews Clinical Oncology*, *9*(8), 471–478. https://doi.org/10.1038/nrclinonc.2012.99

Conde, C., & Cáceres, A. (2009). Microtubule assembly, organization and dynamics in axons and dendrites. *Nature Reviews Neuroscience*, *10*(5), 319–332. https://doi.org/10.1038/nrn2631

Conlin, A., Fornier, M., Hudis, C., Kar, S., & Kirkpatrick, P. (2007). Ixabepilone. *Nature Reviews Drug Discovery*, *6*(12), 953–954. https://doi.org/10.1038/nrd2469

Dagogo-Jack, I., & Shaw, A. T. (2018). Tumour heterogeneity and resistance to cancer therapies. *Nature Reviews Clinical Oncology*, *15*(2), 81–94. https://doi.org/10.1038/nrclinonc.2017.166

Dai, J., Sullivan, B. A., & Higgins, J. M. G. (2006). Regulation of Mitotic Chromosome Cohesion by Haspin and Aurora B. *Developmental Cell*, *11*(5), 741–750. https://doi.org/10.1016/j.devcel.2006.09.018

Davies, C., Hogarth, L. A., Dietrich, P. A., Bachmann, P. S., Mackenzie, K. L., Hall, A. G., & Lock, R. B. (2011). p53-independent epigenetic repression of the p21 WAF1 gene in T-cell acute lymphoblastic leukemia. *Journal of Biological Chemistry*, *286*(43), 37639–37650. https://doi.org/10.1074/jbc.M111.272336

Demaria, S., Volm, M. D., Shapiro, R. L., Yee, H. T., Oratz, R., Formenti, S. C., Muggia, F., & Symmans, W. F. (2001). Development of tumor-infiltrating lymphocytes in breast cancer after neoadjuvant paclitaxel chemotherapy. *Clinical Cancer Research*, *7*(10), 3025–3030.

Derry, W. B., Wilson, L., & Jordan, M. A. (1995). Substoichiometric Binding of Taxol Suppresses Microtubule Dynamics. *Biochemistry*, *34*(7), 2203–2211. https://doi.org/10.1021/bi00007a014

Dhanjal, J. K., Radhakrishnan, N., & Sundar, D. (2017). Identifying synthetic lethal targets using CRISPR/Cas9 system. *Methods*, *131*, 66–73.

https://doi.org/https://doi.org/10.1016/j.ymeth.2017.07.007

Díaz-Martínez, L. A., Giménez-Abián, J. F., & Clarke, D. J. (2007). Regulation of centromeric cohesion by sororin independently of the APC/C. *Cell Cycle*, *6*(6), 714–724. https://doi.org/10.4161/cc.6.6.3935

Dobzhansky, T. (1946). Genetics of natural populations; recombination and variability in populations of Drosophila pseudoobscura. *Genetics*, *31*(May), 269–290.

Drew, Y. (2015). The development of PARP inhibitors in ovarian cancer: From bench to bedside. *British Journal of Cancer*, *113*(S1), S3–S9. https://doi.org/10.1038/bjc.2015.394

Du, Y., Liu, L., Wang, C., Kuang, B., Yan, S., Zhou, A., Wen, C., Chen, J., Wu, Y., Yang, X., Feng, G., Liu, B., Iwamoto, A., Zeng, M., Wang, J., Zhang, X., & Liu, H. (2016). TACC3 promotes colorectal cancer tumourigenesis and correlates with poor prognosis. *Oncotarget*, *7*(27), 41885–41897. https://doi.org/10.18632/oncotarget.9628

Duesberg, P., Stindl, R., & Hehlmann, R. (2000). Explaining the high mutation rates of cancer cells to drug and multidrug resistance by chromosome reassortments that are catalyzed by aneuploidy. *Proceedings of the National Academy of Sciences of the United States of America*, *97*(26), 14295–14300. https://doi.org/10.1073/pnas.97.26.14295

Dull, T., Zufferey, R., Kelly, M., Mandel, R. J., Nguyen, M., Trono, D., & Naldini, L. (1998). A third-generation lentivirus vector with a conditional packaging system. *Journal of Virology*, *72*(11), 8463–8471. https://www.ncbi.nlm.nih.gov/pubmed/9765382

Dumontet, C., & Jordan, M. A. (2010). Microtubule-binding agents: A dynamic field of cancer therapeutics. *Nature Reviews Drug Discovery*, *9*(10), 790–803. https://doi.org/10.1038/nrd3253

Ehrlich, P. (1911). Aus Theorie und Praxis der Chemotherapie. *Folia Serologica VII*, 697–714.

Engel, U., Grosse, R., Goulimari, P., & Knieling, H. (2008). LARG and mDia1 Link G 12/13 to Cell Polarity and Microtubule Dynamics. *Molecular Biology of the Cell*. https://doi.org/10.1091/mbc.E06

Exman, P., Barroso-Sousa, R., & Tolaney, S. M. (2019). Evidence to Date: Talazoparib in the treatment of breast cancer. *OncoTargets and Therapy*, *12*, 5177–5187. https://doi.org/10.2147/OTT.S184971

Fagerberg, L., Hallstrom, B. M., Oksvold, P., Kampf, C., Djureinovic, D., Odeberg, J., Habuka, M., Tahmasebpoor, S., Danielsson, A., Edlund, K., Asplund, A., Sjostedt, E., Lundberg, E., Szigyarto, C. A. K., Skogs, M., Ottosson Takanen, J., Berling, H., Tegel, H., Mulder, J., … Uhlen, M. (2014). Analysis of the human tissue-specific expression by genome-wide integration of transcriptomics and antibody-based proteomics. *Molecular and Cellular Proteomics*, *13*(2), 397–406. https://doi.org/10.1074/mcp.M113.035600

Farmer, H., McCabe, H., Lord, C. J., Tutt, A. H. J., Johnson, D. A., Richardson, T. B., Santarosa, M., Dillon, K. J., Hickson, I., Knights, C., Martin, N. M. B., Jackson, S. P., Smith, G. C. M., & Ashworth, A. (2005). Targeting the DNA repair defect in BRCA mutant cells as a therapeutic strategy. *Nature*, *434*(7035), 917–921. https://doi.org/10.1038/nature03445

Ferlini, C., Cicchillitti, L., Raspaglio, G., Bartollino, S., Cimitan, S., Bertucci, C., Mozzetti, S., Gallo, D., Persico, M., Fattorusso, C., Campiani, G., & Scambia, G. (2009). Paclitaxel directly binds to Bcl-2 and functionally mimics activity of Nur77. *Cancer Research*, *69*(17), 6906–6914. https://doi.org/10.1158/0008-5472.CAN-09-0540

Ferreira, L. T., Orr, B., Rajendraprasad, G., Pereira, A. J., Lemos, C., Lima, J. T., Guasch Boldú, C., Ferreira, J. G., Barisic, M., & Maiato, H. (2020). α-Tubulin detyrosination impairs mitotic error correction by suppressing MCAK centromeric activity. *Journal of Cell Biology*, *219*(4). https://doi.org/10.1083/jcb.201910064

Field, J. J., Pera, B., Calvo, E., Canales, A., Zurwerra, D., Trigili, C., Rodríguez-Salarichs, J., Matesanz, R., Kanakkanthara, A., Wakefield, S. J., Singh, A. J., Jiménez-Barbero, J., Northcote, P., Miller, J. H., López, J. A., Hamel, E., Barasoain, I., Altmann, K. H., & Díaz, J. F. (2012). Zampanolide, a potent new microtubule-stabilizing agent, covalently reacts with the taxane luminal site in tubulin α,β-heterodimers and microtubules. *Chemistry and Biology*, *19*(6), 686–698. https://doi.org/10.1016/j.chembiol.2012.05.008

Flemming, W. (1879). Beitrage zur Kenntniss der Zelle und ihrer Lebenserscheinungen. *Archiv Für Mikroskopische Anatomie*, *16*(1), 302–436. https://doi.org/10.1007/BF02956386

Flemming, W. (1965). Historical paper:Contri butions to the knowledge of the cell and its vital processes. *Journal of Cell Biology*, *25*(1), 3–69. https://doi.org/10.1083/jcb.25.1.3

Fu, W., Chen, H., Wang, G., Luo, J., Deng, Z., Xin, G., Xu, N., Guo, X., Lei, J., Jiang, Q., & Zhang, C.

(2013). Self-assembly and sorting of acentrosomal microtubules by TACC3 facilitate kinetochore capture during the mitotic spindle assembly. *Proceedings of the National Academy of Sciences of the United States of America*, *110*(38), 15295–15300. https://doi.org/10.1073/pnas.1312382110

Fu, W., Tao, W., Zheng, P., Fu, J., Bian, M., Jiang, Q., Clarke, P. R., & Zhang, C. (2010). Clathrin recruits phosphorylated TACC3 to spindle poles for bipolar spindle assembly and chromosome alignment. *Journal of Cell Science*, *123*(21), 3645–3651. https://doi.org/10.1242/jcs.075911

Funk, L. C., Zasadil, L. M., & Weaver, B. A. (2016). Living in CIN: Mitotic Infidelity and Its Consequences for Tumor Promotion and Suppression. *Developmental Cell*, *39*(6), 638–652. https://doi.org/10.1016/j.devcel.2016.10.023

Gadde, S., & Heald, R. (2004). Mechanisms and molecules of the mitotic spindle. *Current Biology*, *14*(18), 797–805. https://doi.org/10.1016/j.cub.2004.09.021

Ganem, N. J., & Pellman, D. (2012). Linking abnormal mitosis to the acquisition of DNA damage. *Journal of Cell Biology*, *199*(6), 871–881. https://doi.org/10.1083/jcb.201210040

Gardner, J. A., Ha, J. H., Jayaraman, M., & Dhanasekaran, D. N. (2013). The gep proto-oncogene Galpha13 mediates lysophosphatidic acid-mediated migration of pancreatic cancer cells. *Pancreas*, *42*, 819.

Gaspari, R., Prota, A. E., Bargsten, K., Cavalli, A., & Steinmetz, M. O. (2017). Structural Basis of cis- and trans-Combretastatin Binding to Tubulin. *Chem*, *2*(1), 102–113. https://doi.org/10.1016/j.chempr.2016.12.005

Gauvin, T. J., Fukui, J., Peterson, J. R., & Higgs, H. N. (2009). Isoform-selective chemical inhibition of mDia-mediated actin assembly. *Biochemistry*, *48*(40), 9327–9329. https://doi.org/10.1021/bi901354z

Gergely, F., Draviam, V. M., & Raff, J. W. (2003). The ch-TOG/XMAP215 protein is essential for spindle pole organization in human somatic cells. *Genes and Development*, *17*(3), 336–341. https://doi.org/10.1101/gad.245603

Gerth, K., Bedorf, N., Höfle, G., Irschik, H., & Reichenbach, H. (1996). Epothilons A and B: Antifungal and cytotoxic compounds from Sorangium cellulosum (Myxobacteria)

production, physico-chemical and biological properties. *Journal of Antibiotics*, *49*(6), 560–563. https://doi.org/10.7164/antibiotics.49.560

Ghandi, M., Huang, F. W., Jané-Valbuena, J., Kryukov, G. V., Lo, C. C., McDonald, E. R., Barretina, J., Gelfand, E. T., Bielski, C. M., Li, H., Hu, K., Andreev-Drakhlin, A. Y., Kim, J., Hess, J. M., Haas, B. J., Aguet, F., Weir, B. A., Rothberg, M. V., Paolella, B. R., … Sellers, W. R. (2019). Next-generation characterization of the Cancer Cell Line Encyclopedia. *Nature*. https://doi.org/10.1038/s41586-019-1186-3

Giannakakou, P., Gussio, R., Nogales, E., Downing, K. H., Zaharevitz, D., Bollbuck, B., Poy, G., Sackett, D., Nicolaou, K. C., & Fojo, T. (2000). A common pharmacophore for epothilone and taxanes: Molecular basis for drug resistance conferred by tubulin mutations in human cancer cells. *Proceedings of the National Academy of Sciences of the United States of America*, *97*(6), 2904–2909. https://doi.org/10.1073/pnas.040546297

Gigant, B., Wang, C., Ravelli, R. B. G., Roussi, F., Steinmetz, M. O., Curmi, P. A., Sobel, A., & Knossow, M. (2005). Structural basis for the regulation of tubulin by vinblastine. *Nature*, *435*(7041), 519–522. https://doi.org/10.1038/nature03566

Giuliano, C. J., Lin, A., Smith, J. C., Palladino, A. C., & Sheltzer, J. M. (2018). MELK expression correlates with tumor mitotic activity but is not required for cancer growth. *ELife*, *7*, 1–23. https://doi.org/10.7554/eLife.32838

Godek, K. M., Venere, M., Wu, Q., Mills, K. D., Hickey, W. F., Rich, J. N., & Compton, D. A. (2016). Chromosomal instability affects the tumorigenicity of glioblastoma tumor-initiating cells. *Cancer Discovery*, *6*(5), 532–545. https://doi.org/10.1158/2159-8290.CD-15-1154

Gomez, C. R., Kosari, F., Munz, J. M., Schreiber, C. A., Knutson, G. J., Ida, C. M., El Khattouti, A., Jeffrey Karnes, R., Cheville, J. C., Vasmatzis, G., & Vuk-Pavlović, S. (2013). Prognostic value of discs large homolog 7 transcript levels in prostate cancer. *PLoS ONE*, *8*(12), 1–7. https://doi.org/10.1371/journal.pone.0082833

Gorrini, C., Harris, I. S., & Mak, T. W. (2013). Modulation of oxidative stress as an anticancer strategy. *Nature Reviews Drug Discovery*, *12*(12), 931–947. https://doi.org/10.1038/nrd4002

Graham B.S., L. D. T. (2020). Cancer, Burkitt Lymphoma. [Updated 2019 Sep 4]. In *StatPearls*

[Internet]. StatPearls Publishing. https://www.ncbi.nlm.nih.gov/books/NBK538148/

Gregory, R. K., & Smith, I. E. (2000). Vinorelbine - a clinical review. *British Journal of Cancer*, *82*, 1907–1913. https://doi.org/https://doi.org/10.1054/bjoc.2000.1203

Grill, S. W., & Hyman, A. A. (2005). Spindle Positioning by Cortical Pulling Forces. *Developmental Cell*, *8*(4), 461–465. https://doi.org/10.1016/j.devcel.2005.03.014

Grueb, S. S., Muhs, S., Popp, Y., Schmitt, S., Geyer, M., Lin, Y. N., & Windhorst, S. (2019). The formin Drosophila homologue of Diaphanous2 (Diaph2) controls microtubule dynamics in colorectal cancer cells independent of its FH2-domain. *Scientific Reports*, *9*(1), 1–14. https://doi.org/10.1038/s41598-019-41731-y

Guo, F., & Liu, Y. (2018). Knockdown of TACC3 inhibits the proliferation and invasion of human renal cell carcinoma cells. *Oncology Research*, *26*(2), 183–189. https://doi.org/10.3727/096504017X14837020772250

Hanahan, D., & Weinberg, R. A. (2011). Hallmarks of cancer: The next generation. *Cell*, *144*(5), 646–674. https://doi.org/10.1016/j.cell.2011.02.013

Hassold, T., & Hunt, P. (2001). To err (meiotically) is human: the genesis of human aneuploidy. *Nature Reviews. Genetics*, *2*(4), 280–291.

He, J. C., Yao, W., Wang, J. M., Schemmer, P., Yang, Y., Liu, Y., Qian, Y. W., Qi, W. P., Zhang, J., Shen, Q., & Yang, T. (2016). TACC3 overexpression in cholangiocarcinoma correlates with poor prognosis and is a potential anti-cancer molecular drug target for HDAC inhibitors. *Oncotarget*, *7*(46), 75441–75456. https://doi.org/10.18632/oncotarget.12254

Heald, R., & Khodjakov, A. (2015). Thirty years of search and capture: The complex simplicity of mitotic spindle assembly. *Journal of Cell Biology*, *211*(6), 1103–1111. https://doi.org/10.1083/jcb.201510015

Healy, J. A., Nugent, A., Rempel, R. E., Moffitt, A. B., Davis, N. S., Jiang, X., Shingleton, J. R., Zhang, J., Love, C., Datta, J., McKinney, M. E., Tzeng, T. J., Wettschureck, N., Offermanns, S., Walzer, K. A., Chi, J. T., Rasheed, S. A. K., Casey, P. J., Lossos, I. S., & Dave, S. S. (2016). GNA13 loss in germinal center B cells leads to impaired apoptosis and promotes lymphoma in vivo. *Blood*, *127*(22), 2723–2731. https://doi.org/10.1182/blood-2015-07-659938

Heilig, C. E., Löffler, H., Mahlknecht, U., Janssen, J. W. G., Ho, A. D., Jauch, A., & Krämer, A. (2010).

Chromosomal instability correlates with poor outcome in patients with myelodysplastic syndromes irrespectively of the cytogenetic risk group. *Journal of Cellular and Molecular Medicine*, *14*(4), 895–902. https://doi.org/10.1111/j.1582-4934.2009.00905.x

Hewit, K., Sandilands, E., Martinez, R. S., James, D., Leung, H. Y., Bryant, D. M., Shanks, E., & Markert, E. K. (2018). A functional genomics screen reveals a strong synergistic effect between docetaxel and the mitotic gene DLGAP5 that is mediated by the androgen receptor. *Cell Death and Disease*, *9*(11). https://doi.org/10.1038/s41419-018-1115-7

Hieronymus, H., Murali, R., Tin, A., Yadav, K., Abida, W., Moller, H., Berney, D., Scher, H., Carver, B., Scardino, P., Schultz, N., Taylor, B., Vickers, A., Cuzick, J., & Sawyers, C. L. (2018). Tumor copy number alteration burden is a pan-cancer prognostic factor associated with recurrence and death. *ELife*, *7*, 1–18. https://doi.org/10.7554/eLife.37294

Höfle, G., Bedorf, N., Steinmetz, H., Schomburg, D., Gerth, K., & Reichenbach, H. (1996). Epothilone A and B-novel 16-membered macrolides with cytotoxic activity: Isolation, crystal structure, and conformation in solution. *Angewandte Chemie (International Edition in English)*, *35*(13–14), 1567–1569. https://doi.org/10.1002/anie.199615671

Holland, A. J., & Cleveland, D. W. (2012). Losing balance: The origin and impact of aneuploidy in cancer. *EMBO Reports*, *13*(6), 501–514. https://doi.org/10.1038/embor.2012.55

Horio, T., Murata, T., & Murata, T. (2014). The role of dynamic instability in microtubule organization. *Frontiers in Plant Science*, *5*(OCT), 1–10. https://doi.org/10.3389/fpls.2014.00511

Hu, Y., Xing, J., Chen, L., Zheng, Y., & Zhou, Z. (2015). RGS22 inhibits pancreatic adenocarcinoma cell migration through the G12/13 α subunit/F-actin pathway. *Oncology Reports*, *34*(5), 2507–2514. https://doi.org/10.3892/or.2015.4209

Huang, Z. L., Lin, Z. R., Xiao, Y. R., Cao, X., Zhu, L. C., Zeng, M. S., Zhong, Q., & Wen, Z. S. (2015). High expression of TACC3 in esophageal squamous cell carcinoma correlates with poor prognosis. *Oncotarget*, *6*(9), 6850–6861. https://doi.org/10.18632/oncotarget.3190

Jacobson, C., & Lacasce, A. (2017). How I treat Burkitt lymphoma in adults. *Blood*, *124*(19), 2913–2921. https://doi.org/10.1182/blood-2014-06-538504.The

Janssen, A., Van Der Burg, M., Szuhai, K., Kops, G. J. P. L., & Medema, R. H. (2011). Chromosome

segregation errors as a cause of DNA damage and structural chromosome aberrations. *Science*, *333*(6051), 1895–1898. https://doi.org/10.1126/science.1210214

Javeed, A., Ashraf, M., Riaz, A., Ghafoor, A., Afzal, S., & Mukhtar, M. M. (2009). Paclitaxel and immune system. *European Journal of Pharmaceutical Sciences*, *38*(4), 283–290. https://doi.org/10.1016/j.ejps.2009.08.009

Jiang, K., & Akhmanova, A. (2011). Microtubule tip-interacting proteins: A view from both ends. *Current Opinion in Cell Biology*, *23*(1), 94–101. https://doi.org/10.1016/j.ceb.2010.08.008

Jinek, M., Chylinski, K., Fonfara, I., Hauer, M., Doudna, J. A., & Charpentier, E. (2012). A programmable dual-RNA-guided DNA endonuclease in adaptive bacterial immunity. *Science*, *337*(6096), 816–821. https://doi.org/10.1126/science.1225829

Jordan, M. A. (2002). Mechanism of action of antitumor drugs that interact with microtubules and tubulin. *Current Medicinal Chemistry - Anti-Cancer Agents*, *2*(1), 1–17. https://doi.org/10.2174/1568011023354290

Jordan, Mary Ann, Thrower, D., & Wilson, L. (1991). Mechanism of Inhibition of Cell Proliferation by Vinca Alkaloids. *Cancer Research*, *51*(8), 2212–2222.

Jordan, Mary Ann, Wendell, K., Gardiner, S., Derry, W. B., Copp, H., & Wilson, L. (1996). Mitotic block induced in HeLa cells by low concentrations of paclitaxel (taxol) results in abnormal mitotic exit and apoptotic cell death. *Cancer Research*, *56*(4), 816–825.

Jordan, Mary Ann, & Wilson, L. (2004). Microtubules As a Target for Anticancer Drugs. *Nature Reviews Cancer*, *4*(April), 236–265. https://doi.org/10.1038/nrc1317

Juneja, J., & Casey, P. J. (2009). Role of G12 proteins in oncogenesis and metastasis. *British Journal of Pharmacology*, *158*(1), 32–40. https://doi.org/10.1111/j.1476-5381.2009.00180.x

Kaelin, W. G. (2005). The concept of synthetic lethality in the context of anticancer therapy. *Nature Reviews Cancer*, *5*(9), 689–698. https://doi.org/10.1038/nrc1691

Kaláb, P., Pralle, A., Isacoff, E. Y., Heald, R., & Weis, K. (2006). Analysis of a RanGTP-regulated gradient in mitotic somatic cells. *Nature*, *440*(7084), 697–701. https://doi.org/10.1038/nature04589

Kalisz, K., Alessandrino, F., Beck, R., Smith, D., Kikano, E., Ramaiya, N. H., & Tirumani, S. H. (2019). An update on Burkitt lymphoma: a review of pathogenesis and multimodality imaging

assessment of disease presentation, treatment response, and recurrence. *Insights into Imaging*, *10*(1), 1–16. https://doi.org/10.1186/s13244-019-0733-7

Kato, T., Watanabe, N., Morishima, Y., Fujita, A., Ishizaki, T., & Narumiya, S. (2001). Localization of a mammalian homolog of diaphanous, mDia1, to the mitotic spindle in HeLa cells. *Journal of Cell Science*, *114*(4), 775–784.

Kavallaris, M. (2010). Microtubules and resistance to tubulin-binding agents. *Nature Reviews Cancer*, *10*, 194. https://doi.org/10.1038/nrc2803

Kelly, P., Casey, P. J., & Meigs, T. E. (2007). Biologic functions of the G12 subfamily of heterotrimeric G proteins: Growth, migration, and metastasis. *Biochemistry*, *46*(23), 6677–6687. https://doi.org/10.1021/bi700235f

Kelly, P., Moeller, B. J., Juneja, J., Booden, M. A., Der, C. J., Daaka, Y., Dewhirst, M. W., Fields, T. A., & Casey, P. J. (2006). The G12 family of heterotrimeric G proteins promotes breast cancer invasion and metastasis. *Proc Natl Acad Sci Usa*, *103*(21), 8173. https://doi.org/10.1073/pnas.0510254103

Khodjakov, A., Cole, R. W., Oakley, B. R., & Rieder, C. L. (2000). Centrosome-independent mitotic spindle formation in vertebrates. *Current Biology*, *10*(2), 59–67. https://doi.org/10.1016/S0960-9822(99)00276-6

Khodjakov, A., Copenagle, L., Gordon, M. B., Compton, D. A., & Kapoor, T. M. (2003). Minus-end capture of preformed kinetochore fibers contributes to spindle morphogenesis. *Journal of Cell Biology*, *160*(5), 671–683. https://doi.org/10.1083/jcb.200208143

Kim, H. S., Lee, K., Kim, S. J., Cho, S., Shin, H. J., Kim, C., & Kim, J. S. (2018). Arrayed CRISPR screen with image-based assay reliably uncovers host genes required for coxsackievirus infection. *Genome Research*, *28*(6), 859–868. https://doi.org/10.1101/gr.230250.117

Kirschner, M., & Mitchison, T. (1986). Beyond self-assembly: From microtubules to morphogenesis. *Cell*, *45*(3), 329–342. https://doi.org/10.1016/0092-8674(86)90318-1

Knowlton, A. L., Lan, W., & Stukenberg, P. T. (2006). Aurora B Is Enriched at Merotelic Attachment Sites, Where It Regulates MCAK. *Current Biology*, *16*(17), 1705–1710. https://doi.org/10.1016/j.cub.2006.07.057

Koike-Yusa, H., Li, Y., Tan, E. P., Velasco-Herrera, M. D. C., & Yusa, K. (2014). Genome-wide

recessive genetic screening in mammalian cells with a lentiviral CRISPR-guide RNA library. *Nature Biotechnology*, *32*(3), 267–273. https://doi.org/10.1038/nbt.2800

Kojima, K. K., & Jurka, J. (2011). Crypton transposons: Identification of new diverse families and ancient domestication events. *Mobile DNA*, *2*(1), 1–17. https://doi.org/10.1186/1759-8753-2-12

Komlodi-Pasztor, E., Sackett, D., Wilkerson, J., & Fojo, T. (2011). Mitosis is not a key target of microtubule agents in patient tumors. *Nature Reviews Clinical Oncology*, *8*(4), 244–250. https://doi.org/10.1038/nrclinonc.2010.228

Kuriyama, R., & Borisy, G. G. (1981). Microtubule-nucleating activity of centrosomes in Chinese hamster ovary cells is independent of the centriole cycle but coupled to the mitotic cycle. *Journal of Cell Biology*, *91*(3 I), 822–826. https://doi.org/10.1083/jcb.91.3.822

Kuukasjärvi, T., Karhu, R., Tanner, M., Kähkönen, M., Schäffen, A., Nupponen, N., Pennanen, S., Kallioniemi, A., Kallioniemi, O. P., & Isola, J. (1997). Genetic heterogeneity and clonal evolution underlying development of asynchronous metastasis in human breast cancer. *Cancer Research*, *57*(8), 1597–1604.

Kwon, M., Godinho, S. A., Chandhok, N. S., Ganem, N. J., Azioune, A., Thery, M., & Pellman, D. (2008). Mechanisms to suppress multipolar divisions in cancer cells with extra centrosomes. *Genes and Development*, *22*(16), 2189–2203. https://doi.org/10.1101/gad.1700908

Laan, L., Pavin, N., Husson, J., Romet-Lemonne, G., Van Duijn, M., López, M. P., Vale, R. D., Jülicher, F., Reck-Peterson, S. L., & Dogterom, M. (2012). Cortical dynein controls microtubule dynamics to generate pulling forces that position microtubule asters. *Cell*, *148*(3), 502–514. https://doi.org/10.1016/j.cell.2012.01.007

Labunskyy, V. M., Hatfield, D. L., & Gladyshev, V. N. (2014). Selenoproteins: Molecular pathways and physiological roles. *Physiological Reviews*, *94*(3), 739–777. https://doi.org/10.1152/physrev.00039.2013

Lammers, M., Meyer, S., Kühlmann, D., & Wittinghofer, A. (2008). Specificity of interactions between mDia isoforms and Rho proteins. *Journal of Biological Chemistry*, *283*(50), 35236–35246. https://doi.org/10.1074/jbc.M805634200

Lan, W., Zhang, X., Kline-Smith, S. L., Rosasco, S. E., Barrett-Wilt, G. A., Shabanowitz, J., Hunt, D.

F., Walczak, C. E., & Stukenberg, P. T. (2004). Aurora B Phosphorylates Centromeric MCAK and Regulates Its Localization and Microtubule Depolymerization Activity. *Current Biology*, *14*(4), 273–286. https://doi.org/10.1016/j.cub.2004.01.055

Lawrence, M. S., Stojanov, P., Mermel, C. H., Robinson, J. T., Garraway, L. A., Golub, T. R., Meyerson, M., Gabriel, S. B., Lander, E. S., & Getz, G. (2014). Discovery and saturation analysis of cancer genes across 21 tumour types. *Nature*, *505*(7484), 495–501. https://doi.org/10.1038/nature12912

Lee, A. J. X., Endesfelder, D., Rowan, A. J., Walther, A., Birkbak, N. J., Futreal, P. A., Downward, J., Szallasi, Z., Tomlinson, I. P. M., Howell, M., Kschischo, M., & Swanton, C. (2011). Chromosomal instability confers intrinsic multidrug resistance. *Cancer Research*, *71*(5), 1858–1870. https://doi.org/10.1158/0008-5472.CAN-10-3604

Lee, J. H., & Berger, J. M. (2019). Cell cycle-dependent control and roles of DNA topoisomerase II. *Genes*, *10*(11). https://doi.org/10.3390/genes10110859

Lee, J. J., & Swain, S. M. (2008). The epothilones: Translating from the laboratory to the clinic. *Clinical Cancer Research*, *14*(6), 1618–1624. https://doi.org/10.1158/1078-0432.CCR-07-2201

Lee, M. O., & Cho, Y. S. (2019). The role of selenium-mediated redox signaling by selenophosphate synthetase 1 (SEPHS1) in hESCs. *Biochemical and Biophysical Research Communications*, *520*(2), 406–412. https://doi.org/10.1016/j.bbrc.2019.09.123

Levesque, A. A., & Compton, D. A. (2001). The chromokinesin Kid is necessary for chromosome arm orientation and oscillation, but not congression, on mitotic spindles. *Journal of Cell Biology*, *154*(6), 1135–1146. https://doi.org/10.1083/jcb.200106093

Li, Q., Ye, L., Guo, W., Wang, M., Huang, S., & Peng, X. (2017). Overexpression of TACC3 is correlated with tumor aggressiveness and poor prognosis in prostate cancer. *Biochemical and Biophysical Research Communications*, *486*(4), 872–878. https://doi.org/10.1016/j.bbrc.2017.03.090

Liao, W., Liu, W., Yuan, Q., Liu, X., Ou, Y., He, S., Yuan, S., Qin, L., Chen, Q., Nong, K., Mei, M., & Huang, J. (2013). Silencing of DLGAP5 by siRNA significantly inhibits the proliferation and invasion of hepatocellular carcinoma cells. *PLoS ONE*, *8*(12), 1–9.

https://doi.org/10.1371/journal.pone.0080789

Lin, A., Giuliano, C. J., Palladino, A., John, K. M., Abramowicz, C., Yuan, M. Lou, Sausville, E. L., Lukow, D. A., Liu, L., Chait, A. R., Galluzzo, Z. C., Tucker, C., & Sheltzer, J. M. (2019). Off-target toxicity is a common mechanism of action of cancer drugs undergoing clinical trials. *Science Translational Medicine*, *11*(509). https://doi.org/10.1126/scitranslmed.aaw8412

Lin, A., Giuliano, C. J., Sayles, N. M., & Sheltzer, J. M. (2017). CRISPR/Cas9 mutagenesis invalidates a putative cancer dependency targeted in on-going clinical trials. *ELife*, *6*, 1–17. https://doi.org/10.7554/eLife.24179

Lin, C. H., Hu, C. K., & Shih, H. M. (2010). Clathrin heavy chain mediates TACC3 targeting to mitotic spindles to ensure spindle stability. *Journal of Cell Biology*, *189*(7), 1097–1105. https://doi.org/10.1083/jcb.200911120

Linch, D. C. (2012). Burkitt lymphoma in adults. *British Journal of Haematology*, *156*(6), 693–703. https://doi.org/10.1111/j.1365-2141.2011.08877.x

Lioutas, A., & Vernos, I. (2013). Aurora A kinase and its substrate TACC3 are required for central spindle assembly. *EMBO Reports*, *14*(9), 829–836. https://doi.org/10.1038/embor.2013.109

Lohr, J. G., Stojanov, P., Lawrence, M. S., Auclair, D., Chapuy, B., Sougnez, C., Cruz-Gordillo, P., Knoechel, B., Asmann, Y. W., Slager, S. L., Novak, A. J., Dogan, A., Ansell, S. M., Link, B. K., Zou, L., Gould, J., Saksena, G., Stransky, N., Rangel-Escareño, C., … Golub, T. R. (2012). Discovery and prioritization of somatic mutations in diffuse large B-cell lymphoma (DLBCL) by whole-exome sequencing. *Proceedings of the National Academy of Sciences of the United States of America*, *109*(10), 3879–3884. https://doi.org/10.1073/pnas.1121343109

Lord, C. J., & Ashworth, A. (2017). PARP inhibitors: Synthetic lethality in the clinic. *Science*, *355*(6330), 1152 LP – 1158. https://doi.org/10.1126/science.aam7344

Love, C., Sun, Z., Jima, D., Li, G., Zhang, J., Miles, R., Richards, K. L., Dunphy, C. H., Choi, W. L., Srivastava, G., Lugar, P. L., Rizzieri, D. A., Lagoo, A. S., Bernal-Mizrachi, L., Mann, K. P., Flowers, C. R., Naresh, K. N., Evens, A. M., Chadburn, A., … Dave, S. S. (2012). The genetic landscape of mutations in Burkitt lymphoma. *Nature Genetics*, *44*(12), 1321–1325. https://doi.org/10.1038/ng.2468

Lu, Y., Chen, J., Xiao, M., Li, W., & Miller, D. D. (2012). An overview of tubulin inhibitors that

interact with the colchicine binding site. *Pharmaceutical Research*, *29*(11), 2943–2971. https://doi.org/10.1007/s11095-012-0828-z

Lui, J. C., Jee, Y. H., Lee, A., Yue, S., Wagner, J., Donnelly, D. E., Vogt, K. S., & Baron, J. (2019). QRICH1 mutations cause a chondrodysplasia with developmental delay. *Clinical Genetics*, *95*(1), 160–164. https://doi.org/10.1111/cge.13457

Lyon-sud, C. H., & Lyon, H. C. De. (2016). Diffuse large B-cell lymphoma : R-CHOP failure — what to do ? *Hematology*, 366–378.

Magidson, V., O'Connell, C. B., Lončarek, J., Paul, R., Mogilner, A., & Khodjakov, A. (2011). The spatial arrangement of chromosomes during prometaphase facilitates spindle assembly. *Cell*, *146*(4), 555–567. https://doi.org/10.1016/j.cell.2011.07.012

Mahoney, N. M., Goshima, G., Douglass, A. D., & Vale, R. D. (2006). Making microtubules and mitotic spindles in cells without functional centrosomes. *Current Biology*, *16*(6), 564–569. https://doi.org/10.1016/j.cub.2006.01.053

Maiato, H., Rieder, C. L., & Khodjakov, A. (2004). Kinetochore-driven formation of kinetochore fibers contributes to spindle assembly during animal mitosis. *Journal of Cell Biology*, *167*(5), 831–840. https://doi.org/10.1083/jcb.200407090

Makino, S., Fukumura, R., & Gondo, Y. (2016). Illegitimate translation causes unexpected gene expression from on-target out-of-frame alleles created by CRISPR-Cas9. *Scientific Reports*, *6*(November), 6–11. https://doi.org/10.1038/srep39608

Margolis, R. L., & Wilson, L. (1977). Addition of colchicine tubulin complex to microtubule ends: The mechanism of substoichiometric colchicine poisoning. *Proceedings of the National Academy of Sciences of the United States of America*, *74*(8), 3466–3470. https://doi.org/10.1073/pnas.74.8.3466

Martino, E., Casamassima, G., Castiglione, S., Cellupica, E., Pantalone, S., Papagni, F., Rui, M., Siciliano, A. M., & Collina, S. (2018). Vinca alkaloids and analogues as anti-cancer agents: Looking back, peering ahead. *Bioorganic and Medicinal Chemistry Letters*, *28*(17), 2816–2826. https://doi.org/10.1016/j.bmcl.2018.06.044

Mastronarde, D. N., McDonald, K. L., Ding, R., & McIntosh, J. R. (1993). Interpolar spindle microtubules in PTK cells. *Journal of Cell Biology*, *123*(6 I), 1475–1489.

https://doi.org/10.1083/jcb.123.6.1475

Matsuda, K., Miyoshi, H., Hiraoka, K., Hamada, T., Nakashima, K., Shiba, N., & Ohshima, K. (2018). Elevated expression of transforming acidic coiled-coil containing protein 3 (TACC3) is associated with a poor prognosis in osteosarcoma. *Clinical Orthopaedics and Related Research*, *476*(9), 1848–1855. https://doi.org/10.1097/CORR.0000000000000379

Matsuda, K., Miyoshi, H., Hiraoka, K., Yokoyama, S., Haraguchi, T., Hashiguchi, T., Hamada, T., Shiba, N., & Ohshima, K. (2017). Clinicopathological and prognostic value of transforming acidic coiled-coil-containing protein 3 (TACC3) expression in soft tissue sarcomas. *PLoS ONE*, *12*(11), 1–14. https://doi.org/10.1371/journal.pone.0188096

Matsuura, S., Matsumoto, Y., Morishima, K., Izumi, H., Matsumoto, H., Ito, E., Tsutsui, K., Kobayashi, J., Tauchi, H., Kajiwara, Y., Hama, S., Kurisu, K., Tahara, H., Oshimura, M., Komatsu, K., Ikeuchi, T., & Kajii, T. (2006). Monoallelic BUB1B mutations and defective mitotic-spindle checkpoint in seven families with premature chromatid separation (PCS) syndrome. *American Journal of Medical Genetics Part A*, *140A*(4), 358–367. https://doi.org/10.1002/ajmg.a.31069

McDonald, K. L., O'Toole, E. T., Mastronarde, D. N., & McIntosh, J. R. (1992). Kinetochore microtubules in PTK cells. *Journal of Cell Biology*, *118*(2), 369–383. https://doi.org/10.1083/jcb.118.2.369

McIntosh, J. R., & Hays, T. (2016). A brief history of research on mitotic mechanisms. *Biology*, *5*(4), 1–38. https://doi.org/10.3390/biology5040055

McNally, F. J. (2013). Mechanisms of spindle positioning. *Journal of Cell Biology*, *200*(2), 131–140. https://doi.org/10.1083/jcb.201210007

McRae, J. F., Clayton, S., Fitzgerald, T. W., Kaplanis, J., Prigmore, E., Rajan, D., Sifrim, A., Aitken, S., Akawi, N., Alvi, M., Ambridge, K., Barrett, D. M., Bayzetinova, T., Jones, P., Jones, W. D., King, D., Krishnappa, N., Mason, L. E., Singh, T., … Hurles, M. E. (2017). Prevalence and architecture of de novo mutations in developmental disorders. *Nature*, *542*(7642), 433–438. https://doi.org/10.1038/nature21062

Megraw, T. L., Kao, L. R., & Kaufman, T. C. (2001). Zygotic development without functional mitotic centrosomes. *Current Biology*, *11*(2), 116–120. https://doi.org/10.1016/S0960-

9822(01)00017-3

Meyers, R. M., Bryan, J. G., McFarland, J. M., Weir, B. A., Sizemore, A. E., Xu, H., Dharia, N. V, Montgomery, P. G., Cowley, G. S., Pantel, S., Goodale, A., Lee, Y., Ali, L. D., Jiang, G., Lubonja, R., Harrington, W. F., Strickland, M., Wu, T., Hawes, D. C., … Tsherniak, A. (2017). Computational correction of copy number effect improves specificity of CRISPR–Cas9 essentiality screens in cancer cells. *Nature Genetics*, *49*(12), 1779–1784. https://doi.org/10.1038/ng.3984

Mitchison, T. J. (2012). The proliferation rate paradox in antimitotic chemotherapy. *Molecular Biology of the Cell*, *23*(1), 1–6. https://doi.org/10.1091/mbc.E10-04-0335

Mitchison, T., & Kirschner, M. (1984). Dynamic instability of microtubule growth. *Nature*, *312*(5991), 237–242. https://doi.org/10.1038/312237a0

Miyamoto, D. T., Perlman, Z. E., Burbank, K. S., Groen, A. C., & Mitchison, T. J. (2004). The kinesin Eg5 drives poleward microtubule flux in Xenopus laevis egg extract spindles. *Journal of Cell Biology*, *167*(5), 813–818. https://doi.org/10.1083/jcb.200407126

Morey, M., Serras, F., & Corominas, M. (2003). Halving the selenophosphate synthetase gene dose confers hypersensitivity to oxidative stress in Drosophila melanogaster. *FEBS Letters*, *534*(1–3), 111–114. https://doi.org/10.1016/S0014-5793(02)03790-0

Mori, T., Kinoshita, Y., Watanabe, A., Yamaguchi, T., Hosokawa, K., & Honjo, H. (2006). Retention of paclitaxel in cancer cells for 1 week in vivo and in vitro. *Cancer Chemotherapy and Pharmacology*, *58*(5), 665–672. https://doi.org/10.1007/s00280-006-0209-6

Mukhtar, E., Adhami, V. M., & Mukhtar, H. (2014). Targeting microtubules by natural agents for cancer therapy. *Molecular Cancer Therapeutics*, *13*(2), 275–284. https://doi.org/10.1158/1535-7163.MCT-13-0791

Muppidi, J. R., Schmitz, R., Green, J. A., Xiao, W., Larsen, A. B., Braun, S. E., An, J., Xu, Y., Rosenwald, A., Ott, G., Gascoyne, R. D., Rimsza, L. M., Campo, E., Jaffe, E. S., Delabie, J., Smeland, E. B., Braziel, R. M., Tubbs, R. R., Cook, J. R., … Cyster, J. G. (2014). Loss of signalling via Gα13 in germinal centre B-cell-derived lymphoma. *Nature*, *516*(7530), 254. https://doi.org/10.1038/nature13765

Musacchio, A. (2015). The Molecular Biology of Spindle Assembly Checkpoint Signaling Dynamics.

Current Biology, *25*(20), R1002–R1018. https://doi.org/10.1016/j.cub.2015.08.051

Musacchio, A., & Salmon, E. D. (2007). The spindle-assembly checkpoint in space and time. *Nature Reviews Molecular Cell Biology*, *8*(5), 379–393. https://doi.org/10.1038/nrm2163

Mustaly, H. M., & Ganem, N. J. (2015). Mitosis: Chromosome Segregation and Stability. *ELS*, 1–7. https://doi.org/10.1002/9780470015902.a0005774.pub2

Nakajima, M., Kumada, K., Hatakeyama, K., Noda, T., Peters, J. M., & Hirota, T. (2007). The complete removal of cohesin from chromosome arms depends on separase. *Journal of Cell Science*, *120*(23), 4188–4196. https://doi.org/10.1242/jcs.011528

Nakano, S., Inoue, K., Xu, C., Deng, Z., Syrovatkina, V., Vitone, G., Zhao, L., Huang, X. Y., & Zhao, B. (2019). G-protein Gα 13 functions as a cytoskeletal and mitochondrial regulator to restrain osteoclast function. *Scientific Reports*, *9*(1), 1–16. https://doi.org/10.1038/s41598-019-40974-z

Nettles, J. H., Li, H., Cornett, B., Krahn, J. M., Snyder, J. P., & Downing, K. H. (2004). The binding mode of epothilone A on α,β-tubulin by electron crystallography. *Science*, *305*(5685), 866–869. https://doi.org/10.1126/science.1099190

Nicholson, J. M., & Cimini, D. (2013). Cancer karyotypes: Survival of the fittest. *Frontiers in Oncology*, *3 JUN*(June), 1–9. https://doi.org/10.3389/fonc.2013.00148

Nieto, Y., Shpall, E. J., Bearman, S. I., McSweeney, P. A., Cagnoni, P. J., Matthes, S., Gustafson, D., Long, M., Barón, A. E., & Jones, R. B. (2005). Phase I and pharmacokinetic study of docetaxel combined with melphalan and carboplatin, with autologous hematopoietic progenitor cell support, in patients with advanced refractory malignancies. *Biology of Blood and Marrow Transplantation*, *11*(4), 297–306. https://doi.org/10.1016/j.bbmt.2005.01.002

Nijman, S. M. B. (2011). Synthetic lethality: general principles, utility and detection using genetic screens in human cells. *FEBS Letters*, *585*(1), 1–6. https://doi.org/10.1016/j.febslet.2010.11.024

Nishida, N., Yano, H., Nishida, T., Kamura, T., & Kojiro, M. (2006). Angiogenesis in cancer. *Vascular Health and Risk Management*, *2*(3), 213–219. https://doi.org/10.2147/vhrm.2006.2.3.213

Nixon, F. M., Gutiérrez-Caballero, C., Hood, F. E., Booth, D. G., Prior, I. A., & Royle, S. J. (2015). The mesh is a network of microtubule connectors that stabilizes individual kinetochore

fibers of the mitotic spindle. *ELife*, *4*(JUNE2015), 1–21. https://doi.org/10.7554/eLife.07635

Noble, R. L., Beer, C. T., & Cutts, J. H. (1958). Role of Chance Observations in Chemotherapy: Vinca Rosea. *Ann. N.Y. Acad. Sci.*, *76*, 882–894.

Nogales, E., & Wang, H. W. (2006). Structural intermediates in microtubule assembly and disassembly: How and why? *Current Opinion in Cell Biology*, *18*(2), 179–184. https://doi.org/10.1016/j.ceb.2006.02.009

Nogales, E., Wolf, S. G., Khant, A., Ludueiiat, R. F., & Downing, K. H. (1995). *Structure of tubulin at 6.5 A and location of the taxol-binding site*. *375*(June), 1–4.

O'Hayre, M., Inoue, A., Kufareva, I., Wang, Z., Mikelis, C. M., Drummond, R. A., Avino, S., Finkel, K., Kalim, K. W., Dipasquale, G., Guo, F., Aoki, J., Zheng, Y., Lionakis, M. S., Molinolo, A. A., & Gutkind, J. S. (2016). Inactivating mutations in GNA13 and RHOA in Burkitt's lymphoma and diffuse large B-cell lymphoma: A tumor suppressor function for the Gα13/RhoA axis in B cells. *Oncogene*, *35*(29). https://doi.org/10.1038/onc.2015.442

Okumura, M., Natsume, T., Kanemaki, M. T., & Kiyomitsu, T. (2018). Dynein–dynactin–NuMA clusters generate cortical spindle-pulling forces as a multiarm ensemble. *ELife*, *7*. https://doi.org/10.7554/eLife.36559

Orr, B., Talje, L., Liu, Z., Kwok, B. H., & Compton, D. A. (2016). Adaptive Resistance to an Inhibitor of Chromosomal Instability in Human Cancer Cells. *Cell Reports*, *17*(7), 1755–1763. https://doi.org/10.1016/j.celrep.2016.10.030

Orth, J. D., Kohler, R. H., Foijer, F., Sorger, P. K., Weissleder, R., & Mitchison, T. J. (2011). Analysis of mitosis and antimitotic drug responses in tumors by In Vivo microscopy and single-cell pharmacodynamics. *Cancer Research*, *71*(13), 4608–4616. https://doi.org/10.1158/0008-5472.CAN-11-0412

Otomo, T., Otomo, C., Tomchick, D. R., Machius, M., & Rosen, M. K. (2005). Structural basis of Rho GTPase-mediated activation of the formin mDia1. *Molecular Cell*, *18*(3), 273–281. https://doi.org/10.1016/j.molcel.2005.04.002

Oudouhou, F., Casu, B., Dopgwa Puemi, A. S., Sygusch, J., & Baron, C. (2017). Analysis of Novel Interactions between Components of the Selenocysteine Biosynthesis Pathway, SEPHS1, SEPHS2, SEPSECS, and SECp43. *Biochemistry*, *56*(17), 2261–2270.

https://doi.org/10.1021/acs.biochem.6b01116

Pampalona, J., Roscioli, E., Silkworth, W. T., Bowden, B., Genescà, A., Tusell, L., & Cimini, D. (2016). Chromosome bridges maintain kinetochore-microtubule attachment throughout mitosis and rarely break during anaphase. *PLoS ONE*, *11*(1), 1–17. https://doi.org/10.1371/journal.pone.0147420

Paracelsus, T. W., & Band 2. (1965). *Die dritte Defension wegen des Schreibens der neuen Rezepte. In: Septem Defensiones 1538. Werke Bd. 2*.

Pereira, D. A., & Williams, J. A. (2007). Origin and evolution of high throughput screening. *British Journal of Pharmacology*, *152*(1), 53–61. https://doi.org/10.1038/sj.bjp.0707373

Peters, J. M., Tedeschi, A., & Schmitz, J. (2008). The cohesin complex and its roles in chromosome biology. *Genes and Development*, *22*(22), 3089–3114. https://doi.org/10.1101/gad.1724308

Pettit, R. K., Pettit, G. R., & Hazen, K. C. (1998). Specific activities of dolastatin 10 and peptide derivatives against Cryptococcus neoformans. *Antimicrobial Agents and Chemotherapy*, *42*(11), 2961–2965. https://doi.org/10.1128/aac.42.11.2961

Pfau, S. J., & Amon, A. (2012). Chromosomal instability and aneuploidy in cancer: From yeast to man. *EMBO Reports*, *13*(6), 515–527. https://doi.org/10.1038/embor.2012.65

Potapova, T. A., Zhu, J., & Li, R. (2013). Aneuploidy and chromosomal instability: A vicious cycle driving cellular evolution and cancer genome chaos. *Cancer and Metastasis Reviews*, *32*(3–4), 377–389. https://doi.org/10.1007/s10555-013-9436-6

Pratt, A. J., & MacRae, I. J. (2009). The RNA-induced silencing complex: A versatile gene-silencing machine. *Journal of Biological Chemistry*, *284*(27), 17897–17901. https://doi.org/10.1074/jbc.R900012200

Prosser, S. L., & Pelletier, L. (2017). Mitotic spindle assembly in animal cells: A fine balancing act. *Nature Reviews Molecular Cell Biology*, *18*(3), 187–201. https://doi.org/10.1038/nrm.2016.162

Quasthoff, S., & Hartung, H. P. (2002). Chemotherapy-induced peripheral neuropathy. *Journal of Neurology*, *249*(1), 9–17. https://doi.org/10.1007/PL00007853

Quintyne, N. J., Reing, J. E., Hoffelder, D. R., Gollin, S. M., & Saunders, W. S. (2005). Spindle multipolarity is prevented by centrosomal clustering. *Science*, *307*(5706), 127–129.

https://doi.org/10.1126/science.1104905

Rampersad, S. N. (2012). Multiple applications of Alamar Blue as an indicator of metabolic function and cellular health in cell viability bioassays. *Sensors (Basel, Switzerland)*, *12*(9), 12347–12360. https://doi.org/10.3390/s120912347

Ran, F. A., Hsu, P. D., Wright, J., Agarwala, V., Scott, D. A., & Zhang, F. (2013). Genome engineering using the CRISPR-Cas9 system. *Nature Protocols*, *8*(11), 2281–2308. https://doi.org/10.1038/nprot.2013.143

Rasheed, S. A., Teo, C. R., Beillard, E. J., Voorhoeve, P. M., Zhou, W., Ghosh, S., & Casey, P. J. (2015). MicroRNA-31 controls G protein alpha-13 (GNA13) expression and cell invasion in breast cancer cells. *Molecular Cancer*, *14*.

Rasheed, S A K, Teo, C. R., Beillard, E. J., Voorhoeve, P. M., & Casey, P. J. (2013). MicroRNA-182 and MicroRNA-200a Control G-protein Subunit -13 (GNA13) Expression and Cell Invasion Synergistically in Prostate Cancer Cells. *J Biol Chem*, *288*, 7986.

Rasheed, Suhail Ahmed Kabeer, Leong, H. S., Lakshmanan, M., Raju, A., Dadlani, D., Chong, F. T., Shannon, N. B., Rajarethinam, R., Skanthakumar, T., Tan, E. Y., Hwang, J. S. G., Lim, K. H., Tan, D. S. W., Ceppi, P., Wang, M., Tergaonkar, V., Casey, P. J., & Iyer, N. G. (2018). GNA13 expression promotes drug resistance and tumor-initiating phenotypes in squamous cell cancers. *Oncogene*, *37*(10), 1340–1353. https://doi.org/10.1038/s41388-017-0038-6

Ravelli, R. B. G., Gigant, B., Curmi, P. A., Jourdain, I., Lachkar, S., Sobel, A., & Knossow, M. (2004). Insight into tubulin regulation from a complex with colchicine and a stathmin-like domain. *Nature*, *428*(6979), 198–202. https://doi.org/10.1038/nature02393

Reddy, A., & Kaelin, W. G. J. (2002). Using cancer genetics to guide the selection of anticancer drug targets. *Current Opinion in Pharmacology*, *2*(4), 366–373.

Rizvi, S. A., Neidt, E. M., Cui, J., Feiger, Z., Skau, C. T., Gardel, M. L., Kozmin, S. A., & Kovar, D. R. (2009). Identification and Characterization of a Small Molecule Inhibitor of Formin-Mediated Actin Assembly. *Chemistry and Biology*, *16*(11), 1158–1168. https://doi.org/10.1016/j.chembiol.2009.10.006

Rizzieri, D. A., Sand, G. J., McGaughey, D., Moore, J. O., DeCastro, C., Chao, N. J., Vredenburgh, J. J., Gasparetto, C., Long, G. D., Anderson, E., Foster, T., Toaso, B., Adams, D., Niedzwiecki, D.,

& Gockerman, J. P. (2004). Low-dose weekly paclitaxel for recurrent or refractory aggressive non-Hodgkin lymphoma. *Cancer*, *100*(11), 2408–2414. https://doi.org/10.1002/cncr.20245

Robinson, W. P., McFadden, D. E., & Stephenson, M. D. (2001). The origin of abnormalities in recurrent aneuploidy/polyploidy. *American Journal of Human Genetics*, *69*(6), 1245–1254. https://doi.org/10.1086/324468

Ruchaud, S., Carmena, M., & Earnshaw, W. C. (2007). Chromosomal passengers: Conducting cell division. *Nature Reviews Molecular Cell Biology*, *8*(10), 798–812. https://doi.org/10.1038/nrm2257

Sahai, E., Alberts, A. S., & Treisman, R. (1998). RhoA effector mutants reveal distinct effector pathways for cytoskeletal reorganization, SRF activation and transformation. *EMBO Journal*, *17*(5), 1350–1361. https://doi.org/10.1093/emboj/17.5.1350

Salic, A., Waters, J. C., & Mitchison, T. J. (2004). Vertebrate shugoshin links sister centromere cohesion and kinetochore microtubule stability in mitosis. *Cell*, *118*(5), 567–578. https://doi.org/10.1016/j.cell.2004.08.016

Sanjana, N. E., Shalem, O., & Zhang, F. (2014). Improved vectors and genome-wide libraries for CRISPR screening. *Nature Methods*, *11*(8), 783–784. https://doi.org/10.1038/nmeth.3047

Sansregret, L., Vanhaesebroeck, B., & Swanton, C. (2018). Determinants and clinical implications of chromosomal instability in cancer. *Nature Reviews Clinical Oncology*, *15*(3), 139–150. https://doi.org/10.1038/nrclinonc.2017.198

Santarella, R. A., Koffa, M. D., Tittmann, P., Gross, H., & Hoenger, A. (2007). HURP Wraps Microtubule Ends with an Additional Tubulin Sheet That Has a Novel Conformation of Tubulin. *Journal of Molecular Biology*, *365*(5), 1587–1595. https://doi.org/10.1016/j.jmb.2006.10.064

Saxton, W. M., & McIntosh, J. R. (1987). Interzone microtubule behavior in late anaphase and telophase spindles. *Journal of Cell Biology*, *105*(2), 875–886. https://doi.org/10.1083/jcb.105.2.875

Schiff, P. B., Jane, F., & Horwitz, S. B. (1979). Promotion of microtubule assembly in vitro by taxol. *Nature*, *277*(5698), 665–667. https://doi.org/10.1038/277665a0

Schmidt, S., Schneider, L., Essmann, F., Cirstea, I. C., Kuck, F., Kletke, A., Jänicke, R. U., Wiek, C.,

Hanenberg, H., Ahmadian, M. R., Schulze-Osthoff, K., Nürnberg, B., & Piekorz, R. P. (2010). The centrosomal protein TACC3 controls paclitaxel sensitivity by modulating a premature senescence program. *Oncogene*, *29*(46), 6184–6192. https://doi.org/10.1038/onc.2010.354

Schneider, L., Essmann, F., Kletke, A., Rio, P., Hanenberg, H., Schulze-Osthoff, K., Nürnberg, B., & Piekorz, R. P. (2008). TACC3 depletion sensitizes to paclitaxel-induced cell death and overrides p21WAF-mediated cell cycle arrest. *Oncogene*, *27*(1), 116–125. https://doi.org/10.1038/sj.onc.1210628

Schneider, Leonid, Essmann, F., Kletke, A., Rio, P., Hanenberg, H., Wetzel, W., Schulze-Osthoff, K., Nürnberg, B., & Piekorz, R. P. (2007). The transforming acidic coiled coil 3 protein is essential for spindle-dependent chromosome alignment and mitotic survival. *Journal of Biological Chemistry*, *282*(40), 29273–29283. https://doi.org/10.1074/jbc.M704151200

Scholey, J. M., Civelekoglu-Scholey, G., & Brust-Mascher, I. (2016). Anaphase B. *Biology*, *5*(4), 1–30. https://doi.org/10.3390/biology5040051

Selvarajah, S., Yoshimoto, M., Park, P. C., Maire, G., Paderova, J., Bayani, J., Lim, G., Al-Romaih, K., Squire, J. A., & Zielenska, M. (2006). The breakage-fusion-bridge (BFB) cycle as a mechanism for generating genetic heterogeneity in osteosarcoma. *Chromosoma*, *115*(6), 459–467. https://doi.org/10.1007/s00412-006-0074-4

Shalem, O., Sanjana, N. E., & Zhang, F. (2015). High-throughput functional genomics using CRISPR–Cas9. *Nature Reviews Genetics*, *16*, 299. https://doi.org/10.1038/nrg3899

Shi, Y. W., Yuan, W., Wang, X., Gong, J., Zhu, S. X., Chai, L. L., Qi, J. L., Qin, Y. Y., Gao, Y., Zhou, Y. L., Fan, X. Le, Ji, C. Y., Wu, J. Y., Wang, Z. W., & Liu, D. (2016). Combretastatin A-4 efficiently inhibits angiogenesis and induces neuronal apoptosis in zebrafish. *Scientific Reports*, *6*(January), 1–11. https://doi.org/10.1038/srep30189

Silkworth, W. T., Nardi, I. K., Scholl, L. M., & Cimini, D. (2009). Multipolar spindle pole coalescence is a major source of kinetochore mis-attachment and chromosome mis-segregation in cancer cells. *PLoS ONE*, *4*(8). https://doi.org/10.1371/journal.pone.0006564

Silljé, H. H. W., Nagel, S., Körner, R., & Nigg, E. A. (2006). HURP Is a Ran-Importin β-Regulated Protein that Stabilizes Kinetochore Microtubules in the Vicinity of Chromosomes. *Current Biology*, *16*(8), 731–742. https://doi.org/10.1016/j.cub.2006.02.070

Singh, P., Thomas, G. E., Gireesh, K. K., & Manna, T. K. (2014). TACC3 protein regulates microtubule nucleation by affecting γ-tubulin ring complexes. *Journal of Biological Chemistry*, *289*(46), 31719–31735. https://doi.org/10.1074/jbc.M114.575100

Skoufias, D. A., DeBonis, S., Saoudi, Y., Lebeau, L., Crevel, I., Cross, R., Wade, R. H., Hackney, D., & Kozielski, F. (2006). S-trityl-L-cysteine is a reversible, tight binding inhibitor of the human kinesin Eg5 that specifically blocks mitotic progression. *Journal of Biological Chemistry*, *281*(26), 17559–17569. https://doi.org/10.1074/jbc.M511735200

Slobodnick, A., Shah, B., Pillinger, M. H., & Krasnokutsky, S. (2015). Colchicine: Old and New. *American Journal of Medicine*, *128*(5), 461–470. https://doi.org/10.1016/j.amjmed.2014.12.010

Smith, C. D., Zhang, X., Mooberry, S. L., Patterson, G. M. L., & Moore, R. E. (1994). Cryptophycin: A New Antimicrotubule Agent Active against Drug-resistant Cells. *Cancer Research*, *54*(14), 3779–3784.

Smith, J. A., Slusher, B. S., Wozniak, K. M., Farah, M. H., Smiyun, G., Wilson, L., Feinstein, S., & Jordan, M. A. (2016). Structural basis for induction of peripheral neuropathy by microtubule-targeting cancer drugs. *Cancer Research*, *76*(17), 5115–5123. https://doi.org/10.1158/0008-5472.CAN-15-3116

Smits, A. H., Ziebell, F., Joberty, G., Zinn, N., Mueller, W. F., Clauder-Münster, S., Eberhard, D., Fälth Savitski, M., Grandi, P., Jakob, P., Michon, A. M., Sun, H., Tessmer, K., Bürckstümmer, T., Bantscheff, M., Steinmetz, L. M., Drewes, G., & Huber, W. (2019). Biological plasticity rescues target activity in CRISPR knock outs. *Nature Methods*, *16*(11), 1087–1093. https://doi.org/10.1038/s41592-019-0614-5

Spicher, K., Kalkbrenner, F., Zobel, A., Harhammer, R., Nürnberg, B., Söling, A., & Schultz, G. (1994). G12 and G13 α-subunits are immunochemically detectable in most membranes of various mammalian cells and tissues. In *Biochemical and Biophysical Research Communications* (Vol. 198, Issue 3, pp. 906–914). https://doi.org/10.1006/bbrc.1994.1129

Stearns, T. (2001). Centrosome duplication: A centriolar pas de deux. *Cell*, *105*(4), 417–420. https://doi.org/10.1016/S0092-8674(01)00366-X

Steinmetz, M. O., & Prota, A. E. (2018). Microtubule-Targeting Agents: Strategies To Hijack the

Cytoskeleton. *Trends in Cell Biology*, *28*(10), 776–792. https://doi.org/10.1016/j.tcb.2018.05.001

Stemmann, O., Zou, H., Gerber, S. A., Gygi, S. P., & Kirschner, M. W. (2001). Dual inhibition of sister chromatid separation at metaphase. *Cell*, *107*(6), 715–726. https://doi.org/10.1016/S0092-8674(01)00603-1

Stewart, S. A., Dykxhoorn, D. M., Palliser, D., Mizuno, H., Yu, E. Y., An, D. S., Sabatini, D. M., Chen, I. S. Y., Hahn, W. C., Sharp, P. A., Weinberg, R. A., & Novina, C. D. (2003). Lentivirus-delivered stable gene silencing by RNAi in primary cells. *RNA*, *9*(4), 493–501. https://doi.org/10.1261/rna.2192803

Stopsack, K. H., Whittaker, C. A., Gerke, T. A., Loda, M., Kantoff, P. W., Mucci, L. A., & Amon, A. (2019). Aneuploidy drives lethal progression in prostate cancer. *Proceedings of the National Academy of Sciences of the United States of America*, *166*(23), 11390–11395. https://doi.org/10.1073/pnas.1902645116

Suzuki, N., Hajicek, N., & Kozasa, T. (2009). Regulation and physiological functions of G12/13-mediated signaling pathways. *NeuroSignals*, *17*(1), 55–70. https://doi.org/10.1159/000186690

Swanton, C., Nicke, B., Schuett, M., Eklund, A. C., Ng, C., Li, Q., Hardcastle, T., Lee, A., Roy, R., East, P., Kschischo, M., Endesfelder, D., Wylie, P., Se, N. K., Chen, J. G., Howell, M., Ried, T., Habermann, J. K., Auer, G., … Downward, J. (2009). Chromosomal instability determines taxane response. *Proceedings of the National Academy of Sciences of the United States of America*, *106*(21), 8671–8676. https://doi.org/10.1073/pnas.0811835106

Swanton, C., Tomlinson, I., & Downward, J. (2006). Chromosomal instability, colorectal cancer and taxane resistance. *Cell Cycle*, *5*(8), 818–823. https://doi.org/10.4161/cc.5.8.2682

Syrovatkina, V., Alegre, K. O., Dey, R., & Huang, X. Y. (2016). Regulation, Signaling, and Physiological Functions of G-Proteins. In *Journal of Molecular Biology* (Vol. 428, Issue 19). https://doi.org/10.1016/j.jmb.2016.08.002

Syrovatkina, V., & Huang, X. Y. (2019). Signaling mechanisms and physiological functions of G-protein Gα 13 in blood vessel formation, bone homeostasis, and cancer. *Protein Science*, *28*(2), 305–312. https://doi.org/10.1002/pro.3531

Takeda, D. Y., & Dutta, A. (2005). DNA replication and progression through S phase. *Oncogene*, *24*(17), 2827–2843. https://doi.org/10.1038/sj.onc.1208616

Tamura, T., Yamamoto, S., Takahata, M., Sakaguchi, H., Tanaka, H., Stadtman, T. C., & Inagaki, K. (2004). Selenophosphate synthetase genes from lung adenocarcinoma cells: Sps1 for recycling L-selenocysteine and Sps2 for selenite assimilation. *Proceedings of the National Academy of Sciences of the United States of America*, *101*(46), 16162–16167. https://doi.org/10.1073/pnas.0406313101

Tan, W., Martin, D., & Gutkind, J. S. (2006). The Gα13-Rho signaling axis is required for SDF-1-induced migration through CXCR. *Journal of Biological Chemistry*, *281*(51), 39542–39549. https://doi.org/10.1074/jbc.M609062200

Tang, Y. C., Williams, B. R., Siegel, J. J., & Amon, A. (2011). Identification of aneuploidy-selective antiproliferation compounds. *Cell*, *144*(4), 499–512. https://doi.org/10.1016/j.cell.2011.01.017

Taylor, A. M., Shih, J., Ha, G., Gao, G. F., Zhang, X., Berger, A. C., Schumacher, S. E., Wang, C., Hu, H., Liu, J., Lazar, A. J., Caesar-Johnson, S. J., Demchok, J. A., Felau, I., Kasapi, M., Ferguson, M. L., Hutter, C. M., Sofia, H. J., Tarnuzzer, R., … Meyerson, M. (2018). Genomic and Functional Approaches to Understanding Cancer Aneuploidy. *Cancer Cell*, *33*(4), 676-689.e3. https://doi.org/10.1016/j.ccell.2018.03.007

Teo, C. R., Casey, P. J., & Rasheed, S. A. K. (2016). The GNA13-RhoA signaling axis suppresses expression of tumor protective Kallikreins. *Cellular Signalling*, *28*(10), 1479–1488. https://doi.org/10.1016/j.cellsig.2016.07.001

Thompson, S. L., Bakhoum, S. F., & Compton, D. A. (2010). Mechanisms of Chromosomal Instability. *Current Biology*, *20*(6), R285–R295. https://doi.org/10.1016/j.cub.2010.01.034

Thompson, S. L., & Compton, D. A. (2008). Examining the link between chromosomal instability and aneuploidy in human cells. *Journal of Cell Biology*, *180*(4), 665–672. https://doi.org/10.1083/jcb.200712029

Thompson, S. L., & Compton, D. A. (2011). Chromosome missegregation in human cells arises through specific types of kinetochore-microtubule attachment errors. *Proceedings of the National Academy of Sciences of the United States of America*, *108*(44), 17974–17978.

https://doi.org/10.1073/pnas.1109720108

Tighe, A., Johnson, V. L., Albertella, M., & Taylor, S. S. (2001). Aneuploid colon cancer cells have a robust spindle checkpoint. *EMBO Reports*, *2*(7), 609–614. https://doi.org/10.1093/embo-reports/kve127

Tobe, R., Carlson, B. A., Huh, J. H., Castro, N. P., Xu, X. M., Tsuji, P. A., Lee, S. G., Bang, J., Na, J. W., Kong, Y. Y., Beaglehole, D., Southon, E., Seifried, H., Tessarollo, L., Salomon, D. S., Schweizer, U., Gladyshev, V. N., Hatfield, D. L., & Lee, B. J. (2016). Selenophosphate synthetase 1 is an essential protein with roles in regulation of redox homoeostasis in mammals. *Biochemical Journal*, *473*(14), 2141–2154. https://doi.org/10.1042/BCJ20160393

Tozer, G. M., Kanthou, C., Parkins, C. S., & Hill, S. A. (2002). The biology of the combretastatins as tumour vascular targeting agents. *International Journal of Experimental Pathology*, *83*(1), 21–38. https://doi.org/10.1046/j.1365-2613.2002.00211.x

Vandecandelaere, A., Martin, S. R., & Engelborghs, Y. (1997). Response of microtubules to the addition of colchicine and tubulin-colchicine: Evaluation of models for the interaction of drugs with microtubules. *Biochemical Journal*, *323*(1), 189–196. https://doi.org/10.1042/bj3230189

Vanneste, D., Ferreira, V., & Vernos, I. (2011). Chromokinesins: Localization-dependent functions and regulation during cell division. *Biochemical Society Transactions*, *39*(5), 1154–1160. https://doi.org/10.1042/BST0391154

Vasudev, N. S., & Reynolds, A. R. (2014). Anti-angiogenic therapy for cancer: Current progress, unresolved questions and future directions. *Angiogenesis*, *17*(3), 471–494. https://doi.org/10.1007/s10456-014-9420-y

Ververi, A., Splitt, M., Dean, J. C. S., & Brady, A. F. (2018). Phenotypic spectrum associated with de novo mutations in QRICH1 gene. *Clinical Genetics*, *93*(2), 286–292. https://doi.org/10.1111/cge.13096

Walczak, C. E., Cai, S., & Khodjakov, A. (2010). Mechanisms of chromosome behaviour during mitosis. *Nature Reviews Molecular Cell Biology*, *11*(2), 91–102. https://doi.org/10.1038/nrm2832

Walker, R. a, Pryer, N. K., & Salmon, E. D. (1987). Dynamic instability of Microtubules. *BioEssays*,

7(4), 149–154.

Wall, M. E., & Wani, M. C. (1995). Camptothecin and Taxol: Discovery to Clinic—Thirteenth Bruce F. Cain Memorial Award Lecture. *Cancer Research*, *55*(4), 753 LP – 760. http://cancerres.aacrjournals.org/content/55/4/753.abstract

Wang, L. H. C., Mayer, B., Stemmann, O., & Nigg, E. A. (2010). Centromere DNA decatenation depends on cohesin removal and is required for mammalian cell division. *Journal of Cell Science*, *123*(5), 806–813. https://doi.org/10.1242/jcs.058255

Wang, Q., Chen, Y., Feng, H., Zhang, B., & Wang, H. (2018). Prognostic and predictive value of HURP in non-small cell lung cancer. *Oncology Reports*, *39*(4), 1682–1692. https://doi.org/10.3892/or.2018.6280

Wang, T., Wei, J. J., Sabatini, D. M., & Lander, E. S. (2014). Genetic screens in human cells using the CRISPR-Cas9 system. *Science (New York, N.Y.)*, *343*(6166), 80–84. https://doi.org/10.1126/science.1246981

Wang, Y., Yu, Y., Li, G. B., Li, S. A., Wu, C., Gigant, B., Qin, W., Chen, H., Wu, Y., Chen, Q., & Yang, J. (2017). Mechanism of microtubule stabilization by taccalonolide AJ. *Nature Communications*, *8*, 1–8. https://doi.org/10.1038/ncomms15787

Wani, M. C., Taylor, H. L., Wall, M. E., Coggon, P., & McPhail, A. T. (1971). Plant antitumor agents. VI. Isolation and structure of taxol, a novel antileukemic and antitumor agent from Taxus brevifolia. *Journal of the American Chemical Society*, *93*(9), 2325–2327. https://doi.org/10.1021/ja00738a045

Weaver, B. A. (2014). How Taxol/paclitaxel kills cancer cells. *Molecular Biology of the Cell*, *25*(18), 2677–2681. https://doi.org/10.1091/mbc.E14-04-0916

Westin, J. R., Mclaughlin, P., Romaguera, J., Hagemeister, F. B., Pro, B., Dang, N. H., Samaniego, F., Rodriguez, M. A., Fayad, L., Oki, Y., Fanale, M., Fowler, N., Nastoupil, L., Feng, L., Loyer, E., & Younes, A. (2014). Paclitaxel, topotecan and rituximab: Long term outcomes of an effective salvage programme for relapsed or refractory aggressive B-cell non-Hodgkin lymphoma. *British Journal of Haematology*, *167*(2), 177–184. https://doi.org/10.1111/bjh.13014

Wignall, S. M., & Villeneuve, A. M. (2009). Lateral microtubule bundles promote chromosome

alignment during acentrosomal oocyte meiosis. *Nature Cell Biology*, *11*(7), 839–844. https://doi.org/10.1038/ncb1891

Winefield, R. D., Entwistle, R. A., Foland, T. B., Lushington, G. H., & Himes, R. H. (2008). Differences in paclitaxel and docetaxel interactions with tubulin detected by mutagenesis of yeast tubulin. *ChemMedChem*, *3*(12), 1844–1847. https://doi.org/10.1002/cmdc.200800288

Wollman, R., Cytrynbaum, E. N., Jones, J. T., Meyer, T., Scholey, J. M., & Mogilner, A. (2005). Efficient chromosome capture requires a bias in the "search-and-capture" process during mitotic-spindle assembly. *Current Biology*, *15*(9), 828–832. https://doi.org/10.1016/j.cub.2005.03.019

Wong, J., & Fang, G. (2006). HURP controls spindle dynamics to promote proper interkinetochore tension and efficient kinetochore capture. *Journal of Cell Biology*, *173*(6), 879–891. https://doi.org/10.1083/jcb.200511132

World Health Organization (WHO). (2019). World health organization model list of essential medicines. In *Mental and Holistic Health: Some International Perspectives*. https://apps.who.int/iris/bitstream/handle/10665/325771/WHO-MVP-EMP-IAU-2019.06-eng.pdf?ua=1

Worzfeld, T., Wettschureck, N., & Offermanns, S. (2008). G12/G13-mediated signalling in mammalian physiology and disease. *Trends in Pharmacological Sciences*, *29*(11), 582–589. https://doi.org/10.1016/j.tips.2008.08.002

Wuster, A., & Madan Babu, M. (2008). Chemogenomics and biotechnology. *Trends in Biotechnology*, *26*(5), 252–258. https://doi.org/10.1016/j.tibtech.2008.01.004

Xu, Y., Rong, J., Duan, S., Chen, C., Li, Y., Peng, B., Yi, B., Zheng, Z., Gao, Y., Wang, K., Yun, M., Weng, H., Zhang, J., & Ye, S. (2016). High expression of GNA13 is associated with poor prognosis in hepatocellular carcinoma. *Scientific Reports*, *6*. https://doi.org/10.1038/srep35948

Yamada, H. Y., & Gorbsky, G. J. (2006). Spindle checkpoint function and cellular sensitivity to antimitotic drugs. *Molecular Cancer Therapeutics*, *5*(12), 2963–2969. https://doi.org/10.1158/1535-7163.MCT-06-0319

Yared, J. A., & Tkaczuk, K. H. R. (2012). Update on taxane development: New analogs and new formulations. *Drug Design, Development and Therapy*, *6*, 371–384. https://doi.org/10.2147/DDDT.S28997

Yasuda, S., Oceguera-Yanez, F., Kato, T., Okamoto, M., Yonemura, S., Terada, Y., Ishizaki, T., & Narumiya, S. (2004). Cdc42 and mDia3 regulate microtubule attachment to kinetochores. *Nature*, *428*(6984), 767–771. https://doi.org/10.1038/nature02452

Younes, A., Ayoub, J. P., Sarris, A., Hagemeister, F., North, L., Pate, O., Mclaughlin, P., Rodriguez, M. A., Romaguera, J., Kurzrock, R., Preti, A., Bachier, C., Smith, T., & Cabanillas, F. (1997). Paclitaxel activity for the treatment of non-Hodgkin's lymphoma: Final report of a phase II trial. *British Journal of Haematology*, *96*(2), 328–332. https://doi.org/10.1046/j.1365-2141.1997.d01-2012.x

Younes, A., Sarris, A., Melnyk, A., Romaguera, J., McLaughlin, P., Swan, F., Rodriguez, M. A., Hagemeister, F., Moore, D., & North, L. (1995). Three-hour paclitaxel infusion in patients with refractory and relapsed non-Hodgkin's lymphoma. *Journal of Clinical Oncology*, *13*(3), 583–587. https://doi.org/10.1200/JCO.1995.13.3.583

Zasadil, L. M., Andersen, K. A., Yeum, D., Rocque, G. B., Wilke, L. G., Tevaarwerk, A. J., Raines, R. T., Burkard, M. E., & Weaver, B. A. (2014). Cytotoxicity of paclitaxel in breast cancer is due to chromosome missegregation on multipolar spindles. *Science Translational Medicine*, *6*(229), 1–11. https://doi.org/10.1126/scitranslmed.3007965

Zasadil, L. M., Britigan, E. M. C., Ryan, S. D., Kaur, C., Guckenberger, D. J., Beebe, D. J., Moser, A. R., & Weaver, B. A. (2016). High rates of chromosome missegregation suppress tumor progression but do not inhibit tumor initiation. *Molecular Biology of the Cell*, *27*(13), 1981–1989. https://doi.org/10.1091/mbc.E15-10-0747

Zasadil, L. M., Britigan, E. M. C., & Weaver, B. A. (2013). 2n or not 2n: Aneuploidy, polyploidy and chromosomal instability in primary and tumor cells. *Seminars in Cell and Developmental Biology*, *24*(4), 370–379. https://doi.org/10.1016/j.semcdb.2013.02.001

Zayac, A. S., & Olszewski, A. J. (2020). Burkitt lymphoma: bridging the gap between advances in molecular biology and therapy. *Leukemia and Lymphoma*, *0*(0), 1–13. https://doi.org/10.1080/10428194.2020.1747068

Zekri, J. M., Hough, R. E., Davies, J. M., Molife, R., Hancock, B. W., & Lorigan, P. C. (2003). Phase II study of docetaxel in patients with relapsed or refractory malignant lymphoma. *British Journal of Cancer*, *88*(9), 1335–1338. https://doi.org/10.1038/sj.bjc.6600914

Zhai, Y., Kronebusch, P. J., & Borisy, G. G. (1995). Kinetochore microtubule dynamics and the metaphase-anaphase transition. *Journal of Cell Biology*, *131*(3), 721–734. https://doi.org/10.1083/jcb.131.3.721

Zhang, J., Grubor, V., Love, C. L., Banerjee, A., Richards, K. L., Mieczkowski, P. A., Dunphy, C., Choi, W., Au, W. Y., Srivastava, G., Lugar, P. L., Rizzieri, D. A., Lagoo, A. S., Bernal-Mizrachi, L., Mann, K. P., Flowers, C., Naresh, K., Evens, A., Gordon, L. I., … Dave, S. S. (2013). Genetic heterogeneity of diffuse large B-cell lymphoma. *Proceedings of the National Academy of Sciences of the United States of America*, *110*(4), 1398–1403. https://doi.org/10.1073/pnas.1205299110

Zhang, J. X., Mai, S. J., Huang, X. X., Wang, F. W., Liao, Y. J., Lin, M. C., Kung, H. F., Zeng, Y. X., & Xie, D. (2014). MiR-29c mediates epithelial-to-mesenchymal transition in human colorectal carcinoma metastasis via PTP4A and GNA13 regulation of β-catenin signaling. *Annals of Oncology*, *25*(11), 2196–2204. https://doi.org/10.1093/annonc/mdu439

Zhang, Jia Xing, Yun, M., Xu, Y., Chen, J. W., Weng, H. W., Zheng, Z. S., Chen, C., Xie, D., & Ye, S. (2016). GNA13 as a prognostic factor and mediator of gastric cancer progression. *Oncotarget*, *7*(4), 4414. https://doi.org/10.18632/oncotarget.6780

Zhang, Y., Tan, L., Yang, Q., Li, C., & Liou, Y. C. (2018). The microtubule-associated protein HURP recruits the centrosomal protein TACC3 to regulate K-fiber formation and support chromosome congression. *Journal of Biological Chemistry*, *293*(40), 15733–15747. https://doi.org/10.1074/jbc.RA118.003676

Zhang, Z., Tan, X., Luo, J., Cui, B., Lei, S., Si, Z., Shen, L., & Yao, H. (2018). GNA13 promotes tumor growth and angiogenesis by upregulating CXC chemokines via the NF-κB signaling pathway in colorectal cancer cells. *Cancer Medicine*, *7*(11), 5611–5620. https://doi.org/10.1002/cam4.1783

Appendix I – Supplementary figures

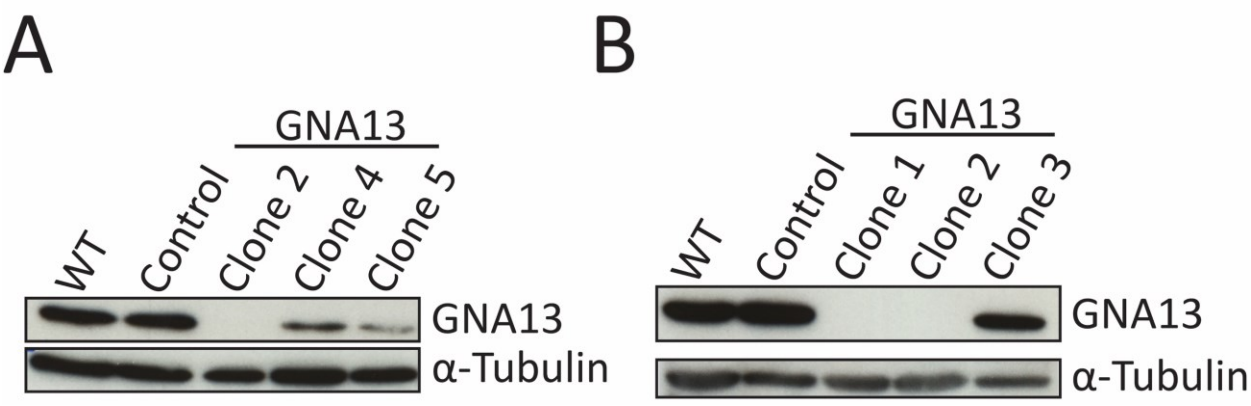

Figure S1. Immunoblots of GNA13 clones validated by TIDE analysis

(A) Immunoblots of NALM6 lines. Clones 4 and 5 were validated by TIDE to have knockout efficiencies >90% but still express GNA13. (B) Immunoblots of U2OS lines. Clone 3 was validated by TIDE to have a knockout efficiency >80% but still expressed GNA13. ≈200 000 cells loaded per well.

Appendix II – Primer and sgRNA Sequences

Gene	Sequence 5’-3’
QRICH1	CCAGGCTGCAGAAATCCCGG
GNA13	CATGGCAGCCCAAGGAATGG
SEPHS1	TGTACCTGAAGTCTCCGGGC
DLGAP5	GAATTGGACATTCCAGATGA
TACC3 (NALM6)	GACCAGGCTGGGCCAGCCAG
TACC3 (U2OS)	GAGGAGGACGACGGTAGGAG

Table S1. sgRNA sequences used to generate clones

sgRNAs were designed by the Tyers lab

Gene	Sequence 5’-3’
QRICH1	CTCACTGATGAATCTTGTTGCTT
	CTCAAAGACACATAACTCTGCTG
GNA13	CCTTCAGAGAGAGGAATTGTG
	TGTGCCTTAGCCTTTCAGTC
SEPHS1	TGGTTTTAGGATGGTCTTGG
	ATGGAACTCGAACAGAGTGG
DLGAP5	AGGCCCCATCACTATAATCC
	CACTGTTACTTGCTTGGTTGG
TACC3	CTCATCAAGGAAGTGGATGC
	TGAGCCCTGTTTTTATCCAG

Table S2. Primers used to amplify exons targeted by sgRNAs

Primers for GNA13, SEPHS1, DLGAP5, and TACC3 were designed by Dr. Benoit Barrette